Laser Powered Actuator

Hongzuo Liu

PhD

University of York

Physics, Engineering and Technology

October 2023

Abstract

Laser Power Transmission (LPT) emerges as a promising and efficient method for wireless power delivery, especially in long-distance applications and harsh environmental conditions. In comparison to other Wireless Power Transmission (WPT) methods, LPT boasts advantages such as a compact device size, focused transmitting direction, and high-power density. This PhD thesis provides an overview of LPT, elucidating the fundamental concepts of the photoelectric emitter, transmission channel, and receiver material. Additionally, it explores recent advancements in diode laser beam combining technology and high-efficiency multi-junction PV materials, discussing recommended LPT devices for simple applications such as laser-powered motors. The versatility of laser-powered actuators to wirelessly drive motors presents distinct advantages in scenarios characterized by high temperatures, radiation, and electromagnetic interference (EMI). A meticulous feedback mechanism is essential for precise motor speed control. This thesis examines wireless techniques for motor speed signal feedback in laser-powered actuators, detailing the structure of light signal transmission, including generation, modulation, and reception processes. A comparative analysis of motor speed collection methods with and without sensors is conducted, considering factors such as cost, reliability, integration, and efficiency. Through simulation, the steady-state characteristics of the system are analyzed under different load torque conditions. A robust speed control method is introduced, utilizing DC motor speed feedback to determine the laser on/off state for speed adjustment. Simulation results demonstrate stable speed control within the controllable range, showcasing the potential of LPT for reliable power delivery in challenging environments. An experiment is conducted to validate the simulation results, using a 150mW and 3W laser primarily to drive a DC motor with converted power from GaAs materials.

Key Words: Laser power transmission, motor actuator, light signal transmission, signal feedback, motor speed sensor, motor speed control, and closed-loop control

Table of Contents

Abstract **2**
Table of Contents **3**
List of Tables **6**
List of Figures **7**
Acknowledgements **9**
Declaration **11**
List of Publications **12**
Nomenclature **13**
Abbreviations **15**
Chapter 1 Introduction **16**
1.1 Background 16
1.2 WPT method comparison 20
1.2.1 APT 21
1.2.2 CPT 21
1.2.3 IPT 22
1.2.4 MPT 22
1.2.5 LPT 23
1.3 Project outline and objectives 24
1.4 The purpose of this work 24
1.5 The structure of this paper 24
Chapter 2 A Review on Laser Power Transmission for Motor Drive in Harsh Hazardous Environmental Application **26**
2.1 Introduction 26
2.2 LPT Review 29
2.2.1 LPT Application History 30
2.2.2 Laser Emitter 32
2.2.3 Transmission through atmosphere 37
2.2.4 Transmission through optical fiber 38
2.2.5 PV materials receiver 41
2.3 Discussion 46
2.4 Future scope 49
2.4.1 Improvement of device conversion efficiency 49
2.4.2 LPT system motor speed control strategy 50

2.5 Summary 50
Chapter 3 Optical Fibre-based Motor Speed Feedback Method for Laser Powered Actuator 52
3.1 Introduction 52
3.2 Light Signal Transmission Structure 53
3.2.1 Light signal emitters 54
3.2.2 Light signal emitter sources 57
3.2.3 Light signal modulation 60
3.2.4 Drive circuit for light sources 61
3.2.5 Light signal receiver 64
3.3 Sensorless Motor Speed Feedback 69
3.3.1 Brushed DC motor 70
3.3.2 Brushless DC motor 71
3.3.3 Induction motor 73
3.4 Motor Speed Feedback by Sensors 75
3.4.1 Encoder for Motor Speed Feedback 76
3.4.2 Position Sensor for Motor Speed Feedback 76
3.4.3 Hall Sensor for Motor Speed Feedback. 78
3.4.4 Vibration Sensor for Motor Speed Feedback. 79
3.5 Discussion 79
3.5.1 Motor speed feedback method for analog light signal modulation. 80
3.5.2 Motor speed feedback method for digital light signal modulation 81
3.5.3 Proposed motor speed feedback method for laser powered actuator 82
3.6 Summary 82
Chapter 4 Simulation on Laser Powered Actuator and its Close-loop Control System 84
4.1 Proposed System Structure and Control Strategy 84
4.1.1Maximum speed and torque under constant incident laser condition 84
4.1.2 Closed-loop control of the motor speed theoretical study 86
4.1.3 Variable torque control by increasing the laser power at the maximum power point of PCM. 89
4.1.4 System efficiency analysis 90
4.2 Simulation Result 92
4.2.1 Applied system parameters 92
4.2.2 Steady-state power point workplace 92
4.2.3 Closed-loop control of the motor speed with laser on/off 95
4.2.4 Closed-loop control of the motor speed with constant torque 96

4.2.5 Closed-loop control of the motor torque 98
4.3 Discussion 100
4.4 Summary 102
Chapter 5 Experiment on Laser Powered Actuator 103
5.1 Introduction 103
5.2 Equipment 103
5.2.1 Laser Enclosure box and interlocks 103
5.2.2 Laser power meter 104
5.2.3 GaAs PCM 104
5.2.4 Lasers 105
5.2.5 DC Motor and Multi-meter 106
5.3 Methods 107
5.3.1 Establishing the Power Density on the PCM (one off set up) 107
5.3.2 Running the Experiment 107
5.3.3 Ending Experiment 108
5.4 Experiment results 109
5.4.1 Beam expand/focus efficiency detection. 109
5.4.2 Output curve with 1mW laser 109
5.4.3 Output curve with 150mW laser 112
5.4.4 Steady-state torque and current measurements 116
5.5 Summary 119
Chapter 6 Conclusions and Future Works 120
6.1 Conclusions 120
6.2 Future work 122
6.2.1 Laser power control strategy 122
6.2.2 Maximum power point control strategy 122
6.2.3 Dual closed-loop control strategy of torque and speed 122
6.2.4 Utilizing light reflection to modulate feedback signal by shutter 123
Appendix 124
1. Design for laser enclosure box. 124
References 125

List of Tables

Table 1-1. Comparison of LPT and other WPT. 23
Table 2-1. The power of 975nm fibre-coupled with LD[28] 32
Table 2-2. Main parameters of PV materials[59] 42
Table 2-3. The relationship between material bandgap and cutoff wavelength and transmission loss [60] 42
Table 2-4. Power conversion efficiency of different types of PV materials 46
Table 2-5. Main parameters comparison of four different types of WPT method. 47
Table 2-6. Comparison of Wire and LPT in harsh hazard application situation. 47
Table 3-1. Comparison of LEDs and LDs 58
Table 4-1. Parameters of PV material block in simulation. 92
Table 4-2. Simulation DC motor main characteristics. 92
Table 5-1: Features and specifications of GaAs used in experiment. 105
Table 5-2. Output power and electric characteristics in different expand/fucus ratio 109
Table 5-3. The value of electrical characteristics from the output of GaAs under 1mW laser 110
Table 5-4. Output I-V-R values of the GaAs irradiated by 150mW laser. 113
Table 5-5. The value of electrical characteristics from the output of GaAs under 150 mW laser 115
Table 5-6. The weight and corresponding current power by STM32 5V port. 116
Table 5-7. The weight and corresponding current power by L450G1 3W laser. 117

List of Figures

Figure 2-1. Special occasions suitable for applicating LPT replace wires. 27
Figure 2-2. Basic LPT Structure. 30
Figure 2-3. Efficiency of LD powered by Pulse wave current supply[27] 32
Figure 2-4. Atmosphere transmission wavelength absorption[5] 37
Figure 2-5. Proposed structure of laser power motor. 48
Figure 2-6. Equivalent circuit of the laser power motor. 48
Figure 2-7. Theoretically analysed efficiency of the motor drive by laser powered system. . 49
Figure 3-1. Schematic structure of a closed-loop control system with wireless feedback signal of laser powered actuator. 54
Figure 3-2. Schematic of the light emitters with each component and signal processing flow. 55
Figure 3-3. The structure of LEDs as a two-layers of N and P type semiconductors with (a) front-illuminated LEDs (FLEDs), (b) side-illuminated LEDs (SLEDs). 59
Figure 3-4. Schematic structure of SLED as a double layer heterojunction grown on N-type GaAs substrate at the top of the diode. 60
Figure 3-5. Analogue modulation circuit for optical signals 62
Figure 3-6. LED digital signal modulation. 63
Figure 3-7. LD digital signal modulation. 64
Figure 3-8. Block diagram of the optical receiver with (a) analogue type and (b) digital type. 65
Figure 3-9. Front end of light receiver with (a) high/low impedance front end and (b) transimpedance front end. 66
Figure 3-10. Receiver noise and its distribution. 69
Figure 3-11. Schematic diagram of encoder. 76
Figure 3-12. One of the vibration sensors method proposed in literature[122]. 79
Figure 4-1. Proposed LPT actuator system structure for DC motor. 85
Figure 4-2. Characteristics of proposed system control method comparing with PWM. 86
Figure 4-3. Proposed system control strategy schematic diagram. 86
Figure 4-4. The proposed system control strategy schematic diagram. 88

Figure 4-5. Time order tendency chart for (a) voltage (b) current (c) rotational speed (d) power point 94
Figure 4-6. Steady-state workplace of power point as a DC motor drive. 94
Figure 4-7. Closed-loop control time order tendency chart for (a) voltage (b) current (c) load torque (d) rotation speed (e) Laser power. 96
Figure 4-8. Constant torque closed-loop speed control time order tendency chart for (a) voltage (b) Current (c) Laser (d) Reference speed (e) Actual speed. 98
Figure 4-9. Closed-loop torque control time order tendency chart for (a) Torque (b) Rotate speed. 99
Figure 4-10. Relationship between maximum torque point and maximum power point for motor work by PCM output. 100
Figure 5-1. Laser enclosure box with interlock. 104
Figure 5-2. GaAs photovoltaic material. 104
Figure 5-3. Multi-meter and motor. 106
Figure 5-4. The schematic setup of the laser. This consists of a laser mount and cooler, laser optical expander and focusing unit, and a GaAs PV cell and mount. The optical expander/focuser cannot focus the laser to a point inside the laser box because it is beyond the wall of an, interlocked, laser enclosure box. 109
Figure 5-5. The electrical characteristics from the output of GaAs under 1mW laser 111
Figure 5-6. The LPT system setup fields 112
Figure 5-7. Output I-V curve of the GaAs irradiated by 150mW laser. 114
Figure 5-8. The electrical characteristics from the output of GaAs under 150mW laser 116
Figure 5-9. Device setup for measurement of torque and current (Powered by 5V port on STM32 board). 117
Figure 5-10. Device setup for measurement of torque and current (Powered by L450G1 3W laser). 118
Figure 6-1. Feedback light signal reflection and generation design. 123

Acknowledgements

First and foremost, I extend my heartfelt gratitude to Dr. Yihua Hu, my primary supervisor, for affording me the incredible opportunity to pursue my Ph.D. studies. Dr. Hu's academic rigor, generosity, and profound intellectual guidance have significantly influenced both my academic pursuits and personal development. Furthermore, Dr. Hu consistently emphasized the importance of maintaining strong research habits, encouraging me to enhance my English proficiency through daily reading aloud and meticulous notetaking. Being his Ph.D. student is a profound honour, and I sincerely hope that my accomplishments align with his high expectations and belief in my potential.

Secondly, I wish to express my gratitude to my co-supervisors, Dr. Mohammad Nasr Esfahani and Dr. Iain Will, for their unwavering support and valuable academic guidance. During our meetings, they attentively listened to my progress reports and provided critical insights. And they help me a lot about the experiment, which makes me improve much scope.

Thirdly, my deepest thanks go to my parents for their unwavering financial support, without which my academic journey would not have been possible. Despite facing numerous challenges, including study transfers, city closures due to the Covid-19 outbreak, visa complications, enrolment issues, and moments of contemplating termination, their guidance and encouragement provided the courage and motivation needed to persevere.

Fourthly, I am grateful to my senior, Dr Yixuan Zhang, for his excellent research recommendations, including structural planning and presentation strategies for journal articles, as well as practical insights into experimental circuit board soldering and transformer winding methods. Special appreciation is extended to my talented colleagues and friends, Xiaotian zhang, Wangjie Lang, Shangming Mei, Yu Nie, Chengdong Xu, Mengyu Cheng and Wangde Qiu, for enriching discussions on future expectations, societal dynamics, and the evolving demands for professionals in industrial development.

Finally, I express my gratitude to the Department of Electronic Engineering at the University of York for its continuous support, providing diverse learning resources. Special thanks to Ms. Camilla Danese for her timely advice and reminders regarding essential activities and assessments at key research junctures.

Declaration

I hereby declare that this thesis is a presentation of original work, and I am the sole author. This work has not been previously presented for an award at this university or any other institution. All sources are duly acknowledged and cited in the references section.

Major contents in Chapter 2 have been published in Power Electronics and Drives, vol. 6, no. 41, pp. 167-184, 2021. The title is ‘Laser Power Transmission and Its Application in Laser-Powered Electrical Motor Drive: A Review’.

Major contents in Chapter 4 have been submitted in Scientific report. The title is ‘Laser Powered Actuator and its Closed-Loop Rotation Speed and Torque Control’.

Hongzuo Liu

May 2024

List of Publications

[1] **H. Liu**, Y. Zhang, Y. Hu, and Z. Tse, “Laser Power Transmission and Its Application in Laser-Powered Electrical Motor Drive: A Review”, *Power Electronics and Drives*, vol. 6, no. 41, pp. 167-184, 2021.

[2] **H. Liu**, Y. Hu, H. Xu, A. Wireko-Brobby, and Y. B. Salamah “Laser Powered Actuator and its Closed-Loop Rotation Speed and Torque Control”, *Scientific Report*, (In minor revision).

Nomenclature

α_{ma}	gas absorb coefficient
α_{pa}	aerosol particle absorb coefficient
α_{ms}	gas scattering coefficient
α_{ps}	aerosol particle scattering coefficient
k	the number of commutator segments
p	the number of pole pairs
S	the number of the ripple peaks in one cycle duration
U	armature voltage
k_e	back potential coefficient of the motor
R	the total resistance of the armature loop
I	the armature current
V_{op}	open circuit voltage
ω_m	maximum speed
T_m	maximum torque
V_{mt}	the voltage at the maximum torque point
I_{mt}	the current at the maximum torque point
k_m	the moment coefficient
T	Torque
ω_r	the reference speed
T_r	the maximum torque under condition of the set speed
$I_m(STC)$	the standard condition values of maximum power point current
$G(STC)$	the standard condition values of irradiance level
P_{laser}	the laser power at the maximum power point

η	the conversion efficiency of the LD
η_d	the differential slope efficiency
D	duty cycle
i	current through the LD
V_{LD}	the voltage through the LD
I_{bias}	the basic current through the LD
I_{th}	the threshold current of LD
$V_m(STC)$	the standard condition values of voltage
G	irradiation level
V_r	the voltage on the resistor
V_m	the voltage on the motor
I_d	laser drive current
P	the output power of the laser

Abbreviations

WPT	Wireless power transmission
APT	Acoustic power transmission
CPT	Capacitive power transmission
IPT	Inductive power transmission
LPT	Laser power transmission
PCM	Photovoltaic conversion material
AGC	Automatic Gain Control
LD	Laser diode
LED	light-emitting diodes
FLED	Front-illuminated LED
SLED	Side-illuminated LED

Chapter 1 Introduction

1.1 Background

Electric motors are an integral part of modern life, powering countless devices and systems that we rely on every day. Their versatile applications span a wide range of industries, from transportation to manufacturing, and they have had a transformative impact on how we live and work. The utilization fields of motors include:

I. Transportation: Electric motors are a driving force behind the rapid evolution of transportation. Electric cars, for example, have gained popularity due to their energy efficiency and environmental benefits. Electric motors in these vehicles provide instant torque, smooth acceleration, and low maintenance requirements. Similarly, electric trains and buses are becoming increasingly common, reducing emissions and noise pollution in urban areas.

II. Industrial Manufacturing: In manufacturing, electric motors are the workhorses behind conveyor belts, robotic arms, and assembly line machinery. They offer precise control, high efficiency, and the ability to operate continuously, contributing to increased productivity and reduced downtime.

III. Aerospace and Aviation: Electric motors play a critical role in modern aircraft, powering systems such as landing gear, flaps, and auxiliary power units. Electric propulsion systems are also being explored for the next generation of environmentally friendly and fuel-efficient aircraft.

IV. Renewable Energy: Wind turbines and solar tracking systems rely on electric motors to adjust the orientation of blades and panels to maximize energy capture. Electric motors help convert renewable energy sources into electricity efficiently.

V. Consumer Electronics: From smartphones to home appliances, electric motors are found in numerous consumer products. Vibrating motors in mobile devices provide tactile feedback, while motors in refrigerators, washing machines, and air conditioners contribute to their functionality and energy efficiency.

VI. Robotics: Electric motors are the muscle behind robots, providing mobility and enabling them to perform a wide range of tasks. Advanced servo motors and actuators are crucial for precise and coordinated movements in industrial robots, medical robots, and even consumer robots like vacuum cleaners.

VII. Medical Devices: In the medical field, electric motors are used in everything from surgical robots and diagnostic equipment to prosthetic limbs and assistive devices for individuals with disabilities. Their precision and reliability are paramount in these applications.

VIII. Entertainment and Amusement: Electric motors power amusement park rides, elevators, and theatre equipment, enhancing our leisure and entertainment experiences. They provide movement and special effects that captivate audiences.

IX. Space Exploration: In space exploration, electric motors are used in satellite orientation systems, robotic arms on spacecraft, and even the wheels of rovers like NASA's Mars rovers. Their reliability is crucial in the harsh conditions of space.

X. Healthcare and Mobility: Electric motors also play a pivotal role in the development of electric wheelchairs and mobility scooters, offering improved maneuverability and accessibility for individuals with mobility challenges.

In general, electric motors are the unsung heroes of modern technology and industry. Their adaptability, efficiency, and reliability have made them indispensable in various sectors, contributing to cleaner and more efficient transportation, enhanced manufacturing processes, and the development of innovative consumer products. As technology continues to advance, electric motors will undoubtedly find new applications and play an even more significant role in shaping our future.

Power transmission through wires is a common and highly effective method, but it does have limitations and drawbacks when used in high-temperature and high-radiation fields, such as those found in certain industrial processes and nuclear facilities. In high-temperature and high-radiation environments, the choice of conductor material becomes critical. Many common conductor materials, such as copper and aluminum, can degrade or become brittle when exposed to extreme heat or radiation, leading to a loss of conductivity and structural integrity. The electromagnetic interference is also a problem, which will influence signal processing.

Resistance and Heat Generation: When electricity is transmitted through a wire, some energy is lost as heat due to the resistance of the conductor material. In high-temperature environments, the resistance of the wire can increase further, leading to greater heat generation and potential overheating issues. Temperature fluctuations can cause the wire to expand and contract. In high-temperature environments, this thermal expansion can lead to mechanical stress on the wire and its supporting structures, potentially causing damage or failure. High levels of radiation can cause ionization and damage to the atomic structure of the conductor material. Over time, this can result in reduced electrical conductivity and increased brittleness, ultimately affecting the wire's performance. Wires used for power transmission are typically insulated to prevent electrical leakage and ensure safety. High temperatures and radiation can degrade the insulation material, increasing the risk of electrical faults, shorts, and safety hazards. In high-temperature and high-radiation environments, maintenance and repair of power transmission systems become more challenging and costly. Access to these areas may be restricted due to safety concerns, and the need for specialized equipment and personnel increases. The harsh conditions in high-temperature and high-radiation fields can significantly reduce the lifespan of power transmission components, including wires and connectors. This necessitates frequent replacements and upgrades, adding to the overall operational costs. Malfunctions or failures in power transmission systems operating in such environments can pose serious safety risks to personnel and equipment. Electrical faults can result in fires, electrical shocks, and other hazards. High-temperature and high-radiation environments can exacerbate energy losses in power transmission systems. Increased resistance, reduced conductivity, and other factors can result in reduced transmission efficiency. Developing and maintaining power transmission systems capable of withstanding extreme temperatures and radiation levels can be prohibitively expensive. This cost factor often needs to be balanced against the benefits of using electricity in these environments. In situations where power transmission is required in high-temperature and high-radiation environments, it's essential to carefully consider the choice of materials, insulation, and overall system design. Engineers often resort to specialized materials and technologies, such as radiation-hardened cables and advanced insulation materials, to mitigate these limitations and ensure the safe and reliable transmission of electrical power in challenging environments. Nonetheless, these solutions are typically more expensive and may require ongoing monitoring and maintenance to ensure continued reliability.

Wireless power transmission (WPT) offers several advantages and benefits when used in high-temperature and high-radiation fields, such as nuclear facilities, industrial processes, and certain aerospace applications. Here are some of the key advantages:

Safety: In high-temperature and high-radiation environments, safety is paramount. WPT eliminates the need for physical wires, reducing the risk of electrical faults, short circuits, and related safety hazards. This is especially crucial in nuclear facilities where any electrical failure could have severe consequences.

Reliability: WPT systems can be designed to be highly reliable. They can incorporate redundancy and fail-safes to ensure uninterrupted power delivery, even in challenging conditions where wired systems might fail due to physical damage or wear and tear.

Maintenance-Free Operation: Without physical wires, there is no risk of wire degradation due to radiation exposure or high temperatures. This means less maintenance is required, reducing downtime and operational costs.

Flexibility and Mobility: WPT allows for greater flexibility in equipment placement and movement within high-temperature and high-radiation environments. Equipment can be easily repositioned or replaced without the need to reroute or replace wiring.

Reduced Contamination Risk: In nuclear facilities, physical wires can serve as conduits for radioactive contamination in the event of a breach. Wireless transmission eliminates this risk, enhancing overall safety.

Scalability: WPT systems can be scalable and adaptable to various power requirements. They can accommodate changes in power needs without the need for extensive rewiring or infrastructure modification.

Remote Power Delivery: In situations where human access is restricted or dangerous, WPT allows for remote power delivery. This is particularly beneficial in the maintenance and operation of robotic systems used in hazardous environments.

Improved Efficiency: Efficiency is one of the bottlenecks for WPT, especially for long distance transmission fields. Advanced WPT technologies can offer high levels of efficiency, reducing energy losses during transmission compared to wired systems. This can result in energy savings and reduced operating costs over time.

Reduced Clutter: In high-temperature and high-radiation fields, wires can create clutter, making it challenging to access and maintain equipment. WPT eliminates this clutter, improving workspace organization and safety.

Futureproofing: As technology evolves, WPT systems can be updated or replaced more easily than wired systems. This allows for the integration of newer, more efficient technologies without extensive rewiring efforts.

Environmental Considerations: In certain high-temperature environments, such as those found in industrial processes, wires and cables can be subject to wear and degradation, leading to environmental concerns. Wireless transmission reduces the need for these materials, contributing to a reduction in waste and environmental impact.

Aerospace and Space Exploration: In aerospace applications, WPT can reduce the weight of electrical systems, which is crucial for fuel efficiency and payload capacity. For hovering light aircraft, it could be powered indefinitely. These could be used for surveillance and communication relays. Additionally, it eliminates the need for physical connectors that can be susceptible to radiation damage in space.

While WPT offers numerous advantages, it's essential to consider factors such as the efficiency of the system, the distance over which power needs to be transmitted, and potential interference issues when implementing this technology in high-temperature and high-radiation environments. Careful system design and consideration of specific application requirements are key to maximizing the benefits of WPT in these challenging fields.

If one of the WPT methods can be used as a DC motor actuator, the drawbacks of wire power transmission in special occasions such as high temperature and high radiation fields will be avoid. On the other hand, based on this WPT method, the characteristics of the wireless motor actuator would be further researched, in order to meeting the requirements of work conditions.

1.2 WPT method comparison

The most used WPT methods include Acoustic Power Transmission (APT), Capacitive Power Transmission, Inductive Power Transmission, Microwave Power Transmission (MPT), and Laser Power Transmission (LPT). Different methods have different transmission distance and power conversion efficiency. The characteristics of the received and converted power will

affect the effect of the motor actuator. It is necessary to analyze and choose one suitable WPT method to as a motor actuator.

1.2.1 APT

Acoustic power transmission is a captivating field of study that delves into the principles governing the efficient transfer of energy through sound waves. This theory explores the dynamic interplay between acoustic signals and the medium through which they propagate, unraveling the intricate mechanisms that underpin the conversion of acoustic energy into a viable form for transmission. Investigating factors such as wave propagation, impedance matching, and the influence of materials, the theory of acoustic power transmission sheds light on how sound waves can be harnessed and directed to transmit power effectively across various mediums. This understanding not only holds significance in fields like telecommunications and underwater communication but also opens avenues for innovative applications in energy transfer and medical technologies. As we delve into the depths of acoustic power transmission theory, we uncover the secrets of harnessing sound as a potent carrier of energy, unlocking new possibilities for sustainable and efficient power transfer systems.

1.2.2 CPT

Capacitive power transmission introduces an intriguing paradigm in the realm of energy transfer, relying on the fundamental principles of electrical capacitance. This theory explores the concept of utilizing capacitors as a means to efficiently transmit electrical power over distances. Unlike traditional methods, capacitive power transmission operates without the need for physical conductors, breaking free from the constraints imposed by conventional wiring systems. At its core, this theory investigates the interaction between electric fields established by capacitors and the transfer of energy across these fields. Key considerations include optimizing capacitor designs which contain improving efficiency, stability and flexibility, addressing issues related to dielectric materials, and ensuring effective power conversion at both ends of the transmission. Capacitive power transmission not only holds promise for revolutionizing energy distribution but also presents opportunities for applications in wireless power transfer, electronic devices, and beyond. By delving into the intricacies of capacitive power transmission theory, we uncover innovative pathways toward a more efficient, wireless, and sustainable future for energy transmission.

1.2.3 IPT

Inductive power transmission is a cutting-edge concept at the forefront of modern energy transfer, leveraging the principles of electromagnetic induction to enable wireless electrical power exchange. This compelling theory delves into the intricacies of magnetic fields and coils, illustrating how alternating currents in a transmitter coil can generate a magnetic field that, in turn, induces voltage across a receiver coil situated within its magnetic influence.

At its core, the theory of inductive power transmission explores the delicate balance between coupling efficiency, resonance tuning, and the optimization of magnetic fields. This dynamic interplay allows for the transmission of electrical energy over short to moderate distances without the need for physical connections. The applications of inductive power transmission span a wide spectrum, from wireless charging pads for everyday devices to more sophisticated implementations in electric vehicles and industrial systems.

Navigating the nuances of this theory unravels challenges related to distance limitations and technological integration. As we delve deeper into the realm of inductive power transmission, we uncover innovative solutions that have the potential to revolutionize the landscape of power distribution, fostering a future where the constraints of traditional wired systems are elegantly surpassed.

1.2.4 MPT

Microwave power transmission represents a pioneering frontier in the realm of wireless energy transfer, harnessing the transformative potential of microwaves for the efficient conveyance of electrical power across space. At its core, this theory delves into the unique characteristics of microwave radiation, particularly its ability to traverse long distances and penetrate various materials without the need for physical conductors.

The theory of microwave power transmission explores the intricacies of generating, transmitting, and receiving microwaves, unravelling challenges related to beam focusing, transmission efficiency, and safety considerations. It showcases how energy can be harvested, converted into microwaves, and then transmitted to a distant location where it is reconverted into electrical power.

1.2.5 LPT

Laser power transmission emerges as a cutting-edge frontier in the landscape of wireless energy transfer, harnessing the precision and focus of laser beams to convey electrical power across space. This groundbreaking theory delves into the fundamental principles of optics, exploring how lasers can be utilized to transmit energy over distances with unprecedented efficiency.

At its essence, the theory of laser power transmission involves converting electrical energy into laser light, which is then precisely directed to a distant location where it is reconverted into electrical power. This process requires meticulous control over the laser beam, addressing challenges related to beam divergence, atmospheric effects, and safety considerations.

The applications of laser power transmission span diverse fields, from beaming power to remote locations, such as satellites or space stations, to providing efficient and targeted energy for terrestrial applications. This theory represents a paradigm shift in the quest for clean and wireless energy solutions, offering a promising avenue for overcoming the limitations of traditional power transmission methods.

Table 1-1. Comparison of LPT and other WPT.

Method	Radiation	Range	Economy	Power Level	Efficiency
APT	No	Short	Cheap	mW	4%
CPT	No	Short	Cheap	kW	90%
IPT	No	Mid	Cheap	kW	98%
MPT	Yes	Far	Expensive	kW	10%
LPT	Yes	Far	Mid	kW	20%

In order to get rid of the limitations and solve the problems of the wired connection, people resorted to wireless power transmission (WPT) approach as a substitute. The WPT method was firstly realized by Tesla in 1914[1], and its basic principle was laid down[2]. Subsequently, more WPT methods were developed, which include acoustic power transmission (APT), capacitive power transmission (CPT), inductive power transmission (IPT), microwave power transmission (MPT) and laser power transmission (LPT), and the comparison of each method is shown in Table 1-1[3-5]. LPT is regarded as a potential means of energy transmission in the future. The LPT has the advantages of flexible and convenient usage, long distance transmission, and it is safer in harsh hazardous fields. Compared with other WPT methods,

LPT has good power conversion efficiency in the far field, lower device size, and long transmission distance. Hence, LPT is more popular in this research.

The literature[5] has discussed a common workflow of the LPT system. Firstly, the power grid sends energy to the current driver of the laser emitter. Then, the laser driver provides a safe and stable current to the laser emitter. Next, the laser emitter transfers laser energy through the medium, which can be the atmosphere or the optical fibre. Finally, the laser power reaches the photoelectric conversion material (PCM) and is converted back to electrical power. A controller monitors all the processes.

1.3 Project outline and objectives

This project will first review the application conditions of the LPT, which includes the utilization fields, power level and power conversion efficiency. The possibility and the performance of LPT motor actuator have been analyzed from the existing practical application. The motor speed feedback method is the main focused point when the closed-loop control system is built. Subjecting to environmental restrictions, the speed feedback signal would be wirelessly transmitted. Consequently, the wireless signal feedback method will be reviewed. The key parts are the collection and the transmission of the speed signal. After building the LPT motor actuator structure, the simulation is figured out to identify the basic principles of the open circuit system and the performance of the closed-loop system. Based on the simulation results, the proposed system is experimentally verified.

1.4 The purpose of this work

Firstly, the relationship between the incident laser power and the output voltage and current, and the motor speed and the torque will be identified in detail. Then, the motor speed control method is designed to keep the motor speed in aimed value in order to meet the work condition. The open and closed-loop control system will be verified in both simulation and experiment.

1.5 The structure of this paper

Chapter 1 introduces the main idea of this research, and the direction and route of the research content.

Chapter 2 gives a review of the LPT system application history, and its structure. According to the existing technology, the laser powered actuator will be proposed, and the efficiency will be analysed in detail.

Chapter 3 discusses wireless signal transmission and find out a way to feedback the motor speed wirelessly. On the other hand, the collection method of motor speed will also be studied in both sensor and sensorless method.

Chapter 4 identifies the designed system by simulation. The open-loop system is mainly combined of a laser, a photovoltaic material and a DC motor. The open-loop system reveals the steady-state characteristics of the system. By modulating the switching frequency of the laser, a closed-loop speed control system is proposed. And the steady-state characteristics of the closed-loop system are also analyzed accordingly.

Chapter 5 conducts experimental verification of the simulation results and explains the relevant processes in detail.

Chapter 6 is the conclusion part of this thesis, and the future work is given to demonstrate the direction of future research and development.

Chapter 2 A Review on Laser Power Transmission for Motor Drive in Harsh Hazardous Environmental Application

Laser Power Transmission (LPT) is considered a potentially efficient way for power delivery, especially in long distance wireless application circumstances and harsh hazardous environmental conditions. In contrast to other WPT (WPT) methods, LPT has many advantages such as lower device size, focused transmitting direction, high power density, etc. With the development of technology, LPT has been widely adopted in several fields. In conservative industries, the utilization of LPT can resolve the limitation problem in a wired connection. The adverse influence in EMI concerning application and high-temperature field can be reduced. This chapter will give a simple review of LPT, and demonstrate the basic concept of photoelectric emitter, transmission channel, and receiver material. Based on the recent research about diode laser beam combining technology and high-efficiency multi-junction PV materials, the advised LPT devices for simple application as laser power motor will be simply discussed.

2.1 Introduction

Energy utilization has become one part of our daily life. Especially, electricity is an extensive energy, which has been widely utilized in transportation, communication, industrial production, and aerospace. Transmission and consumption of energy have changed human production, lifestyle, and promoted the development of society.

The wire connection has the advantage of conductivity, heat resistance, and corrosive resistance, and has usefulness a variety of products, components and connections around the workplace[6]. With the rapid development of technology, the conventional wired transmission method in many emerging application fields has been subjected to lots of limitations and drawbacks, as shown in Figure 2-1. Under the influence of extremely harsh hazard fields like mines and nuclear stations, or under the influence of high nuclear radiation, high temperature or chemical substances, copper wires are prone to becoming weaker, which increases the risk

of serious fire disasters. In a nuclear power plant accident, it can cause high temperatures of thousands of degrees Celsius. This kind of accident has caused serious economic loss and environmental pollution. Where copper wires are used, a field of interference is produced everywhere around them. Any signal may be affected by this field, which compromises security[7]. Although robots[8, 9] can replace humans in hazardous work, if they are designed to carry batteries that must be charged, environmental risks are unavoidable. Wires and batteries both need to have radiation resistance to ensure highly efficient and safe work, or the risk of fire disaster still exists. Moreover, the wired transmission distance is determined by the length of its own. In very far fields, if the length is not long enough or the terminal cannot be reached by wires, the wired connection fails to work. Copper can be more expensive to acquire since it is reliant on a Latin American system of international commerce. It also does not transfer data nearly as swiftly or far as fibre optics does. This means that copper cable is not economically feasible over long distances where it is required[10].

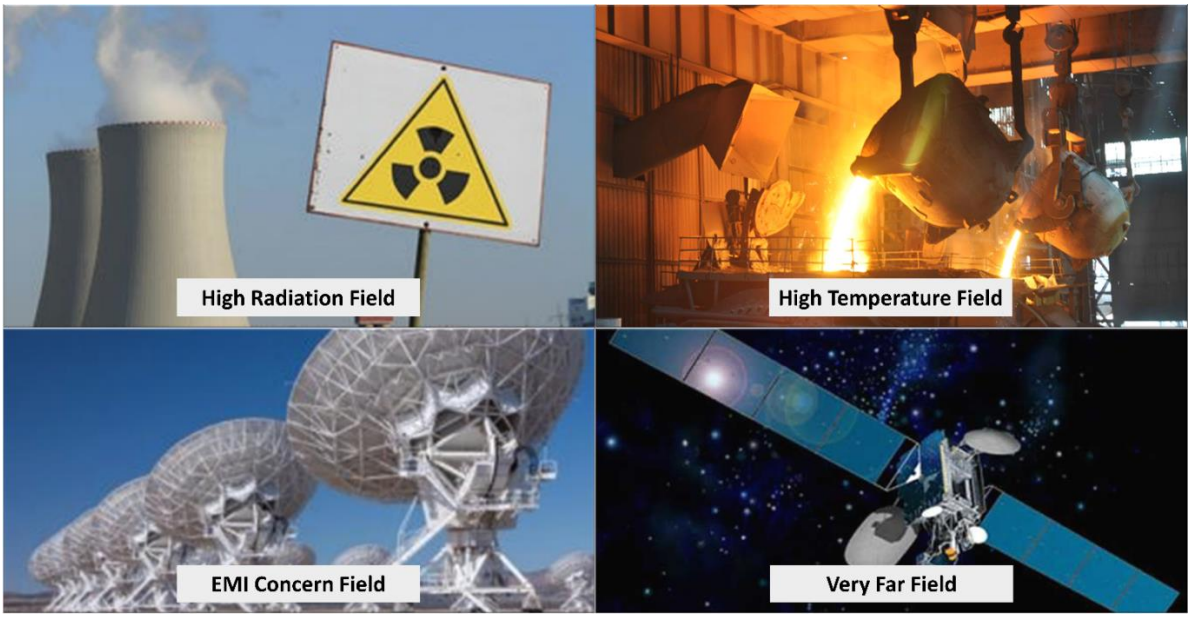

Figure 2-1. Special occasions suitable for applicating LPT replace wires.

WPT (WPT) is a potential method to avoid the wire restriction. In general, some restrictions should be met to implement WPT: 1) Can be transmitted in the atmosphere in an appropriate manner. 2) Can do directional transmission. 3) Can convert energy sources into transmissible energy. 4) Transmitted energy can be converted into usable and required energy types[11]. There are different methods in WPT. Specifically, WPT methods can be classified into two types based on transmission distance: near field transmission and far field transmission. Based on the different power transmission mechanisms, WPT can be divided into four classes:

Capacitive power transmission (CPT), Inductive power transmission (IPT), Microwave power transmission (MPT), and Laser power transmission (LPT). CPT and IPT are near field techniques, and the other two are far field techniques[5]. Considering that LPT has a long transmission distance and large-power output (could reach 5TW[12]), LPT is the suitable choice in WPT.

Laser power has been utilized in several novel areas such as welding and de-icing[13]. Because LPT has flexible workplaces and long-distance transmission capabilities, it can be used to transfer energy to drive the motors, thereby avoiding problems related to EMI, and avoiding high temperature influenced problems of many applications such as deep hole drill in oil industries, aircraft, and robotics, etc. Laser devices have smaller size and easy to implement. Besides, the transmission track of laser is straight, media, and easy to adjust the transfer route. There are two ways for laser transmission: One is tracking through the atmosphere; the other is optical fibre. In atmosphere laser transmission, the power loss should be carefully considered. When transmitted through optical fibre, the power loss would gradually reduce with the transmission distance increased. Typically, optical fibres are made of materials that can withstand high temperatures, so LPT is suitable to be applied in the harsh hazardous situations such as nuclear power plant and high-temperature oil pump.

LPT has many limitations to overcome. The atmosphere is composed of all kinds of gas, such as nitrogen, oxygen, and carbon dioxide. Therefore, if laser travels through the atmosphere or water, there will be different absorption rates and energy losses[14]. If optical fibre is used to direct the laser energy, it can avoid the limitation of laser transmission in various media. It should be considered that one laser emitter may not guarantee enough output power. The recent diode laser-related research is mainly focusing on the multi-diode laser power beam combination technology, which combines the output beams of a set of diode lasers into a high-quality and high-power laser power beam to meet the output demand. Recent research on photovoltaic materials investigates materials with higher conversion efficiency, which also improves the overall system efficiency. The multi-junction GaAs PV materials have higher photovoltaic conversion efficiency than the single-junction GaAs PV materials. Specifically, multi-junction GaAs PV materials can absorb different kinds of wavelength and maximize the light power received. Both technologies are beneficial on improving the LPT system efficiency. And the high temperature would reduce the power conversion efficiency, heat dissipation is necessary.

When the LPT system is used as an actuator, the main point of the research is focused on whether the exiting LPT technology can meet the energy and efficiency demands of motor drives. Therefore, it is necessary to review the LPT system and its components, which is also the focus of this chapter. A general review on the LPT technology and developing level will be given in this chapter. This paper firstly introduces the background and application demand of LPT in section 2.1. Section 2.2 will review the basic model of LPT and recent research progress on each part of LPT including a laser emitter, transmission channel characteristics, and a PV receiver to discuss the optimal application selection. Section 2.3 will discuss and propose an LPT structure and discuss the feasibility of employing LPT for motor drive. Section 2.4 will list the future scope that shows the future direction of improving LPT. The summary will be drawn for the possibility of realizing LPT with the existing condition in section 2.5.

2.2 LPT Review

The basic theory of LPT technology was proposed in 1965 based on the photoelectric effect principle. The structure of LPT is shown in Figure 2-2. On the left side, the laser power supply is used to generate a proper and steady current to Laser Diode (LD). The LD converts electricity to the laser and then transfers it through the channel. The receiver consists of photovoltaics (PV), which is used for absorbing laser power beams to produce current. Besides, a power controller can be added to the system for rectification. All these processes are controlled by a control system.

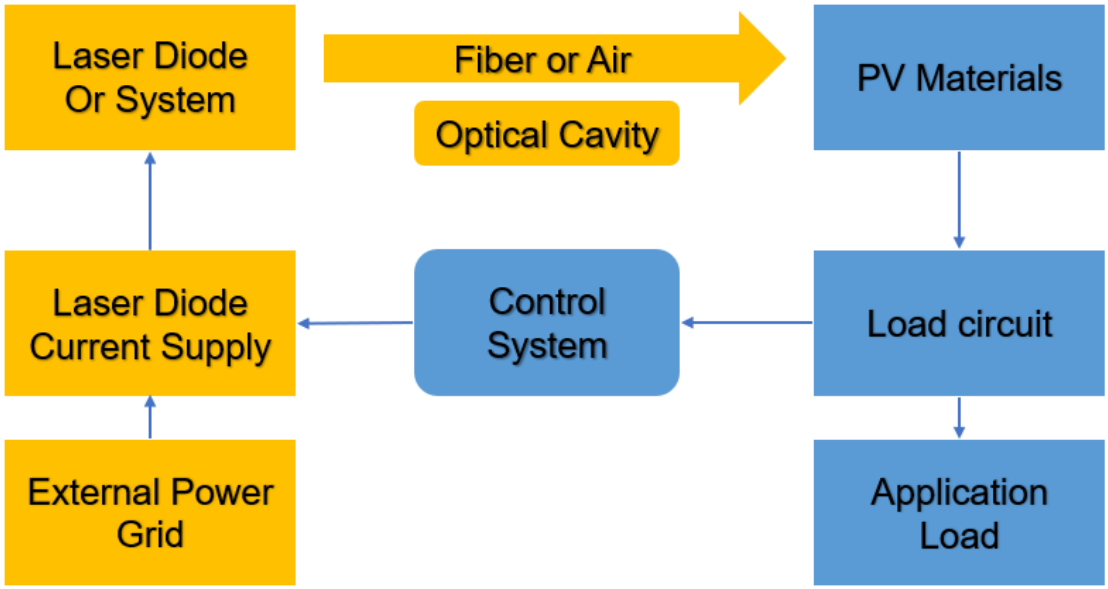

Figure 2-2. Basic LPT Structure.

2.2.1 LPT Application History

LPT is first proposed by NASA for aerospace wireless energy transmission. But due to the limitation of the low convert efficiency in both LD and PV materials, the LPT is hard to apply. In the 21st century, with the developed high-power LD and highly efficient GaAs PV, the LPT technology has gradually been applicated. Many organizations did the LPT experiment and achieved different power delivery efficiency.

In 1985, V.S. Alejnikov et. al. realized the fibre optic laser power transmission, which applied 7W in CO laser and 15W in carbon dioxide laser[15].

In 2002, the EADS Space Transportation facility had an experiment about long-distance laser power transfer on the ground. The experiment used an LD named Nd: YAG, which had 5W output power at the wavelength of 940nm. It provided approximately 1W power for a small car distancing 250m. This experiment proposed the initial application of LPT technology[16].

In 2003, NASA firstly powered micro aircraft by LPT. In this experiment, the aircraft carried a PV material named Ga:InP_2. The Photovoltage conversion efficiency was 17.7% and the diode was 1.5kW adjustable with 50% conversion efficiency. The PV provided 6W of power to a 15m high aircraft and made it fly for 15 minutes[17].

In 2006, the Kinki University initiated the LPT powered micro aircraft study. The chosen laser power was 300W. They achieved 25% transfer efficiency using the GaAs materials and converted 40W power. The aircraft in their design can fly for 1 hour at 50m's high[18].

In 2008 and 2011, D.E.Raible in Cleveland State University introduced the relevant LPT technology, which provided theory support for the real application[19].

In 2009, the US Laser-Motive company experimented with the feasibility of driving the elevator by LPT. The laser power was 1kW. Transfer distance was 1km and total system efficiency was more than 10%[20].

In 2011, Duke University began the research on LPT in the aspect of safety transmission. According to IEC 60825-1, the maximum amount of laser radiation to the human body is relevant to time and wavelength. Commonly, shorter radiation time or higher wavelength is safer for the human body. Thus, Duke University selected 1400nm LD and GaSb PV materials

to form an LPT system successfully to supply power for a telephone in 4m distance[21]. Besides, Chongqing University built a laser power supply network to supply power for a wireless sensor network. The selected 1064nm pumped laser diode can output 3W power with 15% conversion efficiency[22].

In 2013, Tsinghua University proposed a feedback resonance method for laser power transfer. The reflected photon of PV arrays is used to stimulate the emitted photon again, which increased the total transmission efficiency from 4.7% to 6%, comparing with no cavity[23].

In 2014, the Beijing Institute of Technology proposed a type of GaAs PV material that can afford 60 times of standard light irradiation. Then based on this optimal PV material, a 100m LPT experiment was carried out. The results indicate under the irradiation of 793nm laser, the conversion efficiency of PV material was 40% for 24W input laser power, and the total system transfer efficiency was 11.6%[24]. At the same time, Shandong Aerospace Electronic Technology Institute did a verification experiment for LPT to aircraft. The system employed LD with the wavelength of 810nm, laser power of 28W, and the maximum 200m transmission distance to achieve the 15% of the total system transfer efficiency[25].

In 2016, Russian Energy Rocket Space Group Co. Ltd successfully charged one telephone 1.5km away. The experiment device converted laser power into electrical power with 60% transfer efficiency[26]. Besides, Dele Shi et al. in Shandong Institute of Aerospace Electro-technology conducted an onboard experiment on the LPT subsystem. The transmission distance was from 50 to 100m, and the input voltage, current and power were 22V, 4A, and 88W, respectively. The result shows that the received power was 13.43W, and the maximum efficiency was 16.08%[25].

Recently, in 2021, Ali Mohammadnia et. al. studied laser power transmission technology in driving next generation drones. The PV materials were equipped on the drone to receive laser power. The experiment had adopted three different types of PV materials: GaAs, CdTe, and c-Ti PV materials. They received the power of 73.5, 62.6 and 33.2W, respectively. In the transmission distance of 500m, it had the total power transfer efficiency of 12.5%[26].

From the above research, there has been an application supplied by the existing LPT technology. But the system energy transmission efficiency is generally low. The conversion efficiency of LD and PV materials is the main reason that cause the total system power delivery down. However, improving transmission efficiency is still the key breakthrough direction of

the LPT system for supplying sufficient and stable current to the load, and both transmission efficiency and conversion efficiency needs to be improved.

2.2.2 Laser Emitter

Laser emitters play a role in converting electricity power into laser power in LPT technology. The most common type of laser emitter is LD, which uses the photoelectric volt effect of the PN junction to work. The output power efficiency of LD is changed by changing the supply current of the laser power source. The power efficiency of one 975nm LD coupled with fibre optic is shown in Table 2-1. The output power and conversion efficiency of LD is often increased with the supply current raise, but the raise speed of conversion efficiency will decrease. The experiment result studied in literatures[27] have proved that the LD supplied by pulse wave current can achieve better efficiency than that supplied by constant current. As shown in Figure 2-3, the power conversion efficiency will be higher when the duty cycle *D* is lower, since the power density is higher.

Table 2-1. The power of 975nm fibre-coupled with LD[28]

Current J/A	2	3	4	5	6	7	8	9
Laser power P/W	7.6	12.8	18.0	22.6	27.3	31.8	35.9	39.8
Laser power density mW/cm²	26.5	44.6	62.8	78.8	95.2	110.9	125.2	138.8

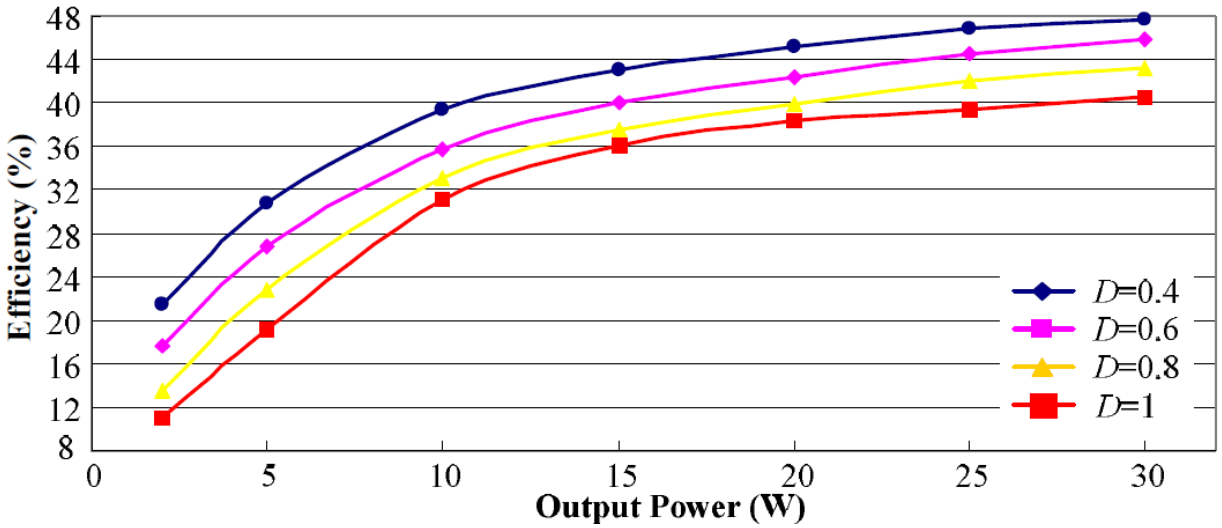

Figure 2-3. Efficiency of LD powered by Pulse wave current supply[27]

Recent research has shown interest in the diode laser combine technology. In this method, all the outputs of every single laser diode are combined into one laser power beam, which obtains

high brightness, high beam quality, and high-power density. For the combined output laser power beam, it ensures to satisfy the demand of power for ending machines that a single laser diode cannot meet. The different systems may have different power perimeters and designed power structures. The output power of these examples is varying from watts to kilowatts. These studies are reviewed as follows:

There was much research done in 2013. M. Röhner et al. present the radiance model of laser diode and how the radiance influenced the power density. The result show that the laser beam combining technology does not increase the radiance more than the initial value. The example used a 200W system model with a 7+1 combined source to pump 400um fibre[29]. H. Zimmer et al. have researched the direct diode laser system which can reach the output power for several kilowatts by applying Beam combining technologies. As the result of using this on the low power laser bars for 6-7 W each, the beam quality has improved by 30%. After that, they improved the laser bar output for 120W and combined 12 such laser bars at 1.4kW for the output of the system and the conversion efficiency was more than 50% in this process. Finally, they designed a 6kW direct diode laser TRU-Diode 6006 which can match output for 4-5kW. This research has proved the spatial and spectral beam combining technology can realize high-brightness multi-kilowatts output laser beam for high command applications from single low power laser emitters[30]. A. Unger et al. described one project named BRIDLE, which aimed to build a direct diode laser system to reach the output for greater than 2kW and efficiency for more than 40% for industry application. If constructed by carbon dioxide lasers, the efficiency can be no more than 20%. Fibre laser was grown well in such application, for it can realize the optical conversion efficiency for 80-85% and the total power efficiency for 30-35%. In a block of the BRIDLE, the single emitter was up to 10W and the total output for this block was 120W in total[31]. T. Brand et al. designed a platform of diode lasers for industrial application at the multi-kilowatts level. The system fibre laser source pump needed 200W power and it had 7 laser bars to combine the one output source. In such system design, they adopted NA 0.22 fibre, which is only 200um. To couple with this fibre, they built a base subunit that contained 5 laser minibars, which satisfied the demand of shape, small size, and laser amount. This unit can give the output for up to 260W, with the current of 40A in central wavelength at 976nm. The photovoltaic conversion efficiency was 52%. To design a high-power system, the system which combined with 4 base subunits was at 800W in a central wavelength of 976nm. For eight base units combined system, the output can reach 1500W. This system can work at five modules in different central wavelengths, which were 915, 940, 980, 1020, and 1060nm. If the current was

45A for each laser minibar, the output could reach 4kW[32]. M.A. Helal et al. did simulation on the laser beam propagation routes and characteristics in the large cavity. They combined several laser diodes to reach a total output of 100-1000W. The basic structure of the high-brightness system was described. The system was contained several diode lasers, which can be single or a group of a laser diode or laser bar. Before the output laser power beam of every single emitter was combined by optical devices, they needed to be collimated with optical collimation devices. In a high-power system, a large volume of the cavity was needed. The output of the beam assembly phase must be ultimately focused on the fibre through further optics. The simulation process was made by software instrument, as Zemax and Speclase. The result showed that the most of beams were coupled into output and some back to the laser diode, and the scatter ray remained was the power loss. The challenge was converting the feedback laser power beams into utilization to reduce the power loss[33]. U. Witte et al. demonstrated one type of high brightness diode laser module which used for pumping applications at the red spectral range. Different types of solid lasers were made of different materials, which needed different beam wavelength of the laser source. As mentioned, the Nd: YAG needs 808nm, the Yb: YAG is 941nm and the Yb3+ doped silica is 975nm, respectively. Seven single emitters were stacked vertically in a ladder shape. The block can reach output for 15.5W with the optical-to-optical conversion efficiency was more than 95%. The factors of power loss were mainly diffraction caused by lens aperture and reflection by the surface of the lens[34]. From the research by Stefan Hengesbach et al, DFB/DBR diode laser module designed by spectral multiplexing was the most efficient way which built on VBGs. The combined multiplexing could reach 97%. There were two concepts of the multiplexing method mentioned. One was Dense Spectral Combining technology, which limits the spacing of the centre wavelength of 4nm. The other was Wavelength beam combining technology, which combines the stable frequency in the external cavity with the diffractive element. The system was designed based on BRIDLE-Project. Five emitters were made one group of bars. The result showed that the multiplexing efficiency in single mode was 97%, and in multi-mode was 85% [35]. The cavity was the important part of the diode laser to deal with the problem of feedback laser power beams. Super large volume cavity studied by S. Bull, S.N. Kaunga-Nyirenda and E.C. Larkins showed the points of how to design this external cavity of diode lasers. As mentioned, both spectral beams combining and coherent beam combining could be adopted in this application to produce high power and good beam quality beam, and duly handle the feedback into the laser. They concluded that not all the laser diode was suitable for equipped a

cavity. Larger was better but would be something wrong in high-order mode. The system stability and efficiency should be considered when designing[36].

In 2015, Dan McCormick et al. shown one type of Diode-pumped alkali-vapor lasers, as the DILAS has grown a source of a laser diode which outputs 2.5kW of fibre optical power at an almost central wavelength at 766.5nm. The 90% was distributed in the power enclosed spectral linewidth. Also, the central wavelength could be controlled in a range of ±0.15nm. Such technology has been applied in fields for different wavelengths and styles, and the power varied from hundreds to thousands of watts[37]. There was one type of fibre-coupled diode laser demonstrated by Ulrich Witte et al. The output could reach 10W and up to 100W. A method called dense wavelength division multiplexing (DWDM) was applied to combine a 5-emitter narrow stripe broad area mini-bar. It used fibre combiner and coarse wavelength beam combining to design this system. In such a designed system, the current supplied to injection was 40A and the measured optical power was 53.2W. The 32.2W was the output power produced by DWDM. The calculated combine efficiency was 60%[38]. The process of high brightness direct diode laser at kilowatts level has been researched by Robin K. Huang et al. The first generation of lasers was carbon dioxide and YAG lasers, which had a small size. As for the second generations were fibre laser and disk laser, they had the benefit of better efficiency. And the third generation was the direct diode. The industrial turn-key 4kW laser system was shown. The system power conversion efficiency was 44% under power for 4kW, at a driving current of 180A. The max current can be 220A, and power can reach 4680W[39]. H. Zimer1 et al. researched a thin-film filter for dense wavelength beam combining technology. The result showed that the output obtained was 550W with electrical to the optical power conversion efficiency of 40% above, which was 10% lower than free direct laser diode. Compared to solid pumped lasers, the direct laser diode had better conversion efficiency and lower cost [40]. There was another high power and high brightness diode laser system in multi-kilowatt level presented by Victor Rossin et al. They adopted broad area diode lasers at a power conversion efficiency of 50% with fibre-coupled modules. The conclusion showed that the improvement can reach 30% of the current generation model for multi-emitter mode[41].

The Distributed Bragg Reflector (DBR) ridge waveguide (RW), which had wavelength stabilized for special pumping application, was demonstrated by Bernd Sumpf in 2016. Tapered laser was the famous way to produce high-power low-diffraction limited beams. For

DBR tarped lasers, they had 12.2W output with 40% conversion efficiency at 25℃under a wavelength of 1064nm[42].

In 2017, Klaus Kleine and Prabu Balu proposed the materials processing powered by the high-power diode laser system. When using solid-state pumped laser systems, the high-power diode lasers were utilized as the pump source. Over 90% of the diode lasers' output was going for the pumping process of the solid lasers and the last small part of the power was directly for materials processing. They combined these emitters or several groups of emitters into one fibre to increase the total output. In the system they were mentioned, a type of stack which was consisted of several laser bars can reach outputs for 50-400W. Then, the combined laser power beam of these laser bar stacks can realize the output power in kilowatts [43]. Meanwhile, Gaëlle Lucas-Leclin et al. discussed the coherent beam combining technology. In on-axis diffracted order, the maximum output power was 7.5W with the beam combining efficiency of 65%. For the power amplifier, five tapered laser bars were combined in a group. The results proved that the beam combining efficiency was 82%, at a supply current of 3A, and it can reach 72% in the maximum current of 6A. The maximum output power was 11.5W [44]. Laser was the new tendency of the way for lighting, replacing existed LED.

In 2019, Anastasiia krasnoshchoka studied two different laser diodes for generating white light. For power concern, the single broad area laser diode can have output for 3.5W at a wavelength of 445nm. The other was a group of blue diode lasers with 8 inside. The output can reach 35W at 450nm. The spot size can be adjusted[45].

From all the research list above, the output of current supply will influence the power efficiency of the LD. If the LD works in a high pulse and low duty cycle state, the power requirements are also very high, especially in accuracy and stability. That will be one limitation of the efficiency improvement. However, the use of efficient power supplies also contributes to the efficiency improvement of LD. Laser power combination technology can be an effective and feasible method to improve the total output power and to meet the demand of the terminal load. The combination efficiency is generally acceptable for the application. But combination system design will increase the complexity of devices, that will cause inconvenient for use. Diode lasers can be considered when a single LD power is insufficient. The challenge of LD is the manufacture technology development.

2.2.3 Transmission through atmosphere

The wavelength between 3-4um or 8-14um is transparent, but laser transfer efficiency in the respective region is low. The range of 780~1100nm can be the window for existing laser power devices to transfer power adequately, as shown in Figure 2-4.

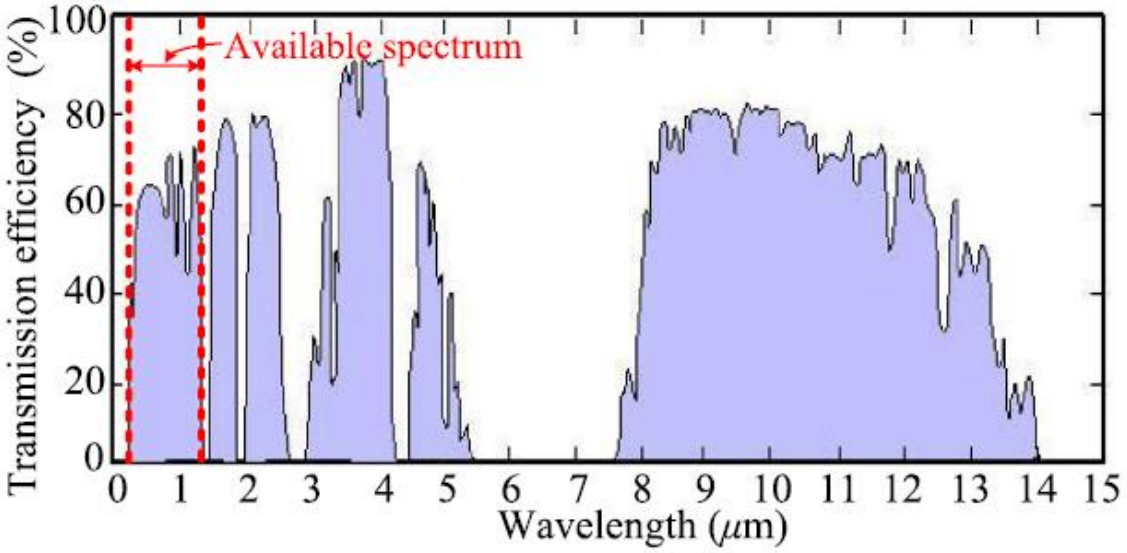

Figure 2-4. Atmosphere transmission wavelength absorption[5]

The observed result of LPT in the atmosphere was studied in literature[14] along with Moderate-resolution atmospheric Transmission (MODTRAN) code-based simulations. The data is collected maximum at 2050nm. This result shows the transparency window from 2025 to 2100nm and below 1960nm the power will be strongly absorbed. This experiment was limited to the low power circumstance between 1W and 10W.

Solar energy outside the earth is attractive to make electricity production. Literature[46] studied the self-focusing of the laser beam in the atmosphere, which helps to assist in delivering powerful laser beams. If the power of beams exceeds the standard self-focusing power, the uncontrolled beams may cause disaster for devices.

When the laser beam is transmitted to the target, a portion of the energy is absorbed by the atmosphere[47]. There are two important influences for laser power transmission. One is the power intensity of the laser will be weaker, which results in a reduction in transmission efficiency. The other more important one is that the atmosphere absorption will heat the channel for LPT. The shape of the laser beam will get distorted, which creates the thermal halo effect. This will further increase the divergence of the laser beam and reduce the intensity. The

relationship between the thermal halo effect and the laser power intensity distribution is nonlinear.

When the laser tracks through the air, atmospheric gas molecules and aerosol particles will absorb and scatter light waves, and then cause the attenuation of laser energy. Laser energy absorbed by the atmosphere per unit volume can be expressed as (2-1):

$$E(z) = \alpha I(z) = \left(\alpha_{ma} + \alpha_{pa}\right) I(z) \tag{2-1}$$

$\alpha_{\_ma}$ and $\alpha_{\_pa}$ are the gas absorb coefficient and the aerosol particle absorb coefficient, respectively. I(z) is the light intensity. The attenuation of the laser caused by absorbing and scattering can be generally presented by the deer theorem. Its differential expression is in (2):

$$dI(z) = \alpha_t(z)dz = \left(\alpha_{ma} + \alpha_{ms} + \alpha_{pa} + \alpha_{ps}\right)dz \tag{2-2}$$

α_{ms} and α_{ps} are the gas scattering coefficient and the aerosol particle scattering coefficient, respectively.

The relationship between the wavelength and absorb is very complex and irregular. A suitable wavelength selection for laser power transfer is important. In addition, the absorption coefficient is constantly changing along the propagation path. When using LPT for short distances, air transmission will be very convenient if nothing stands in the transmission route. Otherwise, laser energy will attenuate as the distance increases. The propagation path will also be offset due to refraction. The challenge is to overcome the power loss and transmission route bending as the distance increases.

2.2.4 Transmission through optical fiber

The key to the realization of optical fibre energy transmission technology is the energy transmission fibre. It has the characteristics of low transmission loss, high damage threshold, and high-temperature resistance. Thus, it can reliably transmit energy in all kinds of extreme environments. When designing the transmission system, the input laser power efficiency, the fibre optical material, and core diameter will be considered. The energy attenuation should be measured. A high energy density laser beam will cause damage to the optical fibre end face. Two aspects are considered in literature[48]: 1) Optical fibre material choosing: Optical fibre materials with low scattering loss should be selected. The material which contains transition metal and OH group has small absortion loss and stable material structure. 2) Optical fibre

structure: The design of a large core diameter is beneficial to reduce the laser power density inside.

The core diameter of single-mode fibre is approximately 2-12um. When the laser is transferred in high power density, the larger size core diameter will be used, because it will influence the performance and life of fibre optic. The laser damage threshold was measured at US Sandia National Laboratories[49]. The result was 215J/ cm^2 that processed by carbon oxide and was 185 J/ cm^2 that not processed by carbon oxide. literature[50] discussed the limitation of the optical fibre transmission that depends on the parameters of the laser power beam, including laser beam diameter and divergence angle. When the laser beam transferred through the fibre, the beam diameter shall be smaller than the fibre diameter. The divergence angle shall not too big, for the beam reflection of the cladding and end face would cause crosstalk to the beam quality.

However, in high-radiation environments, radiation-resistant optical fibres made by special processes must be used to ensure transmission quality. The radiation emitted by nuclear waste can affect the transmission characteristics of optical fibre. This is due to the damage caused by high-energy radiation to the chemical structure of the optical fibre. When fibre-optic transmission is used in a nuclear waste machine, resistant-radiation fibre is needed to ensure the transmission quality. Loss and dispersion are the main parameters for characterization of optical fibre performance. The loss can directly determine the attenuation of light wave energy [51]. The main component of common quartz fibre is silica. When irradiated, the lattice structure of the optical fibre will change. Both the physical and chemical properties of the optical fibre are changed by defects in the lattice. There are three mechanisms that cause changes in optical fibre performance: 1) Radiation-induced absorption (RIA), performing as the absorption of the transmission light by the fibre. 2) Radiation-induced emit (RIE), performing as irradiated optical fibres produce light waves in certain wavelengths. 3) Optical density (the refractive index of the irradiated fibre changes). Among these three mechanisms, RIA is considered to be the main cause of fibre performance decline [52]. This damage will greatly produce the loss of optical fibre. Moreover, the diameter of fibre determines the radiation loss. The experiment shown in literature [52] indicated that with the diameter increased, the loss would decrease. And if the wavelength increased, the loss would reduce.

The methods to improve the resistance radiation performance of optical fibre mainly include resistance radiation design of optical fibre waveguide structure, proper doping of fluorine

element, effective control of manufacturing process, application of peroxide doping technology, pre-irradiation treatment and post-irradiation treatment technology application [53]. Literature [54] proposed a specific way to increase the re-sistant radiation of fibre. First, pre-irradiate the fibre to destroy the part of the easily activated free radicals, atomic defects or loose bonds in fibre, and bond to a stable bond at high temperature. Then by light-fading and hydro-genation process, this process will restore or repair the induced absorption caused by the structural defect of the optical fibre. Finally, deuterium gas treatment is used to reduce the additional loss caused by hydrogenation. Light-fading treatment mainly refers to that under high-intensity laser irradiation. The defects centre of a substance ab-sorbs one or more photons, which will produce free electron heating and self-focusing effects, thereby improving the defect structure of the substance. The low-temperature treatment of liquid nitrogen is mainly to reduce the activation energy of the material, to make the molecular arrangement of the material more orderly, and to reduce the number of internal defects in the material. The experiment process is to intercept the 2.8m polarization-maintaining optical fibre (PMF) after the pre-irradiation treatment of 1.0kGy, and then use a monochromatic laser light source with a wavelength of 980nm and an output power of 100mW to irradiate for 30min. Next, treat the optical fibre with liquid nitrogen for approximately 10min. After the polarization-maintaining fibre is pre-irradiated with 1.0kGy, its loss is greatly increased. Then, through the 980nm laser light-fading treatment on the irradiated fibre, its spectral loss increases a lot, but the signal-to-noise ratio of its loss spectrum is obviously better. Then, after liquid nitrogen treatment, its spectral loss will be greatly reduced, and it is lower than the pristine PMF spectral loss. It shows that the method improves the microstructure of the material and effectively reduces the loss.

Dropping to change the crystal structure of the fibre can also improve the resistance radiation. Literature [55] and [56] have studied the radiation resistance of erbium-doped fibre. The optical fibre doping can change the refractive index of the optical fibre, thus changing the transmission characteristics of the optical fibre. By erbium doping combined with high pressure hydrogen treatment, the RIA is reduced in the experiment measure result. Different doping also results in different radiation resistance. Literature [57] tested the germanium doped (Ge-doped) multi-mode fibre and the fluorine doped (F-doped) radiation resistant standard multi-mode fibre. The experiment result indicated that the F-doped fibre has an obvious effectiveness in light fading than conventional Ge-doped fibre.

Something else worth mentioning is the colour centre, which is produced when the electron energy is higher than the atomic dislocation threshold in silicon dioxide. According to previous studies, the total dose ionization damage effect will not cause permanent damage to optical properties of the fibre. At room temperature, after the irradiation is stopped, the colour centre of the fibre fades after a period. There are many high-energy defect structures in silica fibre. These high-energy defects often form colour centres after being irradiated. The electro-negativity of fluorine is the strongest (stronger than oxygen). Doping with fluorine can produce Si-F bond in the fibre, increase the probability of breaking the network of high-energy defect structures, and reduce the defect concentration in the quartz glass. The light-fading has the opposite effect of radiation, to fix the defects in the lattice. During the process, the light power is higher, the effect of light fade is higher. And the function to reduce the radiation loss is more effective [53].

When laser power transmitted through the optical fibre, the route could be organized in a proper way and the power loss would be lower than atmosphere transmission. But the flexibility in use will be reduced. Especially in high radiation and high temperature environment such nuclear station, the radiation resistance of fibre will directly influence the transmission power quality. The challenge is how to reduce the power loss in long distance and increase the radiation resistance.

2.2.5 PV materials receiver

A suitable photovoltaic conversion material is very important for absorbing laser energy and improving system efficiency. There are hundreds of materials are developed, but the most common photovoltaic materials are Si and GaAs. The main parameters are shown in Table 2-2. The significance of the cut-off wavelength is that it can be used to describe the ability of a material to absorb light. Before the cut-off wavelength, the material absorbs light, but after the cut-off wavelength, the material no longer absorbs light. Silicon is a very common substance, and its production cost is low. But the transfer efficiency is also low due to its sensitivity to 950nm wavelength, and 950nm is not sufficient to deliver power through the air. Because of the breakthrough of the Photoelectric transfer rate of GaAs PV mate-rials, the Laser power transfer energy can have rapid development [58]. The 810nm of best power efficiency of GaAs, which is suitable for LD's wavelength 860nm. During the process of the photoelectric transfer, the power loss includes laser power transmission loss and photo-electric transfer loss. Table 2-

3 has shown the power transfer efficiency in different PV materials. The decibel is a unit of magnitude, expressed in dB, and is defined as "the magnitude difference between two similar power quantities or analogous power quantities when the common logarithm of the ratio of the two is multiplied by 10 to equal 1". The material with a large bandgap has a high upper limit of conversion efficiency, but the loss in optical fibre transmission is larger. This is contradictory for material selection.

Table 2-2. Main parameters of PV materials[59]

Materials	Absorb peak wavelength	Efficiency (%)	Radiation intensity (kW/m²)
GaAs	810nm	40.4	60
		53.4	430
		60	110
Si	950nm	28	110

Table 2-3. The relationship between material bandgap and cutoff wavelength and transmission loss [60]

Materials	Eg(eV)	Cutoff wavelength(nm)	The upper limit of single-junction conversion rate	Losses in standard optical fibres	The light intensity decays to 10%
GaAs	1.42	873	60%	2.5dB/km	4km
$In_{0.35}Ga_{0.65}As$	0.95	1310	45%	0.5dB/km	20km
$In_{0.47}Ga_{0.53}As$	0.74	1550	35%	0.2dB/km	50km
$In_{0.7}Ga_{0.3}As$	0.55	2200	22%	2.2dB/km	5km

GaAs is a typical III-V compound semiconductor materials, although it has the same sphalerite crystal structure as silicon. However, unlike silicon with an indirect bandgap, GaAs is a direct bandgap material, and it has a bandgap width of 1.42eV, which is the best bandgap width that PV materials need. Because GaAs has the best power conversion efficiency that promotes the development and practical application of the LPT system, it has a very outstanding advantage in the application: 1) Direct bandgap structure. GaAs has large light absorb factor; they can quickly absorb the incident light. GaAs can achieve a lower size of devices, for it can absorb 95% of sunlight only needs 5~10um, which is just 10% of silicon materials. 2) Good radiation resistance. The lifetime of minority carriers produced by direct bandgap GaAs is short. Especially in aerospace, the influence of GaAs is lower than that of Si. 3) High-temperature resistance. GaAs materials have a lower temperature coefficient, can adapt to higher working temperatures. 4) High photovoltaic conversion efficiency. Because GaAs have a wider bandgap and better match the sunlight [61].

The power conversion efficiency improvement is the main development direction of the PV materials. Many institutions have made progress in this direction. A three-junction gallium arsenide solar cell developed by Spire Semiconductor achieved a peak efficiency of 42.3%. The latest ground-based solar cell, the C3MJ+, developed by Spectro-lab, a Boeing company, has an average photoelectric conversion efficiency of 39.2%. Japan's Akita University developed an organic material that can convert ultraviolet light into visible light and is transparent to visible light. It used ultraviolet light that solar cells cannot effectively use for photoelectric conversion, thus improve the efficiency of photoelectric conversion. Wake Forest University in the United States increased the amount of sunlight collected by covering the polymer matrix of the cell with a vertical layer of optical fibres as a sun-trapping device. This layer of fibre protrudes from the surface. Sunlight can enter the top of the fibre from any angle, and photons bounce around the inside of the fibre until they are absorbed by the surrounding organic cells. Genie Lens, a US company, developed a polymer film with an embossed microstructure that redirects incoming light and increases its chance of being absorbed. The film can be simply placed on the surface of solar panels to increase their output power. Stanford University has developed a simple and inexpensive way to create large areas of nanoscale textured structures. Researchers precipitated metal and amorphous silicon onto uneven surfaces to create superhydrophobic surfaces and proof-of-concept solar cell devices. The solar cell absorbs 42 percent lighter than a flat surface using the same amount of material[62].

Some research improves the power conversion efficiency of the PV materials concluded in [61]: Yugami et al. chose an 808nm diode laser with an output power of 1W radiate on single-junction single-chip GaAs material. In the area of 4cm², the power receipted is 5W with transfer efficiency could reach 51% [63]. Steinsiek chose the Nd: YAG with 532nm wavelength and 5W output power to drive the small car equipped on an InGaP material. The transmission distance was 300m and PV material power conversion efficiency was 25%[16]. Japan Kinki University chose the output power of 200W with 808nm wavelength laser diode to irradiate the PV materials on the kite fly machine. The PV materials were made of 8 GaAs PV batteries with 28 cm² each. The 0.017W electrical power was gained from the unit area and incident photon-to-electron conversion efficiency was 21% [64]. NASA put the Silicon-based PV materials onto the space elevator, utilizing the telescope system to transmit 1030nm wavelength and 8kW power continuous laser, irradiating on the Silicon-based PV materials to drive the space elevator. The Silicon-based PV array which was comprised of 333 monocrystalline silicon 1m² chips was realizing the power conversion efficiency for 35% [65].

Single junction PV materials have better power conversion efficiency. But they could only absorb one certain wavelength and afford the weaker brightness of incident light. The electrical power gained from the unit area is smaller. This is not conducive to reducing the size of the receiving device. To improve the overall photoelectric conversion efficiency of the material, considered a different type of PV materials could absorb a different certain wavelength of light, people combine different III-V materials according to different bandgap width, to gain the multi-junction PV materials. This material can absorb many different wavelengths, to improve total power conversion efficiency. For InGaP/AsGa/Ga three-junction PV material, its photoelectric conversion efficiency is higher than that of ordinary materials. Still, efficiency will need to be improved to accommodate LPT's evolution. The relevant research is already underway mentioned in [61].

In 2000, Boeing-Spectrolab realized the conversion efficiency at 32.4%, under 372 times the concentration. In the same year, the Shanghai space power supply institute, the ministry of information industry, and other units have also carried out the corresponding research[66-68].

In 2006, Japan Kensuke Nishioka has studied the electricity character of InGaP/AsGa/Ga three-junction PV material which changed due to the incident light brightness and temperature. In this lab, the open-circuit voltage, the short circuit current, the fill factor, and power conversion efficiency were concerned. The brightness range of the incident laser was 1~200 times sunlight, and the material temperature range was 30~240℃. The lab results showed that when the temperature stayed constant, with the incident laser brightness increased, the open-circuit voltage, the short circuit current, and power conversion efficiency would be increasing too. If the brightness stayed constant, with the temperature increased, the open circuit, the fill factor, and the photovoltaic conversion efficiency was decreasing, but the short circuit current was raising [69, 70].

In 2009, American researcher Geffrey S. K et al. have studied the C1MJ and C2MJ three junction GaAs mate-rials' electrical property, under the temperature range of 0~120℃ and incident light range of 1~1000 times sunlight. The result showed that the increase of the incident light brightness would be due to the fill factor and photovoltaic conversion efficiency firstly raising then down. The temperature increasing would cause the fill factor and photovoltaic conversion efficiency decreasing. When the temperature was constant, the peak was located on the 200 times sunlight, and the photovoltaic conversion efficiency peak was under 500 times sunlight[71].

In 2010, the researchers at Hebei University of technology have tested three junctions GaAs PV material to successfully gain the significant electrical parameters. The experiment has measured the maximum photovoltaic conversion efficiency was 22.24%, and the maximum output power was 23.56W, under the condition of 500 times sunlight. Also, once the temperature was raising 1℃, the short circuit current reduced 1.9mA[72].

In 2012, the research on the three-junction GaAs photovoltaic electrical parameters by Yunnan Normal University has shown that under irradiated by 676 times sunlight, the single three-junction GaAs material's short circuit current was 322 times theoretical result, the peak power was 316 larger than the theoretical value, the fill factor and material efficiency was reducing 4.6% and 3.9, respectively, comparing to the theoretical mode[73].

In 2013, the University of Shanghai for Science and Technology successfully built a three-junction GaAs mate-rial mathematic model and theoretically analysed the influence on the electrical characteristic by changing the inci-dent light brightness, and realistically measured the open-circuit voltage and material efficiency changing rule. From the result known that the increase of incident light brightness would aggrandize the open-circuit voltage and conversion efficiency. With the temperature increased, the open-circuit voltage and conversion efficiency decreased[74].

In 2015, Henning Helmers et al. studied how the different temperatures or incident light brightness influenced the GaAs PV materials. During the experiment process, the temperature range was 5~170℃ and incident light brightness was 1~3000 times sunlight. The three-junction GaAs PV materials based on Ga would reduce efficiency under the high-temperature environment, as shown in the result[75].

In 2016, O.Hohn et al. researched under different temperatures that how the laser wavelength influenced the three-junction GaAs PV materials. The result indicated that at a certain temperature, using a certain wavelength of the incident laser and irradiated by matched mixture lasers with the bandgap width of all the subdivision of the GaAs PV materials, which can improve the photovoltaic conversion efficiency[76].

In 2018, Mingzhu Han et al. from Nanjing University of Aeronautics and Astronautics studied different proper-ties of incident lasers that influenced the efficiency of InGaP/GaAs/Ga three-junction PV materials. The experi-mental result indicated that with the property of 7:8:5 with

the incident lasers' wavelength of 532, 808, and 980nm, respectively. The power conversion efficiency was 33.549%, which was the maximum value[61].

Recently, in 2020 Nikolay A et. al. studied the optimization of InGaAs PV material which could achieve the power conversion efficiency more than 50%, with the incident laser wavelength of 1064nm [77].

Table 2-4. Power conversion efficiency of different types of PV materials

PV materials	Si	Single-junction GaAs	Two-junction GaAs	Three-junction GaAs	Multi-junction GaAs
Efficiency	23%	27%	30%	38%	50%

Through the above research, From Table 2-4 it can be confirmed that GaAs material is the first choice of photovoltaic materials. It has the highest photoelectric conversion efficiency at present and has a small device size and convenient application. Moreover, the multi-junction GaAs material can adapt to multi-wavelength laser irradiation, thus reducing the requirements of the emitter and increasing the energy efficiency. The challenge of PV material is to increase the photovoltaic conversion efficiency and optimize the cell arrangement to reduce the internal power loss.

2.3 Discussion

After reading the previous literature, the author found two imperfections. One is that some application experiments only achieved the LPT to supply power to a certain application, and simply measured the parameters of the power transmission. The efficiency improvement of LPT was not further studied. Existing review articles have introduced the development of the overall system and each device in detail and listed some high-efficiency devices and methods to improve efficiency. However, the proposed devices and methods lack practical application cases, and their applications in complex environments have not been explored.

Compared to other WPT (WPT) methods, LPT has outstanding advantages in motor drive. Capacitive power transmission (CPT) and Inductive power transmission (IPT) are called near-field WPT, which have widely used in the new energy source bus charging, mobile phone charging and embedded treating device charging, etc. In such fields, their power transmission efficiency is generally more than 80%. The devices of emitter and receiver are accurately located at the stable position, which ensure the transmission stability, accuracy, and reliability

in a high level. However, the transmission distance of CPT and IPT is too short to satisfy the requirements of long-distance power transmission applications. Usually, MPT and LPT are used in satellite charging and remote drone charging, etc. The efficiency of MPT and LPT are both lower than 20%, but the efficiency of MPT is lower than LPT. The devices of MPT are inconvenient to implement, which causes MPT to become less reliable and stable for use. But microwaves will not be influenced by media change such as different atmosphere condition, the transmission accuracy could be better than LPT. LPT has a lower device size which easy to implement. Reliability and stability will be in a medium level. But in practical applications, the emitter and receiver should be in a straight and route of laser will be bended by air parameter change, which will cause the accuracy down. Considering the transmission efficiency, transmission distance and equipment suitability, the LPT is suitable wireless transmission method for motor drive. The comparison of the four wireless transmission methods is shown in Table 2-5.

Table 2-5. Main parameters comparison of four different types of WPT method.

Method	CPT	IPT	MPT	LPT
Efficiency	High	High	Low	Low
Distance	Short	Medium	Long	Long
Convenience	High	Medium	Low	High
Complexity	Low	Medium	High	Low
Reliability	High	High	Low	Medium
Accuracy	High	High	Medium	Low
Stability	High	High	Medium	Medium

Table 2-6. Comparison of Wire and LPT in harsh hazard application situation.

Method	Wire	LPT
Efficiency	High	Low
High temperature resistant	Low	High
Radiation resistance	Low	High
EMI	Exist	None
Safety	Low	High

The proposed LPT is also aimed at solving the problem of limitation of wired energy transmission in harsh hazard environments. The advantages of LPT are shown in Table 2-6 in detail. Taking the drive motor as an example, the author summarized a minimalist LPT model to achieve high-efficiency transmission applications. It includes an outer current supply, an LD, a type of PCM and a DC motor in Figure 2-5. Because the output current type of PCM is DC,

The DC motor is chosen. The equivalent circuit of this model is shown in Figure 2-6. The function of diode is to obstruct the reverse induced current. This LPT model plays a role in a DC/DC converter between current supply and motor load, so conversion efficiency is the first consideration. Choosing different LD and PV will have different usage conditions and overall efficiency. Judging from the results of the above review, the LD – GaAs is the advised LPT system for a laser power motor, because the 810nm of best power efficiency of GaAs which is suitable for LD's wavelength 860nm. Both LD and GaAs PV materials are the most efficient equipment for energy conversion at present research. The transmission media is atmosphere which in a free space is the most convenient choice. In the condition of the laser transmission route needs to be guided, the media should consider the optical fibre. If the application circumstances are high-temperature or high-radiation, such as nuclear station, the radiation resistance optical fibre can effectively reduce the environment impact, as reviewed in section 2.4.

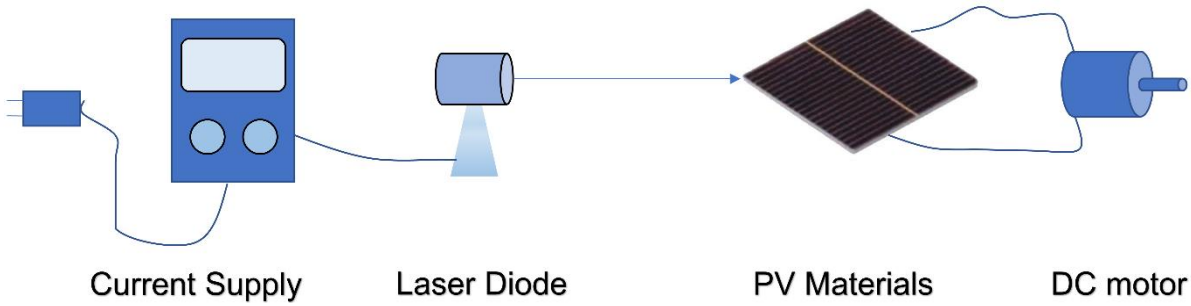

Figure 2-5. Proposed structure of laser power motor.

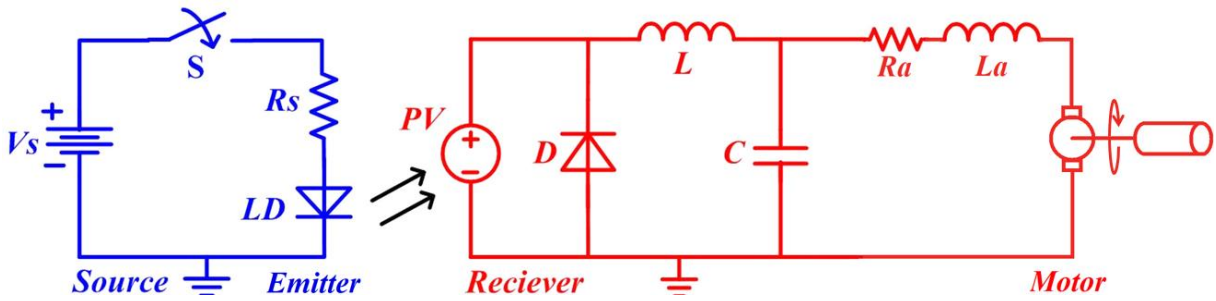

Figure 2-6. Equivalent circuit of the laser power motor.

The total power efficiency of the LPT system is analysed in Figure 2-7. The power efficiency in a current power supply is generally 85%. The power conversion efficiency of LD and PV material from the review result is ideally 60% and 50%, respectively[5]. DC motor commonly has a power efficiency about 80%. Laser transfer process in media is dependent on the specific

conditions, mainly on abortion rate and transmission distance. Theoretically the total system delivery power efficiency is around 20.4%, which ignore the transmission process in media space. This efficiency can achieve the goals required by the motor drive because the power output is enough if the laser is suitable.

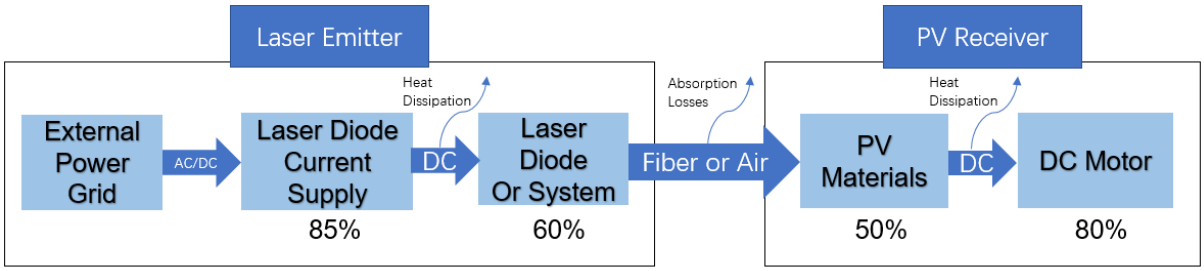

Total Efficiency = 85% × 60% × 50% × 80% = 20.4%

Figure 2-7. Theoretically analysed efficiency of the motor drive by laser powered system.

2.4 Future scope

The author thinks that the research and development direction of LPT to achieve motor drive in future mainly has the following aspects: 1) Improvement of device conversion efficiency. 2) LPT system advanced control strategy. 3) Impact on LPT efficiency in complex environment and improvement methods. Through research progress in these directions, LPT will become a competitive energy transmission method and be widely used.

2.4.1 Improvement of device conversion efficiency

The limitation of LPT in practical applications is mostly the low transmission efficiency. Both LD and PV material do not have the ideal high conversion efficiency. In order to get enough power for the load, two aspects are needed to improve. One is to develop new, more efficient devices of both laser and PV materials. The other is to optimize the operation of the equipment. For example, LD in high efficiency working state requires high accuracy and stability of driving current. In addition to using a stable current source as much as possible, power electronic technology can also be used for rectification to ensure the quality of the LD's drive current. At present, there is little research on power electronics technology rectifying LD driving current. Moreover, the arrangement of the PV unit and the design of the internal circuit will also affect the overall output efficiency. Because the laser power beam density of LD is following the Gaussian distribution, the PV cells that receive insufficient light will become

redundant internal resistance in the loop, reducing the conversion efficiency. By applied a beam expander to expand it as appropriate size that covers the whole surface, the efficiency could be better. Energy efficiency can be improved by optimizing the arrangement of cells and adding electronic components.

2.4.2 LPT system motor speed control strategy

In some extremely harsh environments, such as nuclear station and dusty industrial site, which will also cause the impact on LPT system efficiency. How to eliminate the impact on these occasions and promote the advantages of LPT is also a direction worth exploring. The impact of the complex environment is concentrated on the transmission path. For example, the method to avoid the impact of strong nuclear radiation on atmosphere properties that change the transmission characteristics of lasers in the atmosphere. Excellent radiation-resistant optical fibres also need to be studied. The high temperature resistance and radiation resistance of lasers and photovoltaic materials also need to be further studied and improved.

2.5 Summary

In this chapter an overall review of the LPT system development and exist application examples have been investigated. Existing LPT research has proven that applications powered by laser could be one feasible way. The limitation of this technology is mainly on the transmission efficiency, generally around 20%. In the aspects of laser emitter, transmission media space and PV materials and the power conversion efficiency of the total LPT system is analysed. LD has lower size, easy to implement and use, good alignment of beam and high photovoltaic power conversion efficiency. The accuracy, stability and wave types of the drive current will influence the working efficiency of LD, which could be one direction to improve the efficiency. If single LD is not enough for power demand, the diode laser system can be considered. But this technology will increase the complexity of the emitter device which causes inconvenient for use. When the emitter and receiver are in a straight and need not consider the transmission track, the atmosphere is the best media that saves a few steps for fiber installation and laser collimation. Atmosphere has different wavelength absorb rate, in order to have better transmission efficiency, the chosen wavelength should inside the range of atmosphere transmission window. Air transmission in short distance is convenient, but long-distance transmission will increase the power loss and change the transmission route that reduce the accuracy. The optical fibre can also be used to build the transmission route. In high

radiation environment, the transmission efficiency of fibre will be influenced. So, improving the radiation resistance of fibre is also important. GaAs has the best power conversion efficiency with current technology, due to the band gap is moderate. Back to select LD's wavelength, the best is around 850nm.

Then, by comparing it to other WPT, LPT has long transmission distance and easy for implementation, that is a suitable method as an actuator for motor drive. The proposed structure of the LPT system for motor drive is discussed in detail. This system adopts the high-efficiency equipment under the current technical level summarized by the review and evaluates the overall efficiency of the system. In the future scope, the development direction and expansion ideas of the system are listed in detail, and each aspect will help improve the efficiency and applicability. Especially the state that the system can reach under the optimization by power electronics.

Finally, the proposed LPT to drive the motor is dedicated to avoiding the limitations and losses in wired transmission, especially in harsh hazard environments. From the efficiency of analysis, it can basically meet the needs of wireless transmission.

Chapter 3 Optical Fibre-based Motor Speed Feedback Method for Laser Powered Actuator

Laser powered actuator has the capability to drive a motor wirelessly, offering advantages in specific scenarios due to its adaptability to high temperatures and radiation, flexible usage, and absence of electromagnetic interference (EMI). To establish a precise control system for regulating motor speed, a stringent feedback method is required. Light signal transmission is considered as a viable approach for this purpose. Here wireless techniques for motor speed signal feedback are reviewed for laser power actuators. The structure of light signal transmission are presented through generation resources, modulation and reception processes. The acquisition of motor speed signals through sensorless methods is compared with sensor-based approaches through key principles including cost, reliability, integration, and efficiency. Finally, suitable approaches for the laser-powered actuator are discussed with future opportunities for wireless motor speed feedback methods.

3.1 Introduction

Electric motors play a crucial role in industrial and commercial machinery used across various sectors, from household products to a wide range of industrial applications. The connection of motors to the energy source is commonly supplied by copper wires, while wire connections have certain shortcomings, such as being less flexible, security threats, and electromagnetic interference (EMI) concerns. To overcome these limitations, recently a wireless laser power transmission method has been proposed to use in DC motor actuators [78]. The proposed system structure can realize the operation of a DC motor wirelessly. However, without a feedback component, it is an open-loop system, and the motor rotational speed and output torque cannot be automatically controlled. Therefore, a feedback module is required to constitute a closed-loop control system.

Since the power transmission mode is wireless, the conventional electric signal delivered by wire is unsuitable here. Hence, it is necessary to consider a wireless signal transmission method to employ for the motor speed signal feedback. Optical signal transmission can be considered as a reliable candidate due to its convenience and speed [79]. Generally, an optical signal

transmission system consists of a signal generator and a signal receiver connected to DC motor and controller, respectively. The receiver converts the light signal back to the electric signal for the controller to control the laser output. The light signal is modulated by the generator, which can use different types of light signal modulation, such as analogue modulation and digital modulation. The modulated signal is derived from the motor speed signal, which can be obtained through a sensor or extracted from the current.

Several studies have proposed various methods for reading the motor speed signal [80-83]. This chapter will present and evaluate the most suitable motor speed feedback methods for a laser-powered actuator to create a closed-loop control system. Section 3.2 will present the light signal generation, transmission, and reception process. Section 3.3 will explore sensorless methods of motor speed feedback, and Section 3.4 will review each type of speed feedback sensor. Section 3.5 will discuss the modulation type suitable for the feedback method. Finally, the summary will be provided in Section 3.6.

3.2 Light Signal Transmission Structure

To understand the wireless motor feedback method, one can look at the structure of a closed-loop control systems as shown in Figure 3-1. The proposed speed signal feedback block comprised of a light signal emitter and a light signal receiver. The signal emitter is made up of a modulator, a driver, and a light source. In order to concentrate on showing the signal flow route, the power supply part on the both motor and controller is omitted. The purpose is to combine the electrical terminal signal with the light output by the light source to modulate it, and then couple the modulated light signal to an optical fibre or cable for transmission. A light detector and an amplifying circuit make up the optical receiver. The objective is to convert the optical signal, which is carried across an optical fibre or a cable, into an electrical signal, which is then amplified by an amplification circuit and supplied to an electrical terminal at the receiving end. The function of the light emitter and light receiver in the close loop control system of laser power transmission (LPT) powered motor is shown in Figure 3-1. They can achieve speed feedback wirelessly.

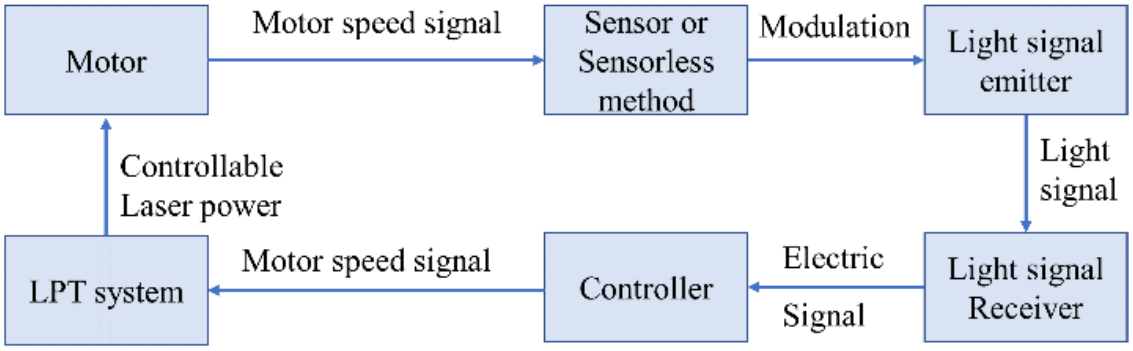

Figure 3-1. Schematic structure of a closed-loop control system with wireless feedback signal of laser powered actuator.

The remainder of this section will discuss the main two components of the wireless feedback signal system as light signal emitters and receivers.

3.2.1 Light signal emitters

The technical requirements of a light signal emitter include [84, 85]:

- Small size and high coupling efficiency with optical fibres.
- The wavelength of the emitted light wave should lie in the three low-loss windows of the fibre (i.e., 0.85μm, 1.31μm and 1.55μm bands).
- Light intensity modulation available.
- High reliability, requiring it to have a long working life and good operational stability (power, polarisation, spectrum, temperature).
- The light power emitted is high enough so that it can be transmitted over long distances.
- Good temperature stability, i.e., when the temperature changes, the output optical power as well as the wavelength change should be within the allowed range.

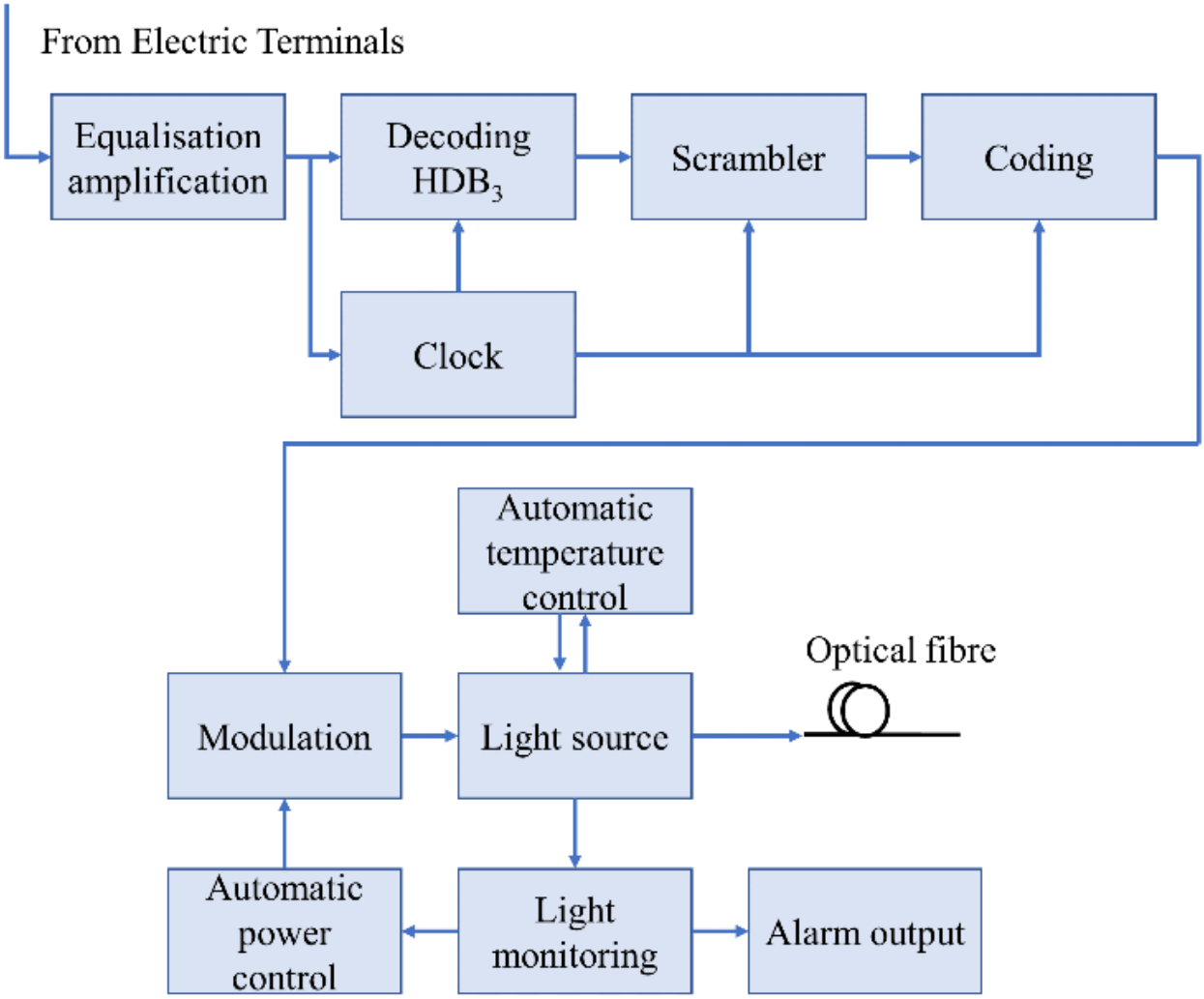

Figure 3-2. Schematic of the light emitters with each component and signal processing flow.

In the fibre optic communication systems, information is carried by light waves emitted by light-emitting diodes (LEDs) or Laser diodes (LDs), where the optical transmitter mainly consists of a modulation circuit and a control circuit. Figure 3-2. shows a schematic of light emitters, where each block in this diagram is describe as following:

1) **Equalisation amplification**

   The HDB_3 stream is transmitted through the cable to produce attenuation and distortion. Therefore, when the signal enters the transmitter, it is first equalised and amplified to compensate for the attenuated level and equalise the distorted waveform.

2) **Decoding**

Since the HDB_3 codes transmitted by PCM systems are bipolar, it is generally not easy to correspond to +1, 0, -1 in the fibre optic communication systems, as the light source can correspond to both light and no light as "0" and "1" codes, respectively. Hence, detection of signal from the PCM terminal is challenging. Thus, after the signal is sent from the PCM terminal to the optical transmitter, the HDB3 code needs to be changed to a unipolar "0" and "1" code by the decoding circuit.

3) **Scrambler**

If there are long "0s" and "1s" in the signal stream, this would make it difficult to extract clock signals. To avoid long "0s" and "1s", a scrambling circuit is added after decoding in order to "destroy" the long "0s" and "1s" streams in a regular manner.

4) **Clock**

Since the decoding and scrambling processes require a clock signal as a basis (time reference), the clock signal in the PCM is taken out by the clock circuit after equalisation and amplification and supplied to the decoding, scrambling, and encoding circuits.

5) **Coding**

Although the decoded and scrambled code can theoretically be transmitted over the optical fibre, from a practical point of view, in order to facilitate uninterrupted error monitoring, to overcome fluctuations in the DC component and to facilitate inter-zone communication, the decoded and scrambled code stream is encoded again to meet the above requirements in the actual optical fibre communication system.

6) **Modulation (drive)**

The encoded digital signal is modulated by a modulation circuit to allow the light emitted by the light source to vary in intensity with the encoded signal stream, creating a corresponding light pulse that is fed to the optical fibres.

7) **Automatic power control (APC)**

The automatic power control circuitry maintains the output optical power of the semiconductor laser at a constant value.

8) **Automatic temperature control (ATC)**

The semiconductor light source is sensitive to temperature. Hence the automatic temperature control circuitry is utilized to maintain the semiconductor laser operating at a constant temperature.

In addition to the circuits in the above sections, the optical transmitter has the following auxiliary circuits:

9) **LD protection circuits**

It slows start-up of bias currents in semiconductor lasers and limiting bias currents from being too large. As the output power of the laser decreases due to aging, the automatic power control circuit will cause the laser bias current to increase, which could burn up the laser if the bias current is not limited.

10) **No light alarm circuit.**

When there is a fault in the optical transmitter circuit, or when the input signal is interrupted, or when the laser fails, the laser will not emit light for a longer period and the delayed warning circuit will give an alarm indication.

3.2.2 Light signal emitter sources

Commonly, there are two types of the laser emitters, i) laser diodes and ii) light-emitting diodes. Laser diodes (LD) are semiconductor devices, which have high output power, high efficiency, and high collimation. Light-emitting diodes (LEDs) are non-threshold devices, where the luminosity changes with the operating current and gradually reaches to a saturation level at high currents. Typically, the operating current of LEDs is 50 mA-100 mA with bias voltage in a range of 1.2 V-1.8 V to provide output power in a mW level. The output power of LEDs reduces at elevated temperatures in the same operating current. For example, the change of temperature from 20°C to 70°C decreases the output power by about half, which is relatively less than LDs. Although comparing to LDs, the output optical power of LEDs is lower and the

spectrum is wider, they are extensively used in medium- and low-rate short-range fibre-optic digital communication systems and fibre-optic analogue signal transmission systems because of their simplicity of use and long life. Regarding the operation difference, LDs and LEDs emit excited radiated light and spontaneous radiated light, respectively. LEDs do not require an optical resonance cavity and have no threshold. The detail comparison of LDs and LEDs is shown in Table 3-1.

Table 3-1. Comparison of LEDs and LDs

LD	LED
High optical power, 1 mW - 10 mW.	Low optical power, only 1mW - 2mW.
Large bandwidth and high modulation rates, 100 MHz - 10 GHz.	Small bandwidth and low modulation rate, 10 - 100 MHz.
Highly directional beam with low divergence.	Poor directionality and high divergence.
High coupling efficiency with optical fibres, up to 80 % or more.	The coupling efficiency to the optical fibre is low, only a few percent.
Narrower spectrum.	Broad spectrum.
The manufacturing process is difficult and costly.	Less difficult and less costly manufacturing process
APC and ATC are required when more stable optical power is required.	Operates over a wide temperature range.
Good linearity of the output characteristic curve.	Saturates easily at high currents.
With pattern noise.	No pattern noises.
Average reliability.	Better reliability.
Short working life.	Long working life.

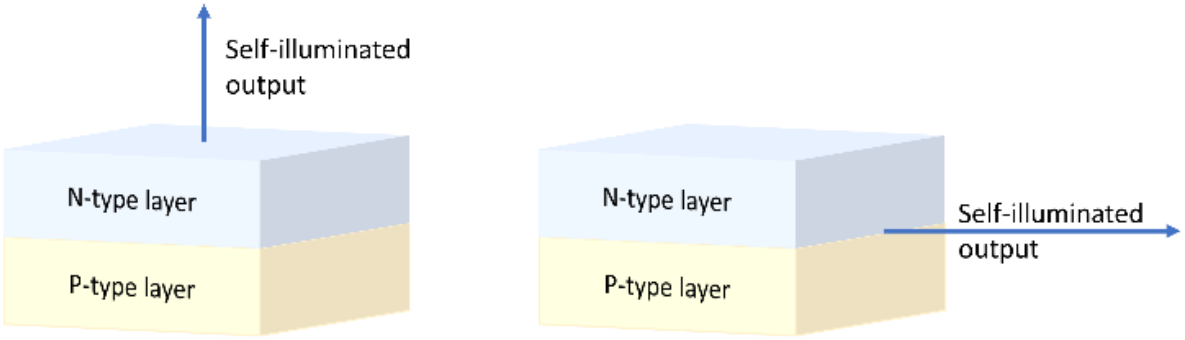

(a) (b)

Figure 3-3. The structure of LEDs as a two-layers of N and P type semiconductors with (a) front-illuminated LEDs (FLEDs), (b) side-illuminated LEDs (SLEDs).

There are two types of LEDs, including side-illuminated LEDs (SLEDs) and front-illuminated LEDs (FLEDs). Compared to FLEDs, SLEDs have larger drive current and smaller output light power. Because the beam radiation angle is smaller and the coupling efficiency of the fibre is higher, the incoming fibre light power is larger than FLEDs. The structure of both SLEDs and FLEDs is shown in Figure 3-3. The SLED structure consists of a double layer heterojunction grown on N-type GaAs substrate at the top of the diode (Figure3-4). The active layer of P-type GaAs is only 1μm to 2μm thick and forms two heterojunctions with N-type AlGaAs and P-type GaAs on either side of it, limiting the carriers and light field distribution in the active layer. The light emission generated in the active layer is coupled through the substrate into the fibre, and due to the high light absorption of the substrate material, a crater is formed in the area directly opposite the active zone by selective etching, allowing the fibre to be directly adjacent to the active zone. A circular contact electrode is formed on the P+GaAs side using the SiO_2 mask technique, thus limiting the current density in the source region of the active layer to approximately 200 A/cm2. The purpose of this structure is to reduce light absorption in the active layer and to give better directionality to the light beam, which is output from the end face of the active layer.

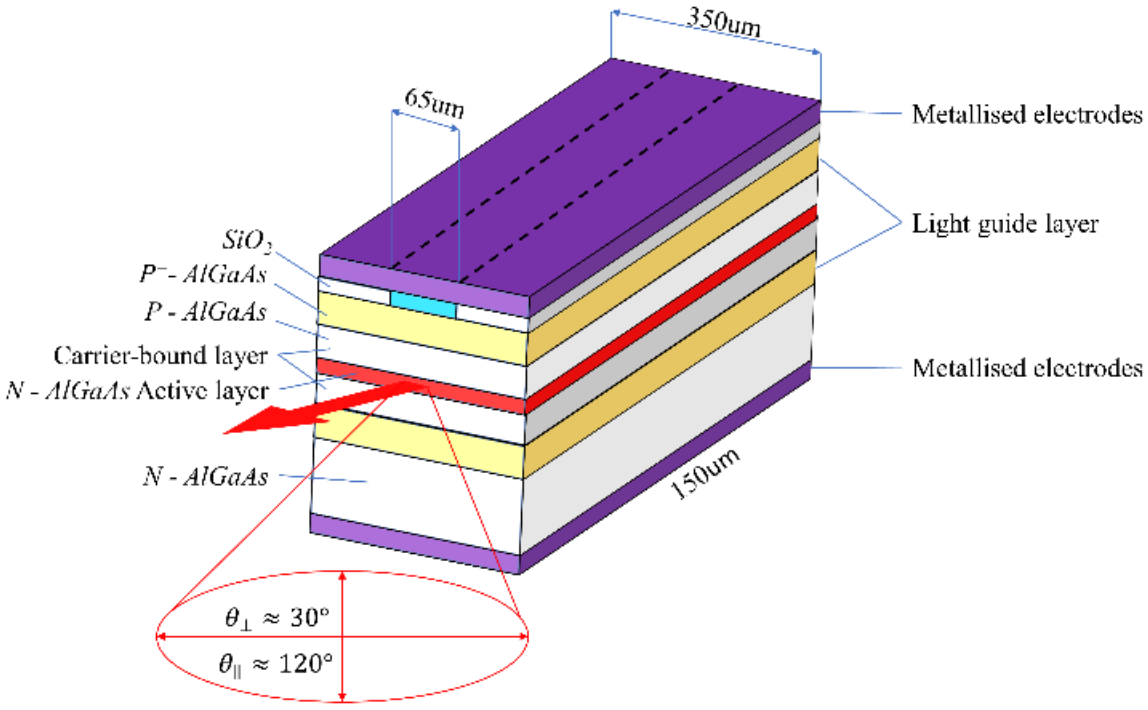

Figure 3-4. Schematic structure of SLED as a double layer heterojunction grown on N-type GaAs substrate at the top of the diode.

3.2.3 Light signal modulation

The process of loading an optical signal onto the emitted beam of a light source is called optical modulation. The modulated light wave is sent through the fibre optic channel to the receiver, where the optical receiver identifies its changes and reproduces the original information, called optical demodulation. The modulation of light sources is divided into two categories:

1) **Direct modulation**

   The transformation of information to be transmitted into a current signal is injected into an LD or LED to obtain the corresponding light signal, using the power modulation method, also known as internal modulation. Only applicable to semiconductor light sources (LD and LED).

2) **Indirect modulation**

   The modulation of laser radiation is achieved by using the electro-optical, magneto-optical, and acoustic-optical properties of a crystal. This modulation method is suitable for semiconductor lasers as well as adapted to other types of lasers.

There are two methods of direct modulation, analogue and digital modulations. Direct modulation of analogue signals is the modulation of a light source with a continuous analogue signal (e.g., voice, TV, etc.). There are two types of analogue modulation: a) using an analogue baseband signal to modulate the light source directly, b) employing a continuous or pulsed RF wave as a subcarrier. In the later type, the subcarrier is first modulated by an analogue baseband signal, and then the modulated subcarrier is used to modulate the optical carrier. Analogue modulation has a lower modulation rate than digital modulation and direct modulation is used. In all communication systems, direct intensity modulation is utilized with LEDs as light sources. The LED analogue modulation principle is to superimpose a continuous analogue signal current on a DC bias current, the appropriate choice of DC bias size, so that the static working point is in the midpoint of the linear section of the light emitting tube characteristic curve, can reduce the non-linear distortion of the light signal.

The signal current is a one-way binary digital signal, with a one-way pulse current of "yes", "no" ("1" code and "0" code) to control the light-emitting tube light or not. In direct modulation, analogue or digital systems are used to control the current flowing through the light-emitting tube to achieve the purpose of modulating the output optical power. LED digital systems are used to modulate the output light power by controlling the current flowing through the light emitting tube. The LD digital systems are usually used in high-speed systems and are threshold devices, which are less temperature stable and have more complex modulation problems than LEDs.

3.2.4 Drive circuit for light sources

In analogue systems, the driver circuitry provides a certain operating point bias current and sufficient signal drive current to enable the light source to output sufficient power. The non-linear distortion must be below -30dB to -50dB, but due to the inherent non-linear distortion of the LED, linear compensation circuits are also required for signal transmission with high quality requirements. LEDs are not very sensitive to temperature and therefore APC and ATC circuits are not generally used. Figure 3-5. shows a simple, yet high-speed common, emitter trans-conductor driver. The base voltage is converted to collector current to drive the light emitter. The transistor operates in Class A operation and the base bias is adjusted so that both the transistor and the light emitter are biased in their respective linear regions. The germanium diode and resistor are connected in series and then in parallel with the LED to act as a shunt at high currents, extending the drive current range and improving the linearity of the LED.

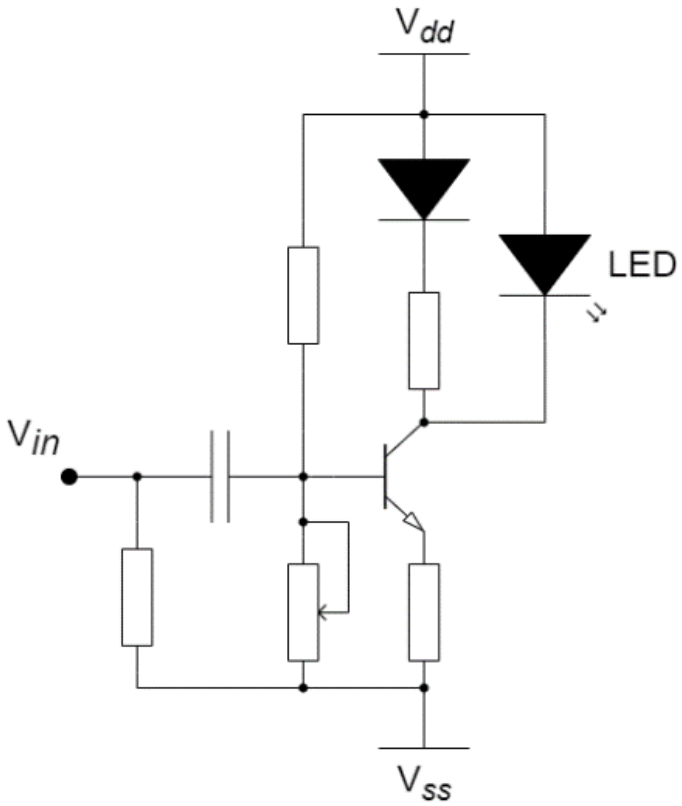

Figure 3-5. Analogue modulation circuit for optical signals

The digital drive circuit for LEDs is mainly used for binary digital signals. The driver circuit should be able to provide "on" and "off" currents of several tens to hundreds of milliamps (mA). Signal current for a one-way binary digital signal, with a one-way pulse of current "with", "without" ("1" code and "0 ") LED digital system is through the control of the current flow through the light tube to achieve the purpose of modulating the output light power. When the code speed is not high, no bias can be added. However, at high code speeds, a small amount of forward bias current is required to help maintain the charge on the diode capacitors.

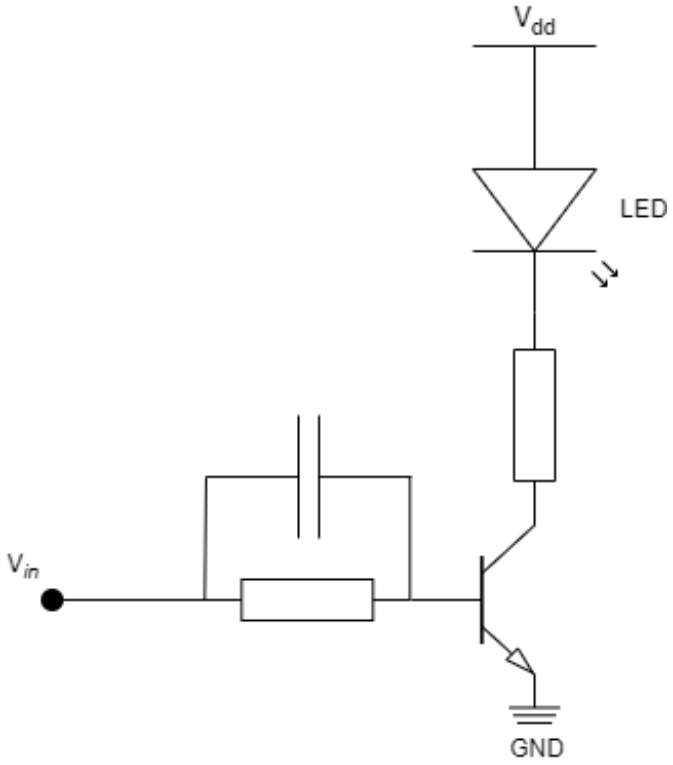

Figure 3-6. LED digital signal modulation.

The LED digital signal modulation circuit has only one stage of common emitter transistor modulation circuit, the transistor is used as a saturation switch and the collector current of the transistor is the injection current of the LED, as shown in Figure 3-6. The signal is accessed from point V_{in}. At "0" code the transistor does not conduct; at "1" code the transistor conducts, so that the injection current is inserted into the LED tube, making the LED tube glow, thus realising the digital signal modulation.

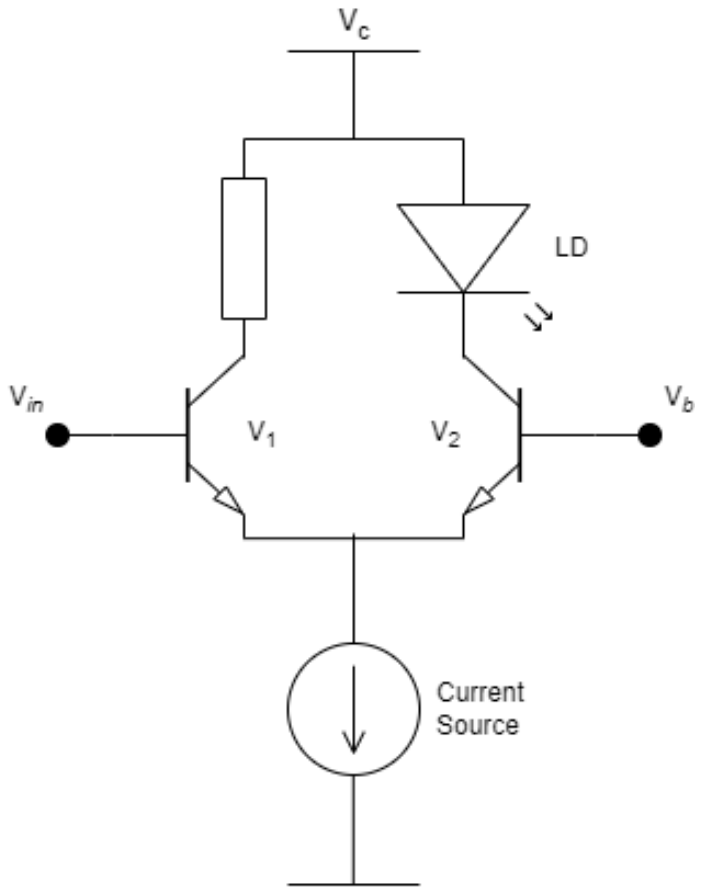

Figure 3-7. LD digital signal modulation.

LD digital systems are usually used in high-speed systems and are threshold devices, which are less temperature stable and have more complex modulation problems than LEDs. As shown in Figure 3-7, V_1, V_2 form a current switch, digital electrical signal V_{in} from the base of V_1 input, where V_b is a DC reference voltage applied to the base of V_2. When the signal is "0" code, V_1's base potential is higher than V_2's base potential, the current source all current flow through V_1's collector, LD connected to V_2 does not glow, as of LD not glowing, equivalent to send "0" code. When the signal is "1" code, V_2 base potential is higher than V_1 base potential, then in turn V_2 conductive, all the current source current flow through the collector branch of V_2, corresponding to the issue of a "1" code.

3.2.5 Light signal receiver

The task of the optical receiver is to recover the information carried by the optical carrier, transmitted by the fibre, with minimal additional noise and distortion. Optical receivers are also available in both digital and analogue receiver forms, as shown in Figure 3-8. They both consist of a photodetector under reverse bias, a low-noise preamplifier and other signal

processing circuitry in a direct detection mode. The digital receivers (b) are more complex than the analogue receivers (a), with equalisation filtering, timing extraction and judgement regeneration, peak detector, and Automatic Gain Control (AGC) amplification circuits after the main amplifier. They operate at high levels and do not affect the analysis of the basic performance of the optical receiver.

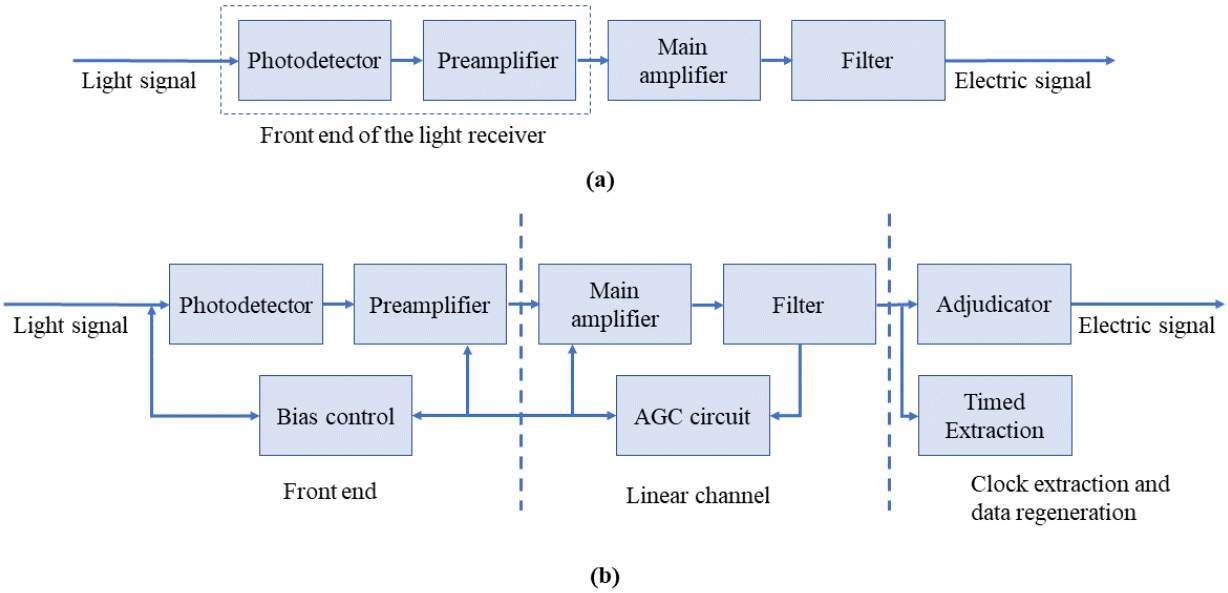

Figure 3-8. Block diagram of the optical receiver with (a) analogue type and (b) digital type.

The following discusses on each part of the light receiver:

1) Front end of light receivers

The front end consists of a photodetector, a bias control circuit and a preamplifier. Its role is to convert the light signal coupled with the photodetector into a time-varying current, which is then pre-amplified (current-to-voltage conversion) for further processing at the back end. It is the core of the optical receiver. It requires low noise, high sensitivity, and sufficient bandwidth. There are three different options for the design of the front end, as shown in Figure 3-9, depending on the requirements of the application:

- **High Impedance Front End**: Field Effect Tube Amplifiers
- **Low Impedance Front End**: Bipolar transistorised amplifier
- **Transimpedance Front Ends**: Transimpedance Amplifiers

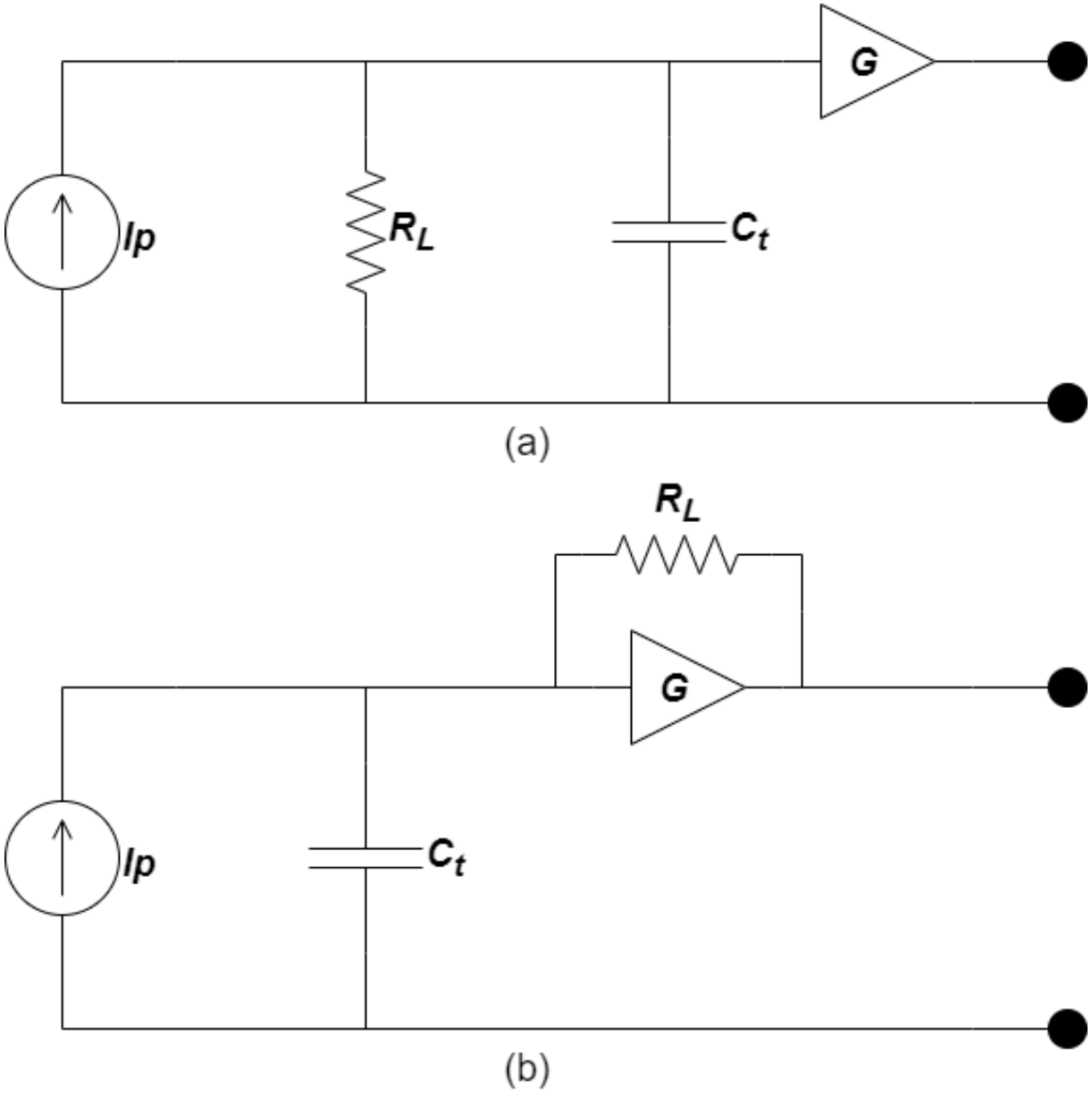

Figure 3-9. Front end of light receiver with (a) high/low impedance front end and (b) transimpedance front end.

The photodetector is the first key component of the light signal receiver, and its role is to convert the received optical signal into an electrical signal. The photodetector is a PN junction with an applied reverse bias. With an incident light, an excited absorption occurs to produce photogenerated electron-hole pairs, where these electron-hole pairs form a drift current under the action of electric field generate a depletion layer. Thus, electron-hole pairs on both sides of the depletion layer can enter the depletion layer due to the diffusion movement to form a diffusion current under the action of the electric field leading to photogenerated current formation. Fiber optic communication requires high efficiency, low noise, low operating voltage, small size, lightweight and long life for optical detection devices. The photodetectors

currently widely used in fibre optic communication systems are the PIN photodiode and the avalanche photodiode APD.

The PIN tube is relatively simple and only requires a bias voltage of 10V to 20V to operate and does not require bias control. But it has no gain effect. Therefore, receivers using PIN tubes are not as sensitive as those using APD tubes. The advantages of PIN photodiodes are low noise, low operating voltage (just over ten volts), long operating life, ease of use, and low price. At the same time, it has a disadvantage of having no multiplication effect. In other words, only a small photocurrent is generated by the same size of the incident light, so the sensitivity of the optical receiver made of it is not high compares to APD. PIN photodiodes can only be used for fibre optic communication over short distances (both small and large capacities are possible).

The APD tube has an internal current gain of 10 to 200 times, which improves the sensitivity of the optical receiver. However, the use of APD tubes is more complex and requires a bias voltage of several tens to 200 V. The temperature variation affects the gain characteristics of the APD tubes more severely. It is often necessary to control the bias of the APD tube or to use temperature compensation measures to keep its gain constant.

In short-range applications, Si devices operating at 850 nm are a relatively inexpensive solution for most links. In long-range links, it is often necessary to operate in 1330 nm and 1550 nm windows, so InGaAs-based devices are commonly used. APD detectors have a carrier multiplication effect compared to PIN detectors and are particularly sensitive but require higher bias voltages and temperature compensation circuits. The choice depends on the specific application.

The weak signal current detected by a photodetector can be converted into a voltage signal by a load resistor and amplified by a preamplifier. However, the preamplifier amplifies the signal and at the same time introduces thermal noise from the amplifier's own resistance and scattering noise from the transistor. When the main amplifier enhances the output signal of the preamplifier, it also amplifies the noise generated by the preamplifier together. The performance of the preamplifier has a very important influence on the sensitivity of the receiver. For this reason, the preamplifier must be low-noise with a wide-bandwidth. The main amplifier is primarily used to provide high gain and to amplify the output signal of the preamplifier to a level suitable for the judgement circuitry required. The output signal level of the preamplifier

is generally in the mV range, while the output signal of the main amplifier is generally 1V to 3V (peak/peak).

2) Linear channel of light receivers

This part of the circuit, consisting of the main amplifier and the equalizer, is called the linear channel, which mainly accomplishes the linear amplification of the signal to meet the requirements of the judgment level. The main amplifier provides a high gain, amplified to a level suitable for the judgement circuit. The function of the equaliser is to shape the distorted digital pulse signal from the main amplifier into a rising cosine waveform that is most favourable to the judgement and with minimum inter-code interference. The output signal of the equaliser is usually divided into two ways, one is converted by the peak detector circuit into a DC signal proportional to the peak value of the input signal, which is fed into the automatic gain control circuit to control the gain of the main amplifier. The other way is fed to the judgement regeneration circuit, which restores the raised cosine signal from the equaliser to a "0" or "1" digital signal. The AGC circuit automatically adjusts the amplifier gain according to the size of the input signal (average) so that the output signal remains constant. This is used to extend the dynamic range of the receiver.

3) Judgement regeneration and clock extraction

Judgement regeneration and clock extraction consists of judgement and clock recovery, which are responsible to recover the raised cosine waveform from the linear channel output into a digital signal. To determine whether it is a "1" or a "0", a verdict is made on the code element of a time slot. If the verdict is "1", then a rectangular "1" pulse is generated by the regenerative circuit; if the verdict is "0", a new "0" is input by the regenerative circuit. To accurately determine the "moment of judgment", accurate clock information is extracted from the signal number stream as a calibration to ensure consistency with the transmitter.

4) Noise characteristics of light receivers

The noise of the optical receiver comes from two sources: one is the noise generated by the optical detector, i.e., multiplication noise and dark current noise. The other is the thermal noise of the amplifier. The receiver noise and its distribution are shown in Figure 3-10.

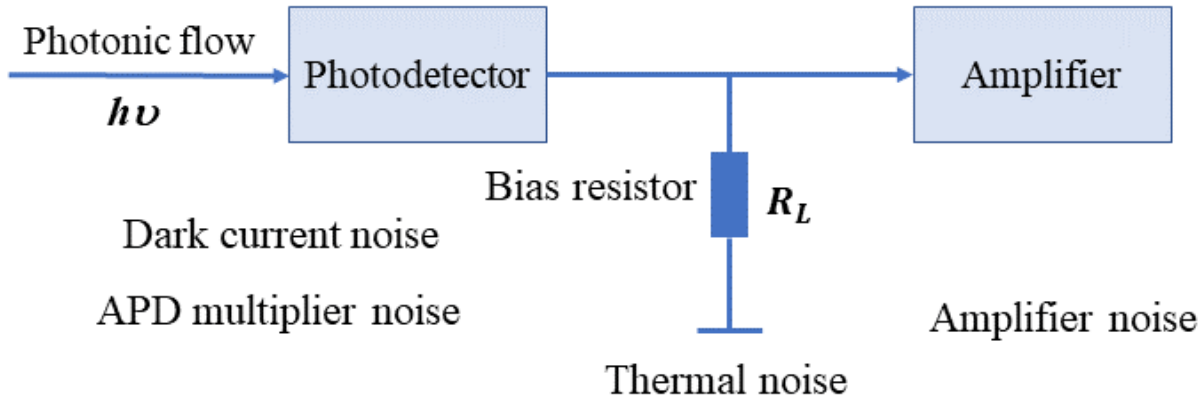

Figure 3-10. Receiver noise and its distribution.

- **Dark-current noise**: During no light signal illuminating the photodetector, some stray light or thermal movement from the outside world will produce some electron-hole pairs causing the photodetector to produce current. This residual current is called dark current.
- **APD multiplication noise**: By using avalanche photodiodes, the random nature of the multiplication process generates additional noise, considered as APD multiplication noise.
- **Thermal noise:** A random pulsation caused by thermal interactions between free electrons and vibrating ions within a conducting medium at a finite temperature creates thermal noise.
- **Amplifier noise:** Characteristics of preamplifier used can be calculated from the amplifier noise equivalent circuit and transistor theory.

3.3 Sensorless Motor Speed Feedback

In modern motor control systems, accurate and reliable feedback of motor speed is crucial for achieving optimal performance and efficiency. Traditionally, motor speed feedback has been obtained using dedicated sensors, such as encoders or hall effect sensors, that directly measure the motor's speed. However, these sensors can add complexity and cost to motor control systems, especially in high-performance or high-volume applications. In recent years, sensorless feedback techniques have emerged as a viable alternative, offering the potential for cost-effective, simplified, and versatile solutions for motor speed control.

Sensorless feedback of motor speed refers to a method of determining the rotational speed of a motor without using dedicated sensors. Instead, sensorless techniques rely on analysing other motor parameters or the back-electromotive force (EMF) generated by the motor to estimate its speed. These techniques leverage the inherent properties of the motor and the interactions between the motor and the load to infer the speed information without any physical sensors.

Sensorless feedback methods have gained significant attention in various motor control applications, including electric vehicles, industrial automation, home appliances, and robotics. They offer several advantages over sensor-based methods, including cost-effectiveness, simplifying design, improving reliability, efficiency, flexibility, and scalability. However, it is important to carefully consider the specific requirements and constraints of the application before choosing a motor control approach, as sensorless feedback methods may have limitations in certain operating conditions or motor types.

In this section, the advantages of sensorless feedback of motor speed will be explored in detail, highlighting how these techniques can provide cost-effective, reliable, and efficient solutions for motor control systems. The benefits of sensorless feedback will be discussed in terms of cost reduction, system simplification, improved reliability, increased efficiency, flexibility, and scalability. Additionally, the potential limitations of sensorless feedback methods will be touched upon, and the importance of careful consideration when selecting a motor control approach will be emphasized.

3.3.1 Brushed DC motor

Sensorless speed signal feedback for brushed DC motors is a technique used to estimate the rotational speed of the motor without using dedicated speed sensors. Instead of relying on external sensors, such as optical encoders or Hall effect sensors, sensorless methods utilize the inherent electrical and/or mechanical properties of the motor to estimate its speed. This approach has gained popularity due to its cost-effectiveness, simplicity, and potential for reduced maintenance requirements.

One commonly used sensorless speed estimation method for brushed DC motors is based on the analysis of back-EMF. When a DC motor rotates, it generates a voltage called the back EMF, which is proportional to its speed. By measuring the motor's terminal voltages and currents, the back EMF can be estimated, and the speed of the motor can be determined from the relationship between the back-EMF and the motor speed [86-89].

Ripple current analysis is another approach used for sensorless speed signal feedback in brushed DC motors. This method involves analysing the ripple current in the motor's armature circuit, which is caused by the commutation of the brushes. The frequency of the ripple current is directly proportional to the motor speed, and by analysing this frequency, the motor speed can be estimated [90-92].

One of the main advantages of sensorless speed signal feedback for brushed DC motors is cost-effectiveness. By eliminating the need for external speed sensors, the overall cost of the motor control system can be reduced, making it more cost-effective, especially for applications where cost is a critical factor. Additionally, sensorless methods are generally simpler in terms of hardware and wiring compared to systems that require external sensors, resulting in simplified motor control circuitry and reduced complexity of the overall system. Another advantage of sensorless speed signal feedback for brushed DC motors is reduced maintenance requirements. External speed sensors, such as encoders or Hall effect sensors, may require periodic maintenance and calibration. In contrast, sensorless methods can eliminate the need for such maintenance requirements, resulting in reduced downtime and increased system reliability. Furthermore, sensorless speed signal feedback methods are scalable and can be easily applied to a wide range of brushed DC motors without the need for motor-specific sensors. This makes it a flexible solution that can be easily scaled for different motor sizes and types.

Generally, sensorless speed signal feedback for brushed DC motors is a cost-effective, simple, and scalable approach for estimating motor speed without the need for dedicated speed sensors. It offers advantages in terms of cost reduction, system simplicity, reduced maintenance requirements, and scalability, making it a popular choice in various motor control applications. However, it is important to carefully select and implement the appropriate sensorless speed estimation method based on the specific requirements and constraints of the motor control system.

3.3.2 Brushless DC motor

Sensorless speed signal feedback for Brushless DC (BLDC) motors refers to the process of estimating the motor speed without using sensors. Instead, various methods are employed to indirectly infer the motor speed by analysing the motor's electrical parameters or back EMF generated during motor operation. This allows for a cost-effective and simplified motor control system without the need for additional sensors.

There are several different techniques used for sensorless speed signal feedback in BLDC motors. Here are some commonly used methods:

1) **Back-EMF Zero Crossing Detection**

   BLDC motors generate back-EMF during operation, which is a voltage induced in the motor windings due to the motion of the rotor. By monitoring the zero-crossing points of the back-EMF waveforms, the motor speed can be estimated [93, 94]. This method is relatively simple and widely used in sensorless BLDC motor control systems.

2) **Model-Based Method**

   Model-based methods involve using mathematical models of the motor to estimate the speed. These models can include parameters such as motor resistance, inductance, and back-EMF constants. By measuring the motor terminal voltage and current, and using these parameters in the model, the motor speed can be estimated [95, 96]. Model-based methods can provide accurate speed estimation but may require more computational resources and system identification.

3) **Signal Injection Techniques**

   Signal injection techniques involve injecting additional signals into the motor windings and analyzing the resulting effects on the motor currents or voltages. By analyzing the changes in the motor currents or voltages, the motor speed can be estimated [97]. Signal injection techniques can provide accurate speed estimation but may require additional hardware and careful calibration.

Advantages of Sensorless Speed Signal Feedback for BLDC Motors:

- **Cost-effective:** Eliminating the need for dedicated speed sensors can reduce the overall cost of the motor control system, making it more affordable for various applications.
- **Simplified System:** Sensorless speed signal feedback eliminates the need for additional sensors, wiring, and signal conditioning, simplifying the motor control system and reducing potential points of failure.

- **Improved Reliability:** With fewer components, sensorless speed signal feedback can lead to improved reliability and reduced maintenance requirements compared to systems that rely on dedicated speed sensors.
- **Higher Efficiency:** Sensorless speed signal feedback can enable faster and more precise speed control, leading to improved motor efficiency and performance.

In general, sensorless speed signal feedback for BLDC motors is a cost-effective and simplified approach to estimate motor speed without using dedicated speed sensors. Various methods such as back-EMF zero crossing detection, voltage and current analysis, model-based methods, and signal injection techniques can be used for sensorless speed signal feedback. These methods offer advantages such as cost-effectiveness, simplified systems, improved reliability, and higher efficiency in motor control applications.

3.3.3 Induction motor

Induction motors are widely used in various industrial and commercial applications due to their robustness, reliability, and cost-effectiveness [98]. However, sensorless speed control techniques have emerged as a promising alternative that eliminates the need for additional sensors, providing cost savings, and improving reliability and performance [99].

One of the key challenges in sensorless speed control of induction motors is obtaining accurate speed feedback without using physical sensors. Several sensorless techniques have been developed for induction motors based on the analysis of the motor's electrical or magnetic characteristics. These techniques can be broadly classified into two categories: model-based methods and sensorless observer-based methods [100].

Model-based methods utilize mathematical models of the induction motor to estimate the rotor speed. These methods typically rely on the measurement of motor terminal voltages and currents and use mathematical algorithms to estimate the rotor speed based on the motor model equations. Some commonly used model-based methods include the rotor resistance estimation method, the stator resistance estimation method, and the parameter identification method [101].

Sensorless observer-based methods, on the other hand, utilize state observers or estimators to predict the rotor speed. These methods typically rely on the measurement of motor terminal voltages and currents and use observer algorithms to estimate the rotor speed based on the

motor's dynamic behaviour. Some commonly used observer-based methods include the extended Kalman filter, the sliding mode observer, and the model reference adaptive system [102-112].

Sensorless speed signal feedback for induction motors offers several advantages over traditional sensor-based methods:

- **Cost savings:** Eliminating physical sensors reduces the overall cost of the motor control system. Sensors, such as encoders or tachometers, can add significant cost to the motor system, especially in large-scale industrial applications. Sensorless speed control can result in cost savings by eliminating the need for additional hardware, installation, and maintenance costs.
- **Increasing reliability:** Physical sensors can be prone to wear and tear, temperature variations, and other environmental factors, which can affect their accuracy and reliability. Sensorless speed control eliminates the risk of sensor failures, resulting to increase system reliability and reduced downtime. This is particularly advantageous in critical applications where system reliability is crucial, such as in industrial automation, transportation, and energy generation.
- **Improving performance:** Sensorless speed control techniques can provide improved dynamic response and higher control bandwidth compared to sensor-based methods. This is because sensorless techniques can provide faster updates of the rotor speed, enabling faster and more accurate motor control. Improved performance can be particularly beneficial in applications that require precise control of motor speed, torque, or position, such as in robotics, machine tools, and high-performance drives.
- **Simplifying motor design:** Sensorless speed control can simplify the motor design by eliminating the need for physical sensors and associated wiring, mounting, and alignment requirements. This can result in a more compact and streamlined motor system, with

reduced complexity and improved ease of installation. It also allows for greater flexibility in motor selection, as sensors do not need to be integrated into the motor design.

- **Enhancing fault detection and diagnosis:** Sensorless speed control techniques can enable real-time monitoring of motor performance and health, allowing for early detection and diagnosis of motor faults. By analysing the estimated rotor speed and other motor parameters, sensorless techniques can detect abnormal motor behaviour, such as rotor faults, bearing wear, or winding degradation, which can help prevent motor failures and reduce downtime.

Sensorless speed signal feedback for induction motors offers several advantages over traditional sensor-based methods, including cost savings, increasing reliability, improving performance, simplifying motor design, and enhancing fault detection and diagnosis. These advantages make sensorless speed control techniques attractive for a wide range of industrial and commercial applications, where accurate and reliable motor control is critical. However, it's important to note that sensorless speed control methods may have limitations in certain operating conditions, and proper design and implementation considerations should be considered to ensure reliable and safe motor operation.

3.4 Motor Speed Feedback by Sensors

Motor speed feedback by sensors is a critical aspect of modern industrial processes and automation systems, allowing for precise monitoring and control of motor performance. Sensors provide real-time data on the rotational speed of motors, enabling industries to achieve higher levels of accuracy, productivity, and reliability in their operations. Accurate measurement and control of motor speed are essential for various industrial applications, such as manufacturing, robotics, transportation, and renewable energy. In this section, the significance of motor speed feedback by sensors will be explored by discussing different types of sensors commonly used for this purpose. This will be followed by discussing benefits each type of sensors offers in terms of performance, efficiency, and safety. Relevant research studies and industrial standards will also be referred to, underscoring the importance of motor speed feedback by sensors in modern industrial systems.

3.4.1 Encoder for Motor Speed Feedback

Motor speed feedback is a crucial aspect in closed-loop control systems of motor-driven technologies, as it enables accurate speed control. One common method for obtaining motor speed feedback is through the use of an encoder, which is a device that converts mechanical motion into electrical signals, as shown in Figure 3-11. Encoders provide high-resolution feedback, allowing precise measurement of motor speed with minimal error [113].

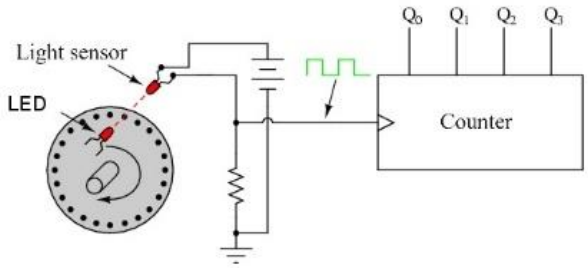

Figure 3-11. Schematic diagram of encoder.

Typically, an encoder consists of a rotating disc with slots or marks, along with a sensor that detects the changes in the disc as it rotates. The sensor generates electrical pulses that are proportional to the speed and direction of the motor. These pulses are then processed by a controller to determine the motor speed and adjust the control signal accordingly.

The use of encoders for motor speed feedback offers several advantages. First, encoders provide accurate and reliable speed measurement, enabling precise control of motor speed in various applications. This is especially important in tasks that require precise positioning or synchronization, such as robotics, automation, and industrial processes [114]. Encoders also offer high resolution control for motor speed, allowing for fine-grained speed control and minimizing speed fluctuations. Moreover, encoders provide real-time feedback, enabling rapid adjustments to changing motor speed requirements. Further research and advancements in encoder technology are expected to continue enhancing motor speed control in the future.

3.4.2 Position Sensor for Motor Speed Feedback

An accurate measurement of the position of a motor rotor is essential for a precise speed control in various industrial applications. Position sensors provide feedback on the rotor's position, allowing for precise control of motor speed and improving the performance and efficiency of motor control systems. Several studies have proposed different approaches for position sensing

in motor speed feedback, including optical, magnetic, and combined sensing techniques [115, 116].

One example of a position sensor for motor speed feedback is a combination of optical and magnetic sensing techniques, which offers high precision and robustness in speed control. The proposed sensor design consists of a custom-designed encoder disk with optical slits and magnetic poles, along with a corresponding sensor head that detects changes in light intensity and magnetic flux. By analysing the output signals from the sensor head, the position of the rotor can be accurately determined in real-time, with positioning accuracy reaching less than 0.1 degree. The sensor is optimized for high resolution of detection, allowing for precise measurement of the rotor's position, which is crucial for applications that require precise speed regulation, such as robotics, automation, and machine tools.

The combination of optical and magnetic sensing techniques in the proposed sensor provides several advantages. Optical sensing offers high resolution and accuracy in detection, while magnetic sensing provides robustness and immunity to environmental factors such as dust, dirt, and temperature fluctuations. This combination allows for a reliable and accurate position feedback, making the sensor suitable for demanding industrial environments.

Furthermore, the low latency of the sensor enables real-time feedback of the rotor's position, allowing for quick and precise adjustments to the motor speed. This is crucial in applications where a rapid change in motor speed is required, such as in high-speed machining or servo motor control.

Quantization errors are part of the system depends on the speed signal extraction method. Some research studies adopt optimization methods to reduce the quantization error. When comparing time interval measurements between continuous pulses and pulse counting in duration, and the measurement of time duration for a variable number of pulses, the speed calculated by FFT (Fast flourier transform) can provide more accurate results in both low- and high-speed ranges [117].

Moreover, correcting the measurement by incorporating other signals as a reference can also help to improve accuracy. In this regard, a study [118] has utilized the encoder corrected with commutation signal obtained from the position sensor of BLDC motor, realizing precise measurement and control of motor speed, providing a method for fast measurements of changes in the direction of rotation.

Other studies have also proposed different approaches for position sensing in motor speed feedback, such as [119] and [120], further highlighting the importance of accurate position sensing in motor control systems.

3.4.3 Hall Sensor for Motor Speed Feedback.

Hall sensors are widely used in motor control systems to provide accurate and reliable feedback on motor speed [120]. A Hall sensor is a type of magnetic sensor that detects variations in the magnetic field and generates an electrical signal based on such changes. These sensors are commonly used in BLDC motors, which are widely used in various applications, such as electric vehicles, industrial automation, and consumer electronics.

Hall sensors are typically placed in the motor housing, near the rotor or stator, and are used to detect the position of the permanent magnets in the motor. As the motor rotates, the position of the magnet's changes, and the Hall sensor generates a pulse signal with a frequency proportional to the motor speed. This pulse signal can then be processed by the motor control system to accurately determine the motor speed.

One of the key advantages of using Hall sensors for motor speed feedback is their high accuracy and reliability. Hall sensors can provide precise speed measurement even at low speeds and can operate in harsh environments, making them suitable for a wide range of applications. Additionally, Hall sensors have a fast response time, allowing for real-time monitoring and control of the motor speed.

In addition to speed measurement, Hall sensors can also be used for commutation in BLDC motors. By accurately detecting the position of the magnets, Hall sensors can determine the appropriate timing for energizing the motor windings, which helps to optimize motor performance and efficiency.

Hall sensors are also relatively inexpensive compared to other types of motor speed sensors, such as optical encoders, which makes them a cost-effective solution for motor control systems.

To illustrate the use of Hall sensors for motor speed feedback, a study [121] conducted experiments on a BLDC motor control system utilizing Hall sensors for speed measurement and commutation. The authors demonstrated that the Hall sensors provided accurate and reliable speed feedback, enabling precise control of the motor speed and improved motor performance.

3.4.4 Vibration Sensor for Motor Speed Feedback.

Vibration sensors can also be used for motor speed feedback, particularly in applications where high accuracy and reliability are critical. Vibration sensors detect changes in the mechanical vibrations of the motor and generate an electrical signal based on the detected changes. This signal can then be processed by the motor control system to accurately determine the motor speed. However, vibration sensors are typically more expensive than Hall sensors and require careful installation and calibration to ensure accurate speed measurement. Additionally, vibration sensors may not be suitable for all types of motors and operating conditions.

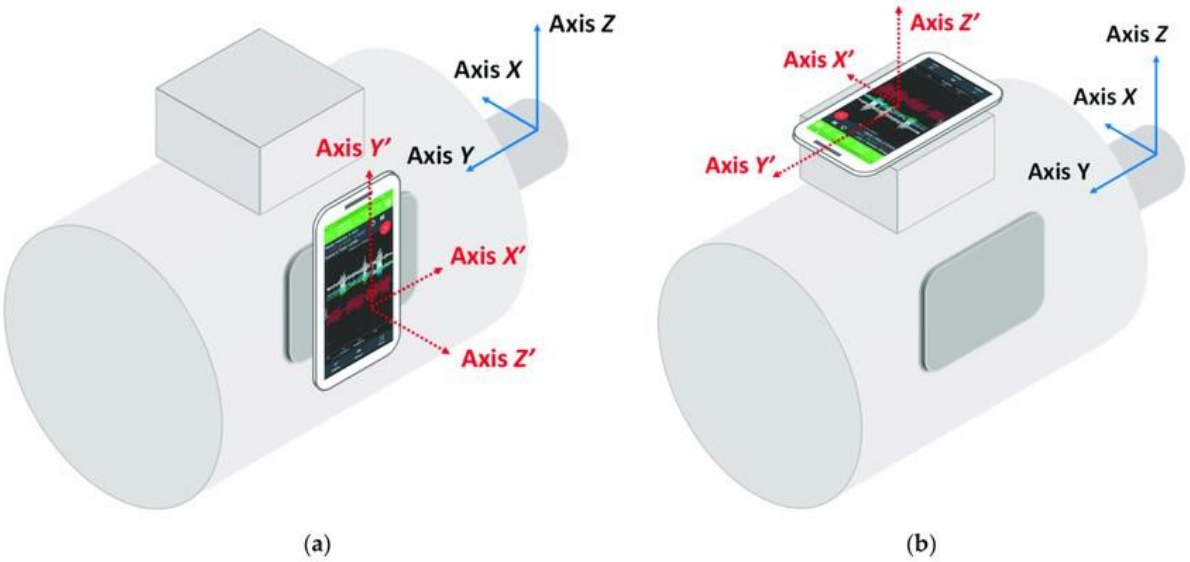

Figure 3-12. One of the vibration sensors method proposed in literature[122].

Typically, vibration sensors are more expensive than Hall sensors. However, a study in the literature [122] presents a low-cost and non-intrusive method for measuring motor speed, as shown in Figure 3-12. This method utilizes the accelerometers integrated on a smartphone to record the vibration signal. The signal is then sent to MATLAB and analysed using an algorithm that recognizes the mechanical frequency of the rotor shaft from the spectrum of the vibration signal. This approach offers an innovative solution for motor speed measurement that is both cost-effective and easy to implement.

3.5 Discussion

Motor speed signal modulation has been widely used in various applications to transmit information about motor performance, control, and status. One of the suitable types of signal

modulation for motor speed is light signal modulation, which can be implemented in analogue or digital form.

In analogue light signal modulation, the motor speed signal is directly translated into changes in the intensity or brightness of a light source, which can be detected and interpreted by a receiver. For instance, the motor speed signal can modulate the intensity of a LED or a laser diode, where the changing intensity of the light corresponds to the varying motor speed. This analogue modulation technique can provide continuous and real-time information about the motor speed, allowing for precise monitoring and control.

On the other hand, digital light signal modulation involves encoding the motor speed information into discrete binary states, typically represented by on/off or high/low states of the light signal. This digital modulation technique can be more robust to noise and interference, and it can support data compression and error correction. Digital light signal modulation can be implemented using various modulation schemes such as amplitude-shift keying (ASK), frequency-shift keying (FSK), and phase-shift keying (PSK), among others[123-128].

The use of light as a medium for motor speed signal modulation offers several advantages. Light signals can be transmitted wirelessly, allowing for remote monitoring and control of motors. Light signals also do not interfere with electrical signals, making them suitable for applications in electrically noisy environments. Additionally, light signals can be easily directed and focused, enabling precise and targeted communication.

3.5.1 Motor speed feedback method for analog light signal modulation.

If the speed feedback signal is processed in analogue form, such as using a current voltage sensorless speed control method, it involves transmitting the current and voltage information as light signals to a signal receiver at the appropriate amplitude. The calculated speed signal, obtained through an estimation method, can be directly modulated to correspond to the intensity of the light signal.

The analogue signal of motor speed estimation method has many types, which include synchronous speed tracking [129], and inject voltage commands in synchronously rotating reference frame [130]. The speed feedback method with higher precision should be selected according to the actual situation. However, it's worth noting that analogue signal processing may have limitations in terms of signal quality and noise immunity compared to digital signal

processing. Analogue signals can be susceptible to signal degradation and noise, which may affect the accuracy of the speed feedback information. Additionally, analogue signal processing may require careful calibration and adjustment to maintain accuracy over time.

3.5.2 Motor speed feedback method for digital light signal modulation

Many sensorless methods or sensors are extracted the speed signal from the gained original pulse signals, which are suitable for digital modulated light signals. Digital signal will be easy to translate and conduct, which can simplify the system complexity.

In sersorless method, the motor speed signal is extracted in the pulse or peak of the current signal. In brushed DC motor, due to the brush will run at different position of the segment when commutation, the resistance in armature loop will change which cause the current ripple [91]. Different number of segments will produce different number of ripples when motor has run in one cycle. The motor speed can be determined by the time cost in counting the number of ripple peaks in one cycle duration. The relationship between the segment number and the number of ripple peaks in one duration is shown as formula (3-1):

$$\begin{cases} S = 2 \cdot k \cdot p, & k\ is\ odd \\ S = k \cdot p, & k\ is\ even \end{cases} \tag{3-1}$$

where k is the number of commutator segments and p is the number of pole pairs. The S is the number of the ripple peaks in one cycle duration which can be generated as a digital signal of motor speed by light signal transmission. This method is weak at high-speed range, with high error. In order to optimize the feedback result, the method called Kalman filter estimator is fused with the original feedback result [92]. The performance at high-speed range is improved.

In induction motor, the speed can be determined by pulses from slot harmonics included in the negative-sequence current, and a method of elimination of saturation harmonics using high-pass filter. The rotor speed is estimated by counting the zero-crossing points of the slot harmonics [131]. The speed value then can be set as digital signal and transferred by light signal.

Some type of sensors which can generate pulse signals are suitable for digital modulation. For example, Hall sensor can detect the position of the rotor in the shaft. In the time duration, the number of pulse or segments of rectangular wave will be produced as it is proportion to the motor speed, for hall sensor could just detect some part of positions of rotor [132].

3.5.3 Proposed motor speed feedback method for laser powered actuator

In order to wirelessly transfer signals, light signal transmission is considered the most suitable method for laser-powered actuators. The key factor lies in the type of signal generation. There are two types of light signal generation: analogue and digital. The choice between them depends on the type of motor speed signal obtained from the motor. Different methods of motor speed feedback will yield different types of motor speed signals. The corresponding modulation structure depicted in Figure 8.

Among the closed-loop motor speed feedback methods for laser-powered actuators, the sensorless motor speed feedback method offers several advantages such as cost-effectiveness, simplified system design, and improved efficiency. It is widely regarded as the primary choice. The ripple counting method used in brushed DC motors can generate digital pulse signals, which are suitable for digital light signal modulation. This method is ideal for laser-powered actuators.

However, if high accuracy is required for a specific application, sensors are necessary. These sensors can provide precise signal feedback, which can be further enhanced by integrating them with algorithms to improve reliability. It is important to note that using sensors will increase system complexity and cost.

3.6 Summary

This section focuses on exploring a wireless method for motor speed signal feedback in laser powered actuators. Considering its high efficiency and conductivity, light signal transmission is chosen as the wireless transfer method. The light signal transmission system consists of a light emitter and a light receiver, which are reviewed in this study. When it comes to the light emitter, LEDs are preferred over LDs due to their better signal modulation capabilities and energy-saving characteristics. The main consideration for light signal modulation revolves around two types: analogue and digital. To ensure efficient operation and compatibility with the system, it is important to select a motor speed feedback method that aligns with the signal type. The sensorless method stands out due to its cost-effectiveness, simplified system design, and improved efficiency. For laser powered actuators, the proposed ideal method for motor speed feedback involves the use of the ripple counting technique with digital light signal modulation, specifically designed for brushed DC motors. If higher accuracy is required,

incorporating sensors along with optimization algorithms becomes necessary. This combination allows for precise signal feedback and enhances reliability. However, it's important to note that the inclusion of sensors also leads to increased system complexity and cost implications.

Chapter 4 Simulation on Laser Powered Actuator and its Close-loop Control System

The wire connection under harsh environmental conditions (high temperature or high radiation) results in many limitations. Laser power transmission (LPT) is regarded as a convenient conduit for power delivery wirelessly. LPT has many benefits, which include zero electromagnetic interference, immunization from temperature and radiation, and long transmission distance. Based on the LPT structure, an LPT powered actuator system is proposed. Studying through simulation, the steady-state characteristic of the system is analysed, and the result shows the steady-state characteristic mainly depends on the load torque. A robust speed control method is proposed by feedback of the DC motor speed to determine the laser on/off state to adjust the speed. The simulation result indicates that in the analysed-controllable range, the speed is stably controlled.

4.1 Proposed System Structure and Control Strategy

4.1.1Maximum speed and torque under constant incident laser condition

The proposed LPT actuator for DC motors consists primarily of the energy transmission and load blocks. The energy transmission block is by LPT, which contains a laser diode and a PCM. LD is a type of electric-to-photo equipment that has a high conversion efficiency, a smaller size, and requires less power to operate. The PCM is different to solar panels in that it has high power conversion efficiency at a certain wavelength of the incident laser. In general, the energy transmission block will transmit energy as efficiently as possible. In the load block, there is just a DC motor without any amplifiers. This is under consideration to simplify the system and reduce energy consumption. Hence, LD is the only controllable equipment in this system.

The first step is to identify which power point of the PCM drives the DC motor in a steady state with a certain external loading. The system schematic structure is mainly shown in Figure 4-1. The irradiance lever of the laser emitter is adjustable, and the PCM is mainly concerned about the irradiance level received. The DC motor is connected at the end of the PCM with a changeable external load torque. The system is proposed to work under high radiation and

harsh conditions, hence on the receiver side the most common power electronics devices often utilized are no longer needed. Therefore, power electronics devices such as capacitor or battery are not used. The photoelectric energy will directly drive the DC motor and other devices and realize their basic working condition operation.

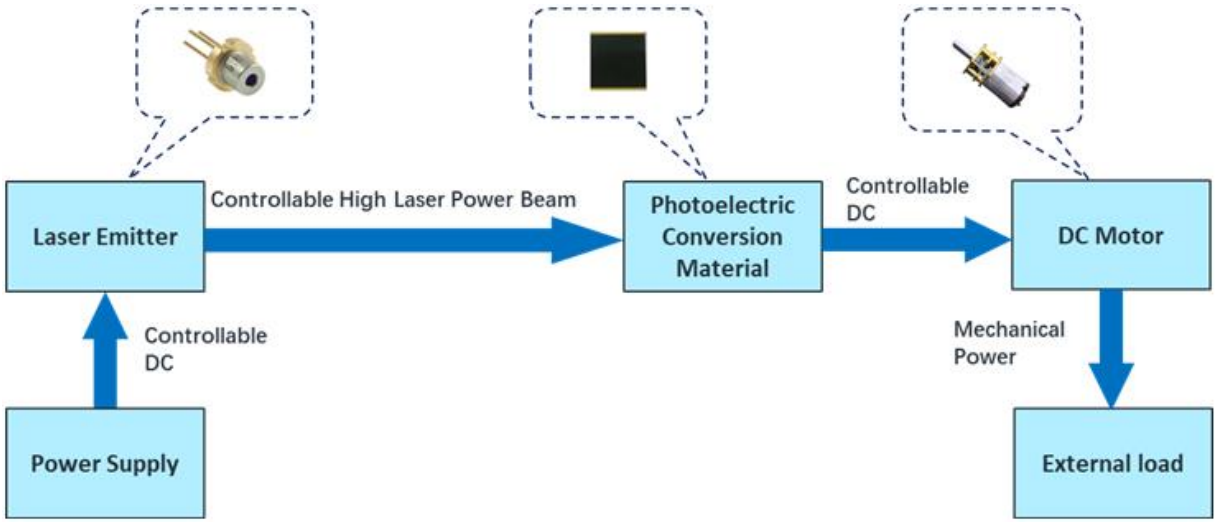

Figure 4-1. Proposed LPT actuator system structure for DC motor.

Theoretically, as for the application of a DC motor, the rotation speed ω is determined by the equation which is given as:

$$U = k_e\omega + RI \tag{4-1}$$

In this formula, the U is the armature voltage, k_e is the back potential coefficient of the motor, or torque constant, which is related to the structural parameters of the motor. The R is the total resistance of the armature loop, whereas I is the armature current.

From this formula, it can be observed that if the motor reaches the highest speed, the armature voltage will be at its maximum value at which stage the current is zero. In Figure 4-5, the maximum value of the voltage is the open circuit voltage V_{op}. Consequently, the theoretical maximum speed of the motor can be expressed as:

$$\omega_m = \frac{V_{op}}{k_e} \tag{4-2}$$

On the contrary, when the motor speed is at 0, it will have the maximum output torque. It is different from the open circuit voltage in that the power point cannot be the short circuit current point because the voltage cannot be zero. In a DC motor, the output torque is directly

proportional to the armature current. Therefore, the power point of the maximum output torque Tm will be a known point when the motor is working at the maximum current it can reach.

For analysis of the maximum torque point by a mathematical method, the current is proportional to the external load torque. When the speed is zero, by substituting in formula (4-1), the maximum load torque will satisfy the equation as:

$$I_{mt} = \frac{V_{mt}}{R} \tag{4-3}$$

where V_{mt} and I_{mt} are the voltage and current at the maximum torque point, respectively. This point is on the output curve of the PCM.

4.1.2 Closed-loop control of the motor speed theoretical study

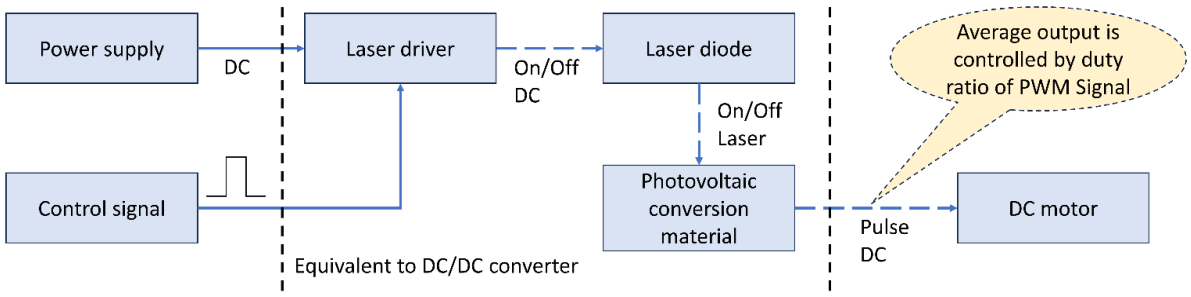

Figure 4-2. Characteristics of proposed system control method comparing with PWM.

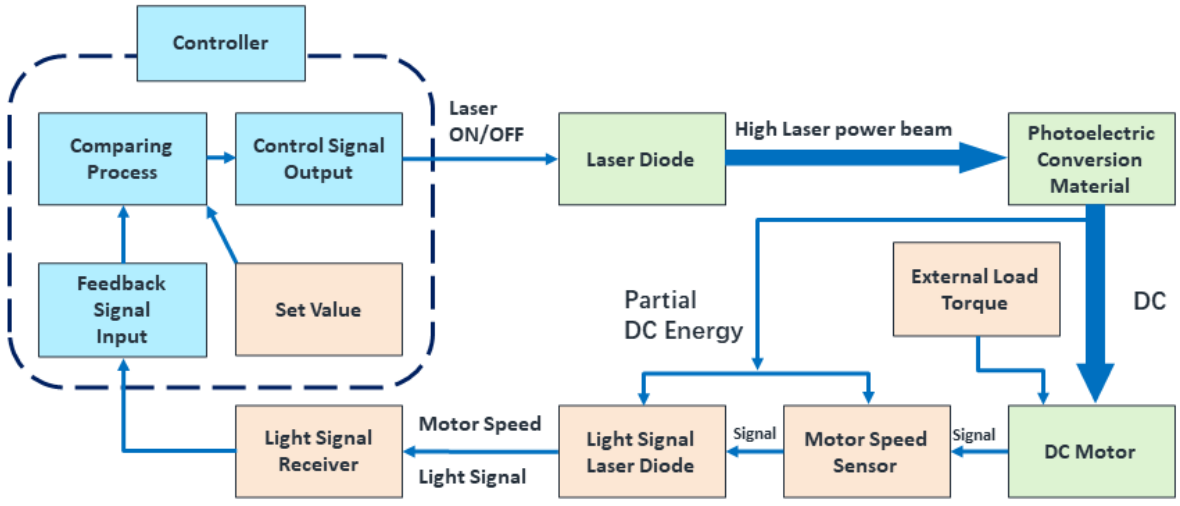

Figure 4-3. Proposed system control strategy schematic diagram.

In existing DC control strategies, the PWM method is widely used, and its basic principle is to adjust the duty cycle of a square wave signal in order to get the average output current adjusted.

If the laser emitter were driven by a pulse-controlled source to deliver a pulse laser to the PCM, the average output power could be theoretically changed. For the motor side, its control effect on the motor is the same as the PWM, as shown in Figure 4-2. The LPT system is equivalent to a DC/DC converter and the steady-state average output of PCM will be determined by the duty ratio. Since the existing research has not shown the exact relationship between the incident laser and the external load torque, an adaptive control method cannot be adopted yet. Under this condition, a robust control is proposed to adjust the laser on and off. The key element of the system is giving feedback of the motor speed to the control unit to determine whether to open or close the laser. The control logic is that if the actual motor speed is less than the reference value, then the laser is on. If not, turn the laser off. Since the speed of optical signal propagation is much greater than the change in motor speed which only varies in 0 to 70 rpm, the delay problem can be ignored. Based on this method, the closed-loop control system structure is shown in Figure 4-3. The system aims at maintaining the DC motor speed at a default value. The controller is in front of the LD, which receives the rotation speed signal from the DC motor and determines the laser on/off status to change the output of PCM to control the DC motor speed by comparing it with the set value. The control block diagram is exhibited in Figure 4-4. The system is proposed to work under high radiation and harsh conditions. Hence on the receiver side the most common power electronics devices are no longer applicable. Therefore, power electronics devices are not used. The photoelectric energy will directly drive the DC motor and other devices and realize their basic working condition operation.

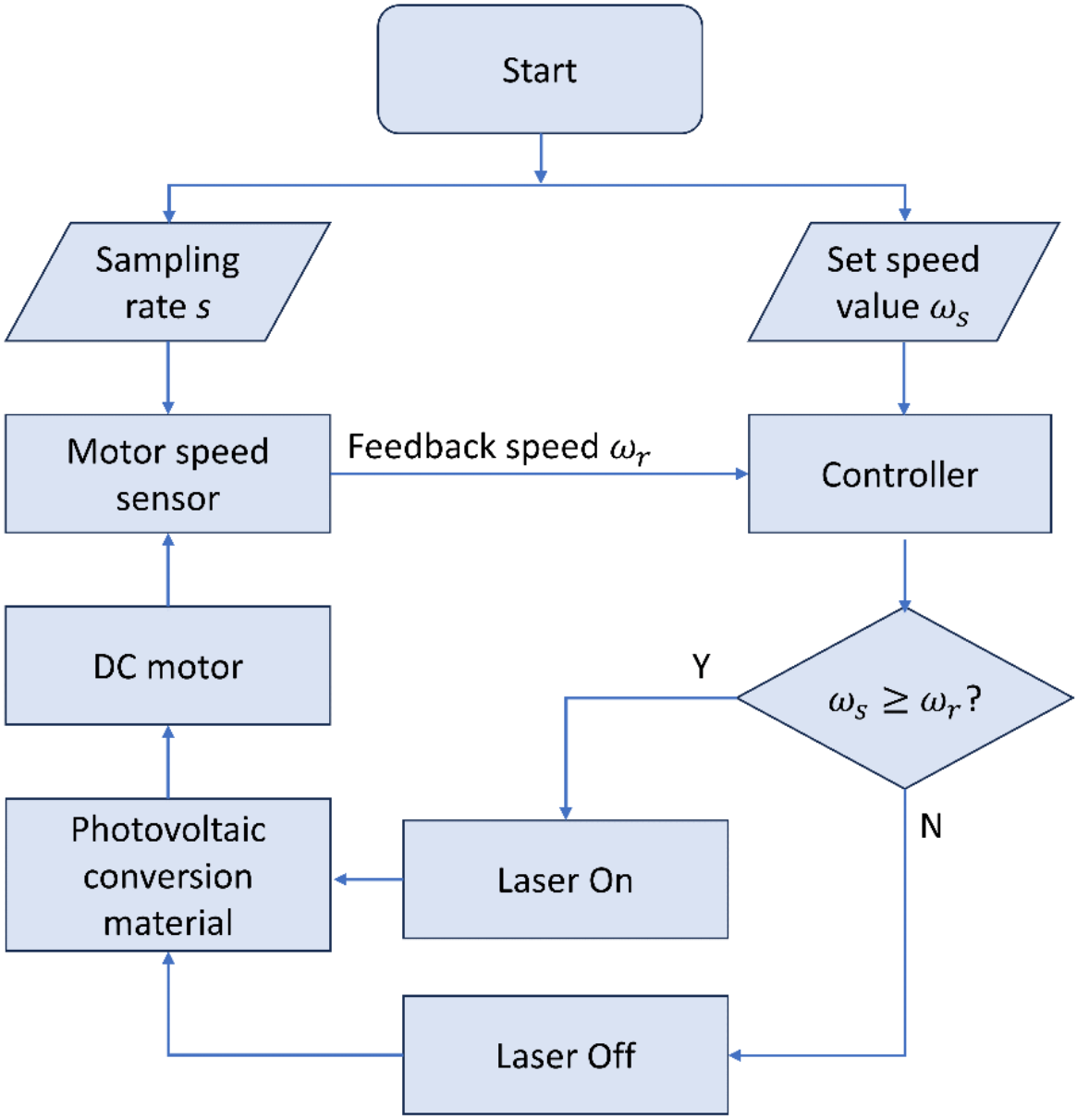

Figure 4-4. The proposed system control strategy schematic diagram.

When the reference value of the motor speed is set, the upper load torque the DC motor can afford is limited. This is because the over torque will reduce the upper speed of the motor, which causes the reference value to become unreachable. Theoretically, the output torque of the DC motor is proportional to the armature current. The equation is shown as:

$$T = k_m I \tag{4-4}$$

Where the k_m is the moment coefficient. Under the condition in which the speed is set, according to formula (4-1) (4-4), the maximum torque T_r under condition of the set speed ω_r can be calculated as:

$$T_r = k_m(\frac{U-k_e\omega_r}{R}) \tag{4-5}$$

The $\omega_r$is the reference rotation speed. Hence, when $0<T<T_r$, the proposed method works. If $T_r<T<T_m$, the motor will still work but cannot reach the reference motor speed.

On the other hand, when the external load torque is constant and the speed is variable, that means the system will have a maximum rotating speed. If the set speed is greater than this maximum value, the laser will be continuously on and work at maximum speed. According to formular (4-1), (4-3), the maximum motor rotation speed can be written as:

$$\omega_r = \frac{Uk_m-TR}{k_ek_m} \tag{4-6}$$

Where ω_r represents the maximum rotating speed with a certain torque *T*. Consequently, when $0<\omega<\omega_r$, the system can be controlled at the desired speed. If the set speed is larger than this maximum speed, it is unreachable.

4.1.3 Variable torque control by increasing the laser power at the maximum power point of PCM.

The literature[133] indicates the relationship between the current at the maximum power point I_m and the irradiance level $G(W{\cdot}m^{-2})$. Considering that the temperature influence is ignored, the equation is given as:

$$I_m(G) = I_m(STC)\frac{G}{G(STC)} \tag{4-7}$$

$I_m(STC)$ and $G(STC)$ are the standard condition values of maximum power point current and irradiance level, respectively. When the irradiance level changes, the spot size S (m^2) does not change. With laser power $P = GS$, and using formula (4-4), the laser power at the maximum power point P_{laser} with torque T can be expressed as:

$$P_{laser} = T\frac{P(STC)}{I(STC)k_m} \tag{4-8}$$

This formular can be regarded as the closed-loop feedback function to determine the output power of the laser when the external load torque changes. However, by means of this method the motor is working under the condition of the maximum power point of one certain laser power. If the torque at the maximum load torque point as described in formula (4-3) is less than this maximum power point, the motor speed cannot be determined. When the load torque increases, to determine whether the torque can be driven by increasing the laser power as

exhibited in formula (4-8), the maximum power point under the condition of this power value should be at the right side of the maximum torque point. Considering that the maximum torque point satisfies formula (4-3), the maximum power point needs to satisfy the equation as shown below:

$$\frac{V_m}{I_m} > \frac{V_{mt}}{I_{mt}} = R \tag{4-9}$$

In the equation, V_m is the voltage at its maximum power point, and R is the total resistance of the armature loop. By this method, the motor can be driven by increasing the laser power when the load torque increases, but the upper limit of the external load torque is determined by formular (4-9). When out of range, the motor shows excessive load.

4.1.4 System efficiency analysis

The power efficiency of a current power supply is generally 85%[5]. The power conversion efficiency of LD and PCM from the review result is ideally 60% and 50%[5], respectively. A DC motor commonly has a power efficiency of about 80%[134]. The laser transfer process in media is dependent on the specific conditions, mainly on the abortion rate of the media and transmission distance. Theoretically, the total system delivery power efficiency is around 20%. The transmission power loss through atmosphere and fibre are mainly determined on the absorption rate of the components in air or the absorption of the fibre inner wall material, and the transmission distance. It is assumed that the situation is to work within tens of meters of the site rather than a long distance, so the transmission power loss can be neglected here. Although the transmission efficiency is low, the efficiency is enough to be used as a motor drive if the received and converted energy can satisfy the basic working conditions by choosing a suitable and powerful sufficient laser emitter. The energy requirements and efficiency of the receiving end will become the reference for selecting laser energy and power supply.

When the LD is working at the pulse mode, relevant studies show that for the same average power, the smaller duty cycle will have a larger efficiency. The equation of the relationship between the current and the output of the LD is shown in formula (4-10)[135], and the equation to express the conversion efficiency of LD in pulse mode is shown in formula (4-11)[27, 136].

$$P = \eta_d(i + I_{bias} - I_{th}) \tag{4-10}$$

$$\eta = \frac{D\eta_d(i+I_{bias}-I_{th})}{V_{LD}(Di+I_{bias})} \tag{4-11}$$

Where η and η_d are the conversion efficiency of the LD and the differential slope efficiency, respectively. The P is the output power of the LD. The D is the duty cycle of the pulse mode LD. The i and V_{LD} are the voltage and current through the LD. The I_{bias} is the basic current through the LD, which is a constant. The I_{th} is the threshold current of LD. If the current to the LD is less than the I_{th}, the LD cannot turn on.

In the control strategy of this paper, the altitude of the LD is set as a constant for 3W, which means the current is also a constant according to equation (4-10) and the average power of the LD is proportional to the duty cycle D. The equation (11) can be rewritten as:

$$\eta = \frac{\eta_d(i+I_{bias}-I_{th})}{V_{LD}(i+\frac{I_{bias}}{D})} \tag{4-12}$$

To turn on the laser, it should guarantee $i + I_{bias} - I_{th} > 0$. When the $I_{bias} > 0$, the increase of the D will cause the η to raises, which means the smaller duty cycle D will obtain a smaller conversion efficiency of LD. If $I_{bias} = 0$, the efficiency is only determined by the current to the LD and cannot be influenced by duty cycle D.

Literature[137] figures out that the conversion efficiency of PCM depends on the irradiation level of the incident laser. The relationship is expressed at equation (4-13).

$$\eta_{PCM} = \frac{V_m(STC)I_m(STC)}{SG(STC)} ln(e + b\Delta G) \tag{4-13}$$

Among these parameters, $V_m(STC)$ and $I_m(STC)$ are the standard condition values of voltage and current. ΔG represents the difference between known irradiation level G and the standard value $G(STC)$. Constants b is the compensation coefficients, which can be obtained by fitting many experimental data. It is worth noting that e is the base of the natural logarithm.

From equation (4-13), it can be easily found that the conversion efficiency of PCM depends on the irradiance lever of incident laser. The higher irradiance level will result in a higher conversion efficiency. Overall, increasing both the power and duty cycle of LD are helpful to enhance the total system efficiency.

4.2 Simulation Result

4.2.1 Applied system parameters

By comparing volt-ampere characteristics and power point movement, it can intuitively grasp the feasibility and the operation rules of the entire system. Based on the obtained steady-state parameters of the system, the control strategy can be effectively designed. The parameters of the applied PCM are exhibited in Table 4-1. Because the adopted laser diode is 3W, considering the idea efficiency is 50%, the output power would be 1.5W. The tested motor is set as a permanent magnet DC motor, and the main characteristics are shown in Table 4-2.

Table 4-1. Parameters of PV material block in simulation.

Maximum Power (W)	1.5
Open circuit voltage Voc (V)	2
Short-circuit current Isc (A)	1.7
Voltage at maximum power point Vmp (V)	1.5
Current at maximum power point Imp (A)	1
Temperature coefficient of Voc (%/deg·C)	-0.36099
Temperature coefficient of Isc (%/deg·C)	0.102

Table 4-2. Simulation DC motor main characteristics.

Armature resistance (Ω)	0.006
Armature inductance (H)	0.0012
Torque constant (N·m/A)	1.8

4.2.2 Steady-state power point workplace

Firstly, the steady-state characteristics of the system are studied, which include armature voltage, armature current, and motor rotation speed, to determine the steady-state influence factors. The external load torque is changed from 0 to 3 in diverse groups. Due to this part of the simulation just identifying the characteristics of the steady-state work status of the DC motor, the temperature is set for 25 °C as the standard condition and the distance attenuation is not considered. The incident is 3W. The power output of PCM is set at 1.5W because it corresponds to the ideal maximum photo-electric conversion efficiency of 50%.

As shown in Figure 4-5(a), the voltage gradually rises until it finally reaches the steady-state value. This steady-state value decreases as the external load torque increases. When the current first reaches the short-circuit value in Figure 4-5(b), it begins to fall and eventually settles at the steady-state value. This steady-state value of the current is also determined by the motor load torque, which satisfies formula (4-4). As a result, because they are proportional, the higher the external load torque, the higher the armature current. After the current drops, the voltage starts to rise. The steady-state voltage is determined by the steady-state current at a certain power point. The rotation speed tends to increase continuously until it reaches the steady-state value, as shown in Figure 4-5(c), and it is also determined by the steady-state current. According to Figure 4-5(d), the steady-state power point begins at the open circuit voltage point and increases as the load torque increases. When the load torque is gradually approaching the maximum power torque, power then goes down to the maximum output torque point. Hence, the output at the maximum power point is not holding the maximum output torque, and there will be a maximum work efficiency torque value at the maximum output torque according to formula (4-4).

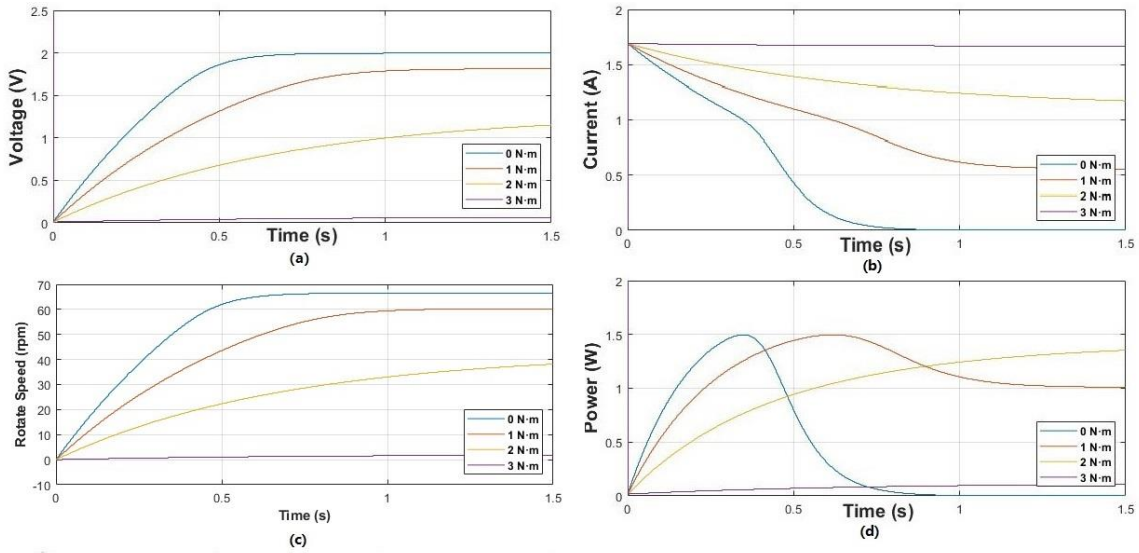

Figure 4-5. Time order tendency chart for (a) voltage (b) current (c) rotational speed (d) power point

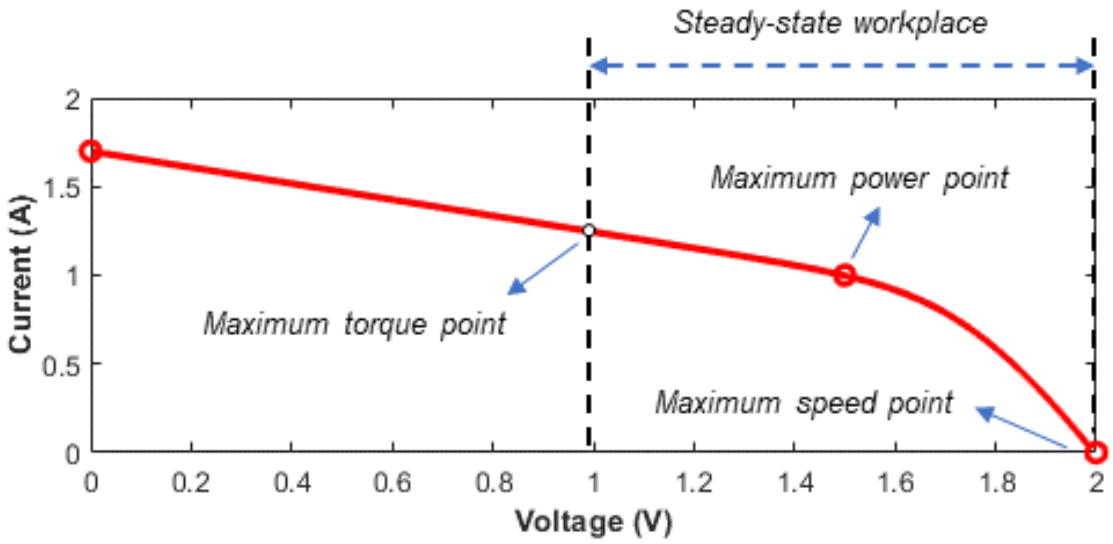

Figure 4-6. Steady-state workplace of power point as a DC motor drive.

According to the results in Figure 4-5, the proposed LPT system could realize the motor actuator function. The output current, voltage, and motor speed are mainly dependent on the external load, and the steady state workspace is between the maximum output torque point and the open circuit voltage power point, which is shown in Figure 4-6. From formula (4-2), it is known that the maximum speed point is also the open circuit voltage point. If the load torque is greater than the maximum output torque, the work point will move from the maximum speed point to the maximum power point and then fall to the maximum torque point.

Another thing that needs attention is that at zero time, there is a peak in the voltage curve with a high value. In order to observe the tendency of the whole curve, the axis is narrowed. By analysing this phenomenon, the motor load is a resistive inductive load. When the laser is on at 0 time, the current is 0A. According to formula (4-1), the voltage will be very high. This produces such a high voltage peak. When the current is increased to the maximum current value to accelerate the motor, the voltage goes down to the normal level.

The efficiency of the LPT system is mainly determined by the efficiency of the laser and PCM. The laser works on continuous mode, so the efficiency is constant. The efficiency of PCM is changed by steady state work power point moves. Hence, if the output power of PCM is higher, the total system efficiency will also be higher. The maximum power point will have the maximum total system efficiency.

4.2.3 Closed-loop control of the motor speed with laser on/off

For the same experiment equipment above, the laser on/off controller is added. This controller mainly controls the laser on/off status by comparing the received motor speed signal and the preset motor speed value. In this simulation experiment, the reference speed value is set as 30 rpm. The load torque is a random value which varies from 0 to 3, as in the affordable range. The torque is changed every 0.5 seconds to detect the adjusting effect. As the typical PWM frequency is lower than 10kHz, it will reduce the steady-state fluctuation range in real application, and the controllable range of low-speed and high-speed intervals with higher switching frequency requirements becomes narrower.

Generally, the speed is well controlled in the controllable range as shown in Figure 9. The voltage vibrates at a large altitude when the load changes. Because the laser is in pulse mode, the steady-state voltage fluctuates around the steady-state value. The current starts at the short circuit current value. After a fluctuation, it reaches the steady state. As compared with the load torque, the steady-state current value is approximately proportional to the load torque, as in formula (4-4). Every time the load torque is changed, the current will change after a certain fluctuation. Within 2~2.5s, 3.5~4s and 9~10s, the torque is too large to exceed the control range described in formula (4-5). From 4~9s, the load torque is within the controllable range, the speed is equal to the aimed value. Consequently, in these periods, the laser keeps on, but the speed cannot reach the aimed value. In other periods, the laser works in pulse mode in which case the speed is controlled well.

One thing worth noticing is that every time the load changes, the voltage has two peaks in different directions, with the upward one emerging larger than the downward one. At the same time, the current tends to have a peak with the direction been determined by whether the steady-state value is going up or down. Under the condition of the external load torque increases, the steady-state value increases, and the current is rapidly increased as the laser keeps on. This increased current becomes the up peak. From formular (4-1), if the motor load is a resistive inductive load, the voltage downward peak appears. When the motor speed reaches the pre-set value, the motor brakes and gets into a steady state. This break action needs the laser off to decrease the current. Consequently, the voltage will rapidly increase at this moment to become the upward peak. On the contrary, if the external load torque decreases, the laser will first turn off to slow down the motor speed. Hence, the flow dramatically drops. This

action causes the downward peak. According to formula (4-1) and the characteristics of resistive inductive load, the voltage upward peak appears. When the speed is down to the reference speed value, the laser changes to turn on. This acceleration action causes the current to rise, and the voltage suddenly drops to produce the downward peak. Because these actions happen in an extremely brief time, they do not significantly affect the accuracy of the control system but do introduce some requirements for tolerance of the equipment.

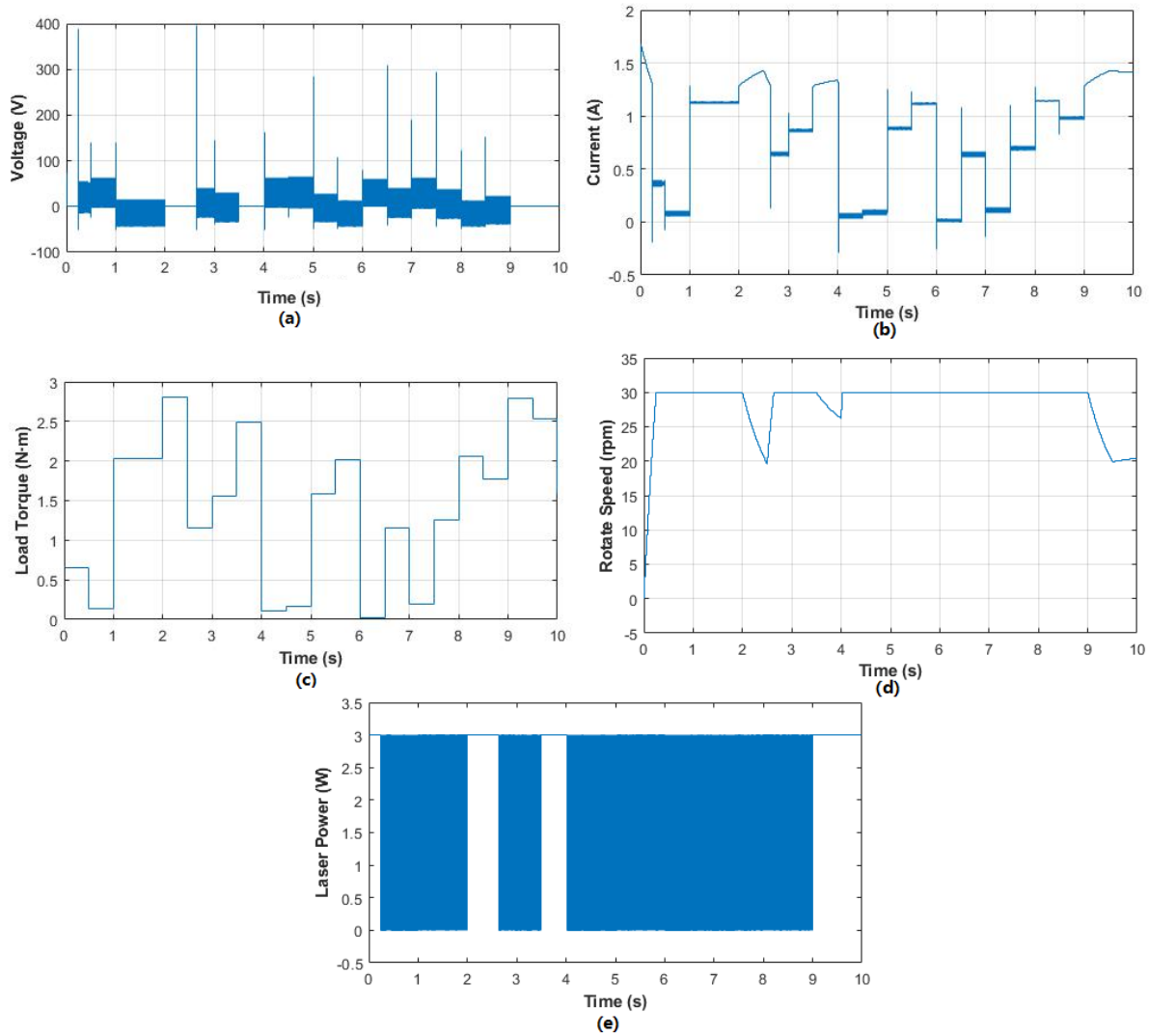

Figure 4-7. Closed-loop control time order tendency chart for (a) voltage (b) current (c) load torque (d) rotation speed (e) Laser power.

4.2.4 Closed-loop control of the motor speed with constant torque

In this model, the load torque is set as a constant of 1 N·m, and the reference speed is a variable from 0 to 120 rpm. The reference speed changes every second. This part of the simulation is

to capture how the characteristics reveal themselves at different speeds and with the same external torque.

From Figure 4-8, the voltage is also vibrating at the steady state. Generally, the average value of each part is approximately equal. The steady-state current at every part is the same as well. This situation further proves that the steady-state voltage and current are determined by the external load torque. Because the external load torque is constant, the steady-state current is proportional to the external load torque and the steady-state voltage is determined by formula (4-1). When the reference speed is out of the controllable range, as the formula (4-6) exhibits, the laser will stay continuously on, and the speed will be at the maximum speed under this external torque. It is clear that the steady-state current is constant between the intervals of 2~5s and 6~8s according to Figure 4-8. In 4~5s and 7~8s, the speed value is constantly at the maximum under the condition of the torque. The vibration will increase as the difference between the reference and maximum speeds increases. This is due to the steady state on/off duty ratio of the laser being larger when the reference speed is closer to the maximum speed.

The peaks also happen in voltage and current curves. Compared with the speed change in Figure 4-8 (d) and (e), the speed acceleration and brake obviously prove the peak direction of current. When the motor is accelerating, the peak is upward. When the motor is braking, the peak is downward.

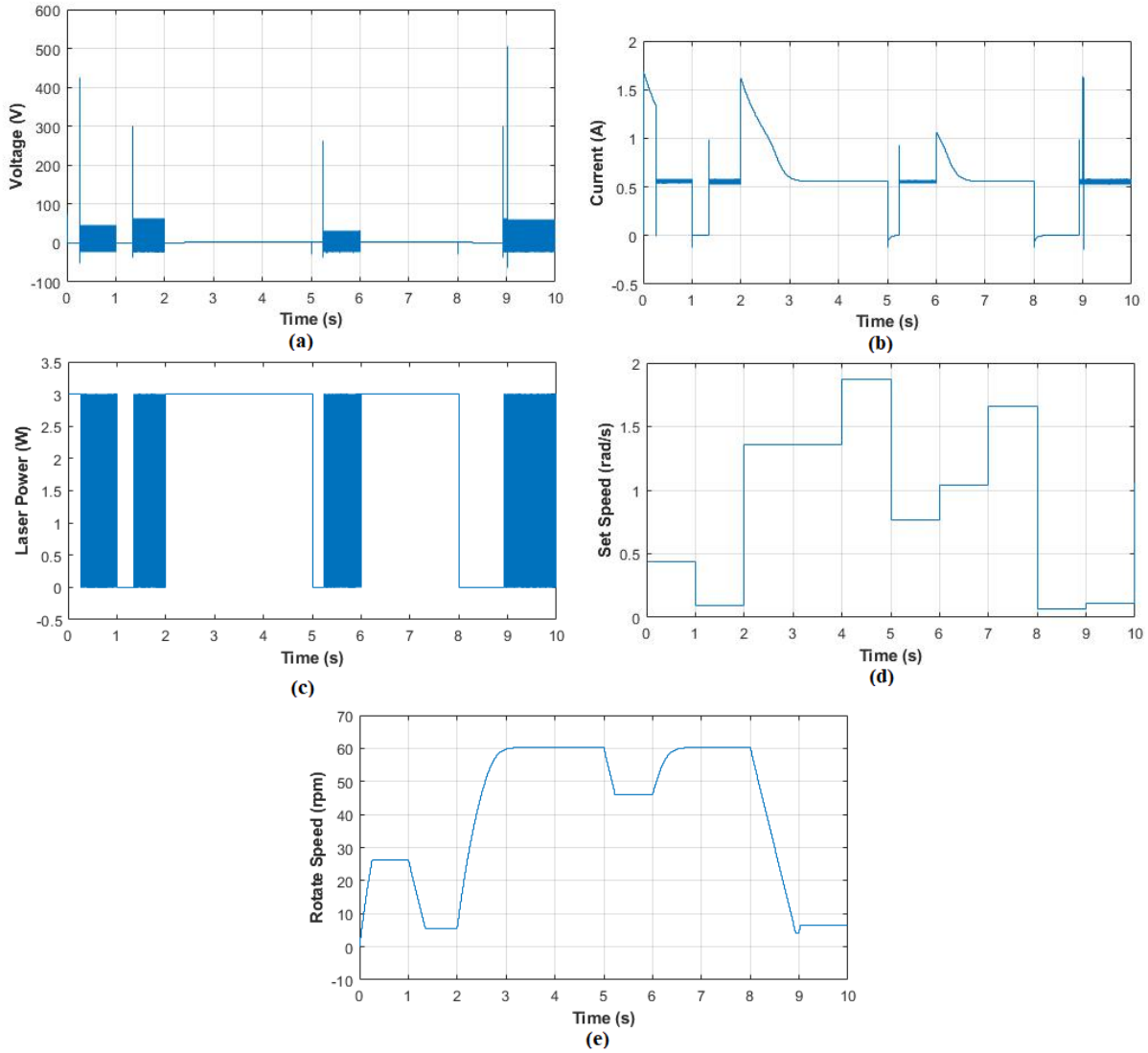

Figure 4-8. Constant torque closed-loop speed control time order tendency chart for (a) voltage (b) Current (c) Laser (d) Reference speed (e) Actual speed.

4.2.5 Closed-loop control of the motor torque

In this part of the simulation, the external load torque is set as a random variable, and the range is from 0 to 10 N·m. As formula (4-8) expresses, the incident laser power is determined by the feedback signal of the external load torque. The external load changes every 0.5s. The result is shown in Figure 4-9.

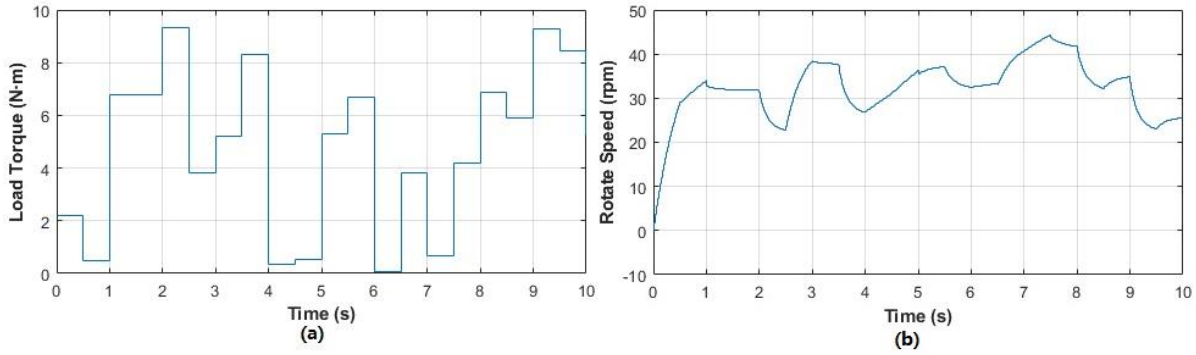

Figure 4-9. Closed-loop torque control time order tendency chart for (a) Torque (b) Rotate speed.

From Figure 4-9, it is obvious that the motor can be driven at this range of the external load torque when the motor speed is greater than 0. One thing to keep in mind is that when the load torque is rapidly increased, for example, 2~2.5 s, 3.5~4 s, and 9~9.5 s, the speed decreases rapidly. This is because of formula (4-9). When the laser power increases, the maximum power point is gradually approaching the maximum torque point of the PCM output. Another observation is that when the load torque rapidly decreases, the speed suddenly accelerates to a large value.

The relationship between the maximum power point and maximum torque point under this control method is shown in Figure 4-10. Besides increasing the external load torque, if the inner resistance becomes larger, the maximum power point will also be closer to the maximum torque point. If the maximum torque point is on the right side of the maximum torque point, the motor cannot be driven. Consequently, the maximum torque is reached when the work point is moved at the maximum torque point with the laser power increasing.

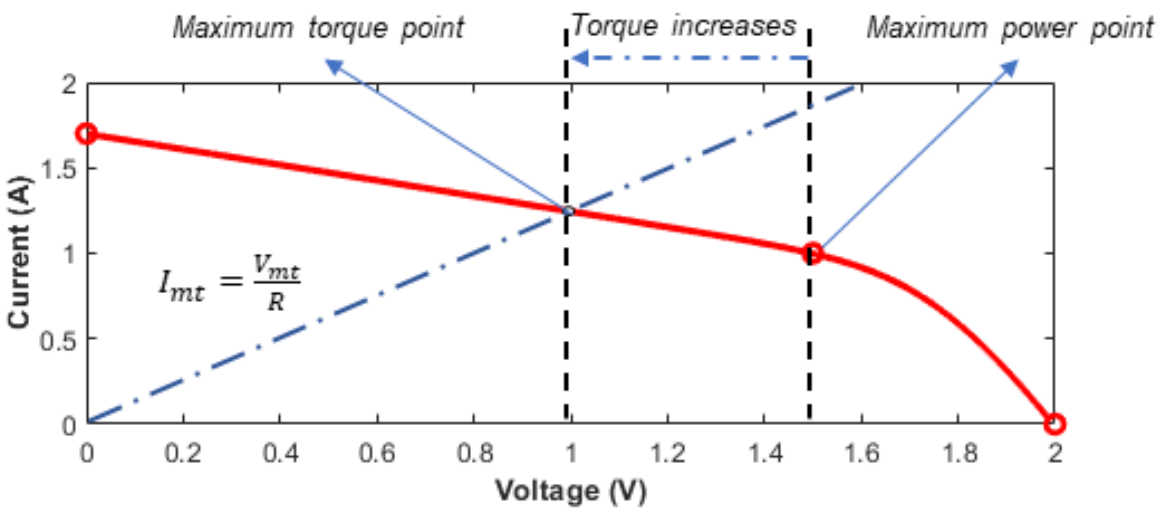

Figure 4-10. Relationship between maximum torque point and maximum power point for motor work by PCM output.

4.3 Discussion

The LPT system can work as a DC motor actuator, as the results show. Without power electronics elements, directly driving the motor can simplify the energy integration and control processes and avoid external energy losses. The simulation work has found out that the motor armature voltage and current in steady state strictly corresponds to the point on the output curve of the PCM. By changing the external load torque, the current becomes proportional to the external load torque. This is the key rule when the external torque changes to determine the current. When the current is obtained, the voltage can be found on the curve by corresponding to the current, as shown in the simulation data. Based on this rule, the steady state workplace is proposed between the maximum torque point and the maximum speed point. After theoretical analysis, the maximum speed point is the same as the open circuit voltage point and the maximum torque point is determined by formular (4-3). At the maximum speed point, the external load torque is zero. And the speed at the maximum torque point is also zero. This steady state workplace mainly demonstrates when the motor is working, the values of the voltage and the current will be at a certain point inside the range. This will be an important criterion to judge whether the motor can be driven by the LPT system. Consequently, if the laser power is not changed, the external torque should be no more than the value corresponding to the maximum torque point.

In the application of motors, it is often necessary to control the speed. If the speed is set as a constant value and the load torque varies, the average input power of the laser to the PCM needs to be changed. By changing the laser work mode as an on/off pulse it can change the input power, thereby achieving the desired speed control. The laser on/off is determined by comparing the feedback speed value with the set value. If the set value is larger, the laser is on. Otherwise, the laser is off. The control simulation result shows the motor is almost controlled at the set value. At some point, the external load torque is out of the upper limitation, this scenario is described in formula (4-5), where the laser is continuously on, and speed cannot reach the set value. On the other hand, when the load torque is constant, the rotating speed varies. By the same control method, the speed is also controlled at the set value except in areas which are out of the acceptable range which is described in formula (4-6). The steady-state current of the average confirms that the current is determined by the load. While stable control is achieved, there are two limitations that need to be addressed. One is the issue of the laser on/off switching frequency being extremely high; requirements for practical devices need to be demonstrated by practical experiments. The other encumbrance is that the laser power is a constant. If the control range wants to expand, the laser power needs to be increased. By analyzing the relationship between the current at the maximum power point and the corresponding laser power, it becomes evident that if the load torque is known, the laser power can be determined. Consequently, the feedback signal of the external load torque can build up a closed-loop control system according to formula (4-8). The simulation result shows that within the limitation range of formula (4-9), the motor can be driven by increasing the laser power when the external load torque rises.

The above control methods work within a certain controllable range in insistences where the application is out of acceptable control range, the system cannot work. The system set up for the simulation was performed at low power levels. If the system were applied to large motor such as in several kilo watts, high-power lasers would be needed at current conversion efficiencies. This requires PCM with properties that can withstand high-power laser light. In addition, the impact of thermal radiation caused by high-power lasers on other equipment will also be taken into consideration. In general, this application at high power levels depends on the advancement of device technology. There is no need for high dynamic performance because no power electronics are used, only basic steady-state control is possible and is only required to meet the fundamental operating conditions.

4.4 Summary

In this chapter, an LPT motor actuator has been proposed to achieve long-distance wireless power transmission to drive a motor and control its speed. The power transfer efficiency of the examined LPT system is 20.4%, which is sufficient to become a motor actuator and it has been proven that the proposed control method can decrease the total system efficiency. The maximum and minimum motor rotation speed and torque have been calculated using the DC motor formula and PCM output characteristics. In addition, a method to control the motor speed by adjusting the laser turn-off has been proposed. This uses motor speed feedback value to compare with the set value to determine the laser on/off. The maximum torque after setting the speed is also given theoretically. Beyond the torque value, the system is outside of the controllable range. In the simulation to verify the steady-state characteristics, the steady-state power point mainly changes with the external load torque. The steady-state power point is finally located between the maximum torque point and the maximum speed point. At the 0-time will produce a high voltage peak, this is due to characteristic of resistive inductive load of DC motor. Within the control range, the rotation speed of the DC motor is stable at the set value, and the laser works in pulse mode. In this period, the load torque is out of control range, the laser is continually on, and the speed cannot reach the aim value. When the load torque is constant and the reference speed is variable, if the speed is larger than the maximum controllable speed, the laser will also be continuously on, and the motor will work at this maximum speed value. When the reference speed or external load torque is changed, the peak direction of current is to index the motor acceleration or braking to approach the next steady state. The voltage peak is determined by current changing rules.

The control range is mainly limited by the laser power and load torque. The key direction of the future work is to expand the control range by using the feedback signal of the load torque to control the amount of the laser power. The variable load, which is added to adjust the maximum power point to increase the total system efficiency and control the speed at the same time, will also be a way to promote the application.

Chapter 5 Experiment on Laser Powered Actuator

5.1 Introduction

In this section, the practical experiment will be conducted to identify the result which is gotten from the simulation work. High-powered lasers are deployed to illuminate a GaAs PCM. The PCM is subsequently used to power an electrical motor. Because the class 4 laser is used in atmosphere transmission, it will be hazard to both operator and flammable substances. In order to ensure the safety of the experiment process, a laser enclosure box is designed to prevent laser spillage. The voltage and current of the PCM output will be measured by a multi-meter. A STM32 NUCLEO F303RE board is used to read the speed value from the encoder on the DC motor. The increase the load of the motor will be by hanging weights.

5.2 Equipment

5.2.1 Laser Enclosure box and interlocks

There is a purpose-built lightproof metal box, with lid and safety interlock. If the lid is opened, the laser is instantly turned off. There is a key controlled, laser interlock, override switch for the initial laser alignment stage. This allows the laser to be switched on, with the lid open, during beam alignment. There are laser interlocks on the window blinds and lab door (which has a ‘laser on’ illuminated sign. If any of these are opened, the laser will be instantly turned off.

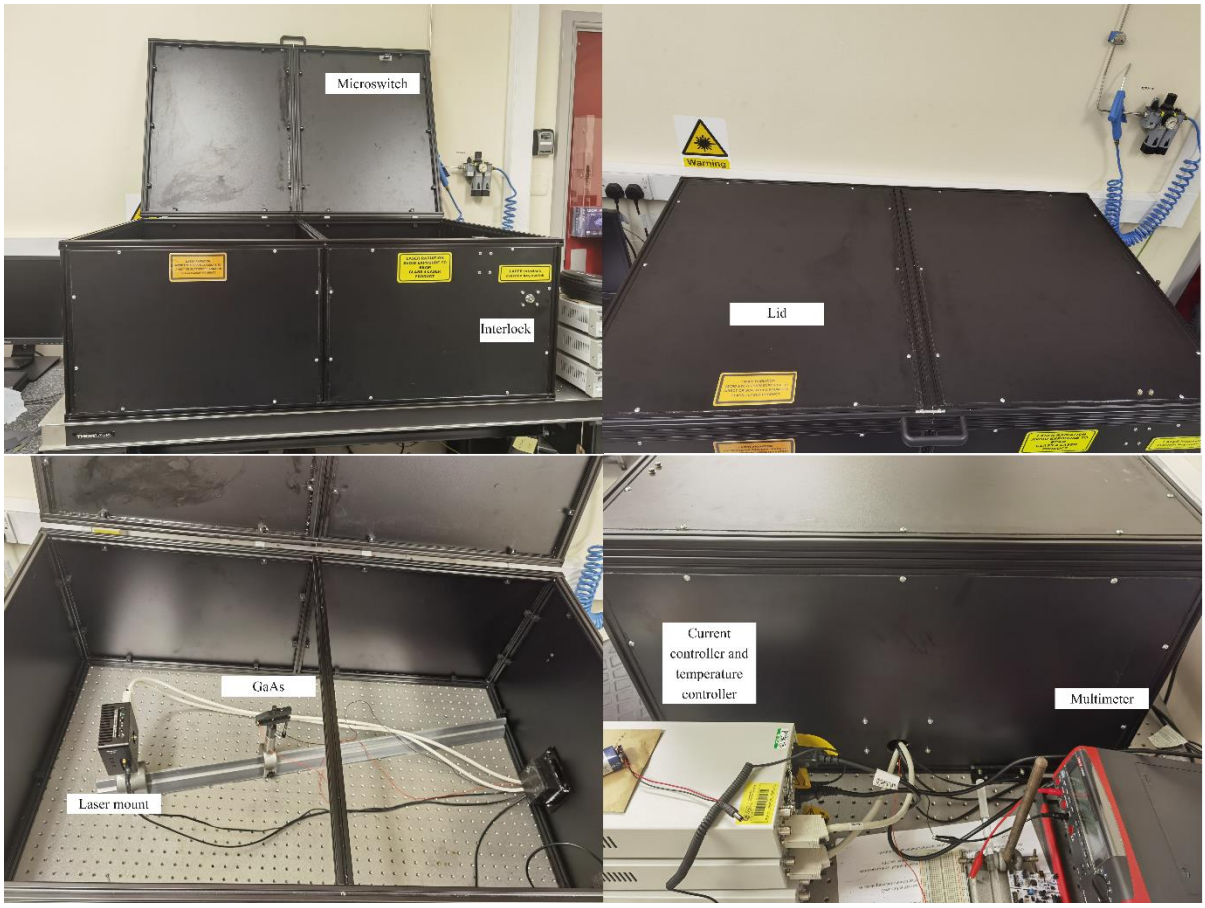

Figure 5-1. Laser enclosure box with interlock.

5.2.2 Laser power meter

A Thorlabs S121C 500 mW (400-1100 nm) light meter will be used to measure the laser output.

5.2.3 GaAs PCM

A HASUNOPTO GaAs with product No. HGSC-A100B-1N will be utilized as the PCM.

Figure 5-2. GaAs photovoltaic material.

The features and specifications include in Table 5-1:

Table 5-1: Features and specifications of GaAs used in experiment.

Features	Specification
High conversion efficiency three junction gallium arsenide battery	The typical efficiency of the chip is higher than 30%
Schottky bypass diode	The effective area of the chip is 99mm^2.
Low thermal resistance packaging for high thermal conductivity	The working temperature is -40℃ to 100℃
Ceramic substrate	Maximum tolerance temperature 180℃
Stress reducing stress design.	Thermal resistance below 0.23 centigrade /W
Gold band bonding	The substrate material can be customized according to customer needs (Al_2O_3, AlN).
Lead-free low void hole rate welding	Aluminium base, copper base, etc.
Plug and pull connection terminal.	The product has passed the IEC62108 test
Automatic encapsulation, high reliability	Through CQC golden sun certification

5.2.4 Lasers

- 642 nm, Pmax = 150 mW, Imax = 350 mA, continuous wave (HL6385DG)
- 447 nm, P_{max} = 3200 mW, I_{max} = 2500 mA, continuous wave (L450G1)

5.2.5 DC Motor and Multi-meter

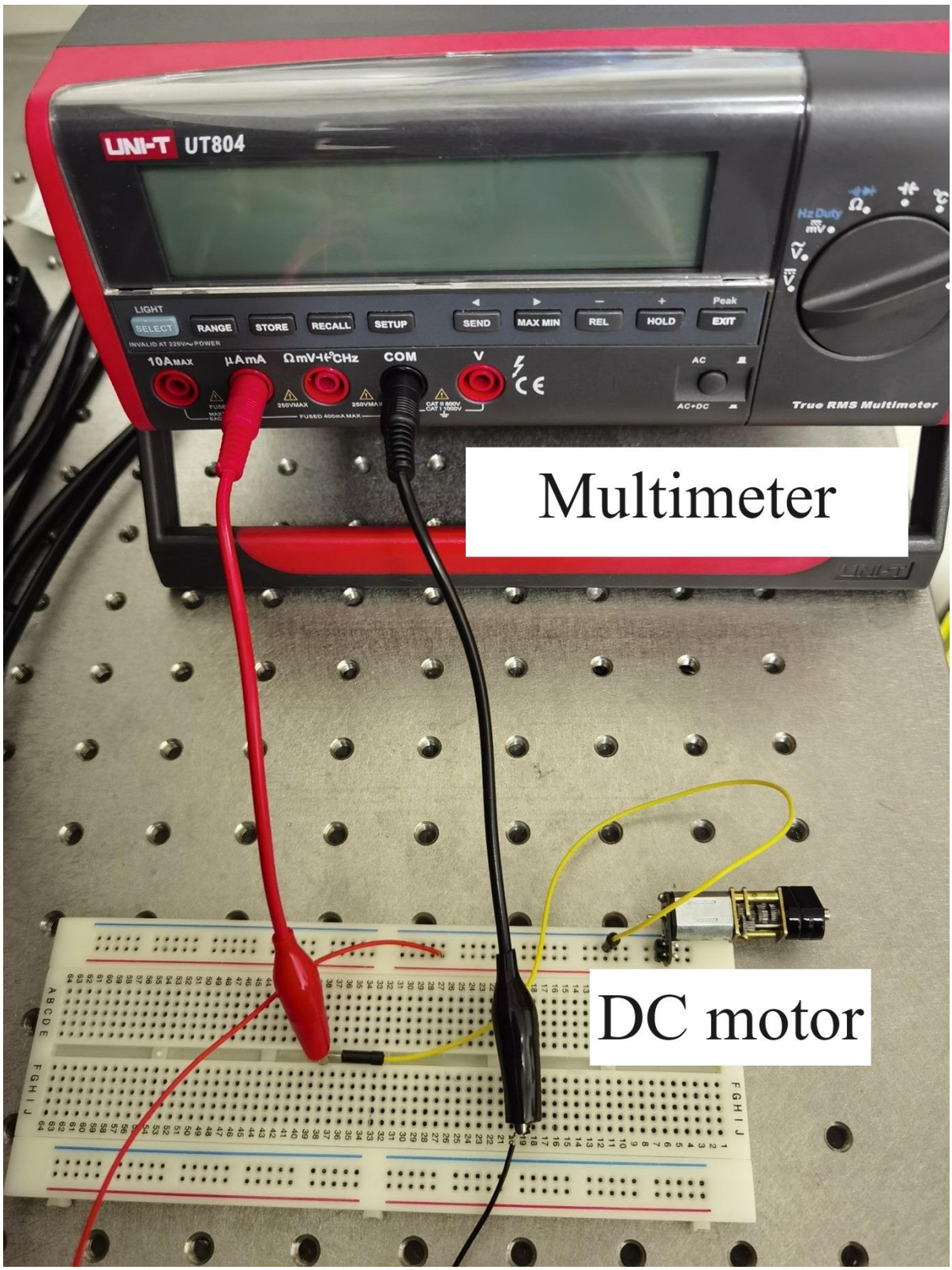

Figure 5-3. Multi-meter and motor.

- 3.3V, 20mA no-load current, DC motor (COM0802).

- LINI-T multi-meter (UT804)

The set up is shown in Figure 5-3.

5.3 Methods

Lasers must only be operated when they are attached to the beam expander/focusing device, see Figure 5-4. This makes viewing of the unexpanded beam impossible. DO NOT adjust the hard mechanical stop, that limits the spots size. The hard stop will be set so that the focus point of the laser is beyond the walls of the laser box and thus it is physically impossible to achieve dangerous laser intensities during the set-up stage. DO NOT use the laser outside of the box.

5.3.1 Establishing the Power Density on the PCM (one off set up)

1. Set the power limit on the laser controller to less than 5 mW.
2. Wear the provided set-up goggles. Switch on the laser and align the laser onto the power meter.
3. Place the provided 15% filter in front of the power meter and close the lid. Ensure the laser interlock is activated and the key is removed from the key switch. The filter is used to ensure the laser does not damage the power meter at high power settings. It also extends the power meter's measurement range.
4. Ensure, again, that the lid to the laser box is closed, then set the laser to the maximum required power and record the output value.
5. Repeat step 4 for different power settings, including those used in the laser alignment stage. This is done to calibrate the actual output of the laser after it has passed through the optical system. Plot this data in order to produce a calibration curve for later experiments.
6. Replace the optical meter with the PV cell. Ensure it is in the same location, distance and orientation as that of the power meter. The amount of light falling on the PV cell is known, by using the calibration curve in future experiments. The x axis is the power setting on the laser power supply, and the y axis is the reading from the power meter. These calibration curves account for optical losses in the set up.

5.3.2 Running the Experiment

- Close the lid and disengage the laser override switch.

- Increase the power on the laser control supply in increments, up to full power, to test the motor. Use the calibration sheet to determine the actual power reaching the PV cell and compare this with the torque on the motor.
- Consider varying the laser spot size. Ideally it should cover the whole PV cell. Follow steps 1 to 2, in section 3.1, to set the spot size.

5.3.3 Ending Experiment

- **Turn off the laser.**
- Ensure the laser interlock override is **NOT** disengaged.
- Allow the laser power supply to run down, i.e. for the capacitors therein to discharge.
- lift the lid on the laser box to access the set-up if necessary.

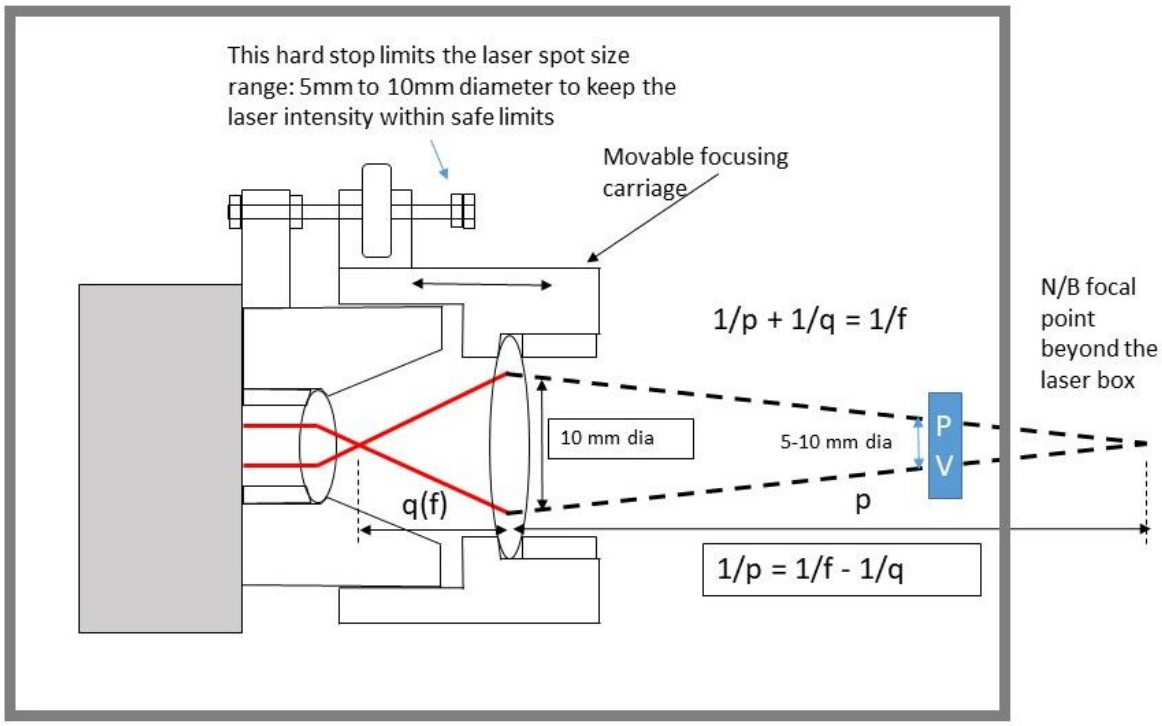

Figure 5-4. The schematic setup of the laser. This consists of a laser mount and cooler, laser optical expander and focusing unit, and a GaAs PV cell and mount. The optical expander/focuser cannot focus the laser to a point inside the laser box because it is beyond the wall of an, interlocked, laser enclosure box.

5.4 Experiment results

5.4.1 Beam expand/focus efficiency detection.

On GaAs PCM, only the part where is illuminated will generate electricity. The other part will become the load. This situation will cause total efficiency down. But for a single cell, stronger irradiation also achieves higher conversion efficiency. Therefore, this experiment will use a 1mW laser, to detect the output in different ration on both expand and focus the beam. The result is exhibited below:

Table 5-2. Output power and electric characteristics in different expand/fucus ratio

Ratio	Laser Power(mW)	Voltage(V)	Current(μA)
1：1.5	0.74	1.9166	44.66
1：2	0.82	1.9271	45.21
1：3	0.86	1.9266	50.44
1：4	0.96	1.9258	49.68
1.5：1	0.78	1.9226	46.68
2：1	0.85	1.9177	46.35
3：1	0.89	1.9166	46.96
4：1	0.9	1.9228	49.03

From the result, it is obvious that both expand and focus can increase the total power conversion efficiency. The more ratio will have the more efficiency. Comparing expand and focus, expand is better than focus.

5.4.2 Output curve with 1mW laser

This work is to identify the output characteristics of the PCM when connects a motor with different resistor in series. This work will be helpful to determine the power devices when connecting with a stopped motor. As 1mW laser is too small to drive the motor, other power

output from PCM can be used to drive other electrical appliances. The result is shown below in Table 5-3:

Table 5-3. The value of electrical characteristics from the output of GaAs under 1mW laser

R (Ω)	I(μA)	V(mv)	V_r (mv)	V_m (mv)
0	50.36	0.88	0	0.88
20	50.54	1.83	0.99	0.82
30	50.4	2.33	1.49	0.88
50	50.32	3.39	2.55	0.88
100	50.47	5.88	5.05	0.82
150	50.64	8.41	7.55	0.82
200	50.6	10.91	10.06	0.82
300	50.91	15.9	15.02	0.82
510	50.25	26.6	25.75	0.82
750	52.72	40.34	39.09	0.85
1000	52.1	53.01	52.19	0.85
1600	51.8	83.06	82.29	0.83

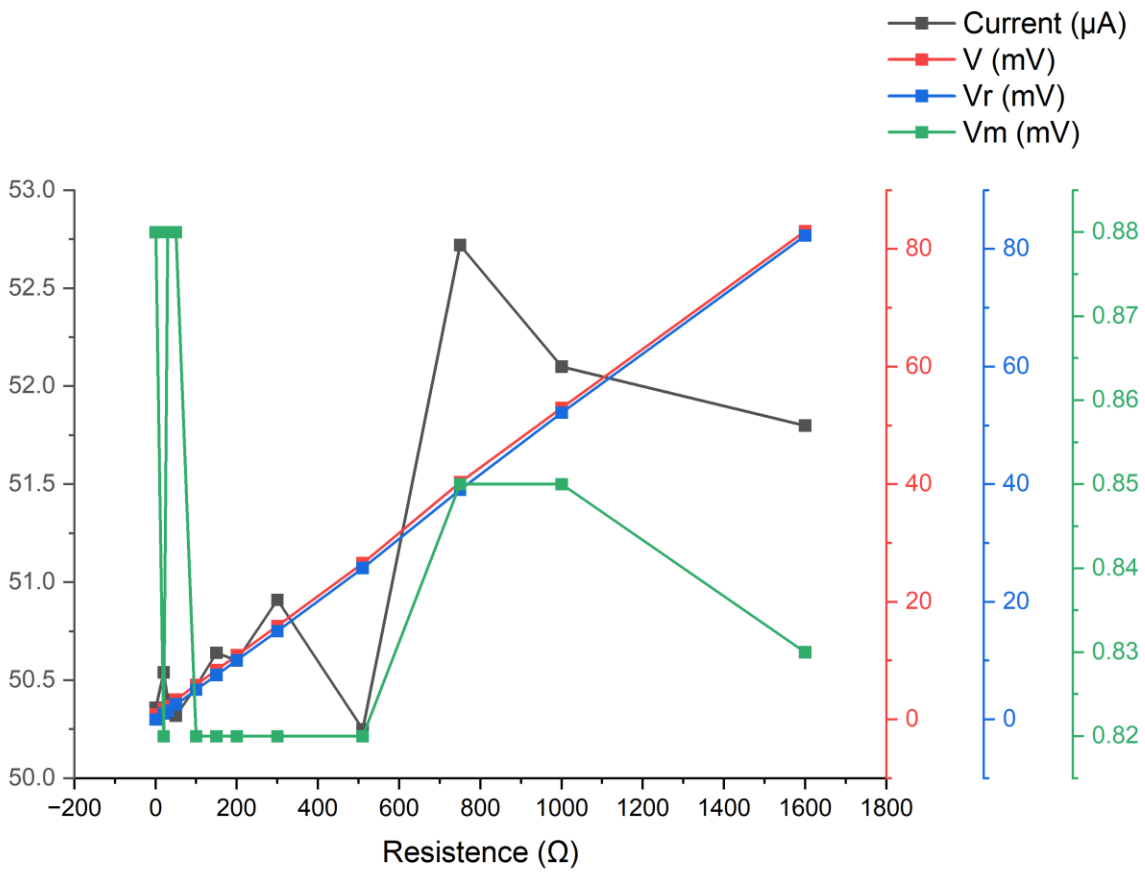

Figure 5-5. The electrical characteristics from the output of GaAs under 1mW laser

The R is the resistance in series of the motor. The I is the circuit current, and the V is the total voltage. The V_r is the voltage on the resistor, and the V_m is the voltage on the motor.

As we can see in the Figure 5-5, the current and the V_m is almost no change at all. This indicates that the DC motor works as a state resistance here. The other energy goes to the resistor, which increases the total output power and the power conversion efficiency of the PCM. On the one hand, the total voltage V and the resistor voltage V_r is proportional to the resistor, which increase as the resistor increases. On the other hand, the motor voltage is changed as the current changes. This indicates that increase the current will not only the torque increases, but also rise the motor speed.

5.4.3 Output curve with 150mW laser

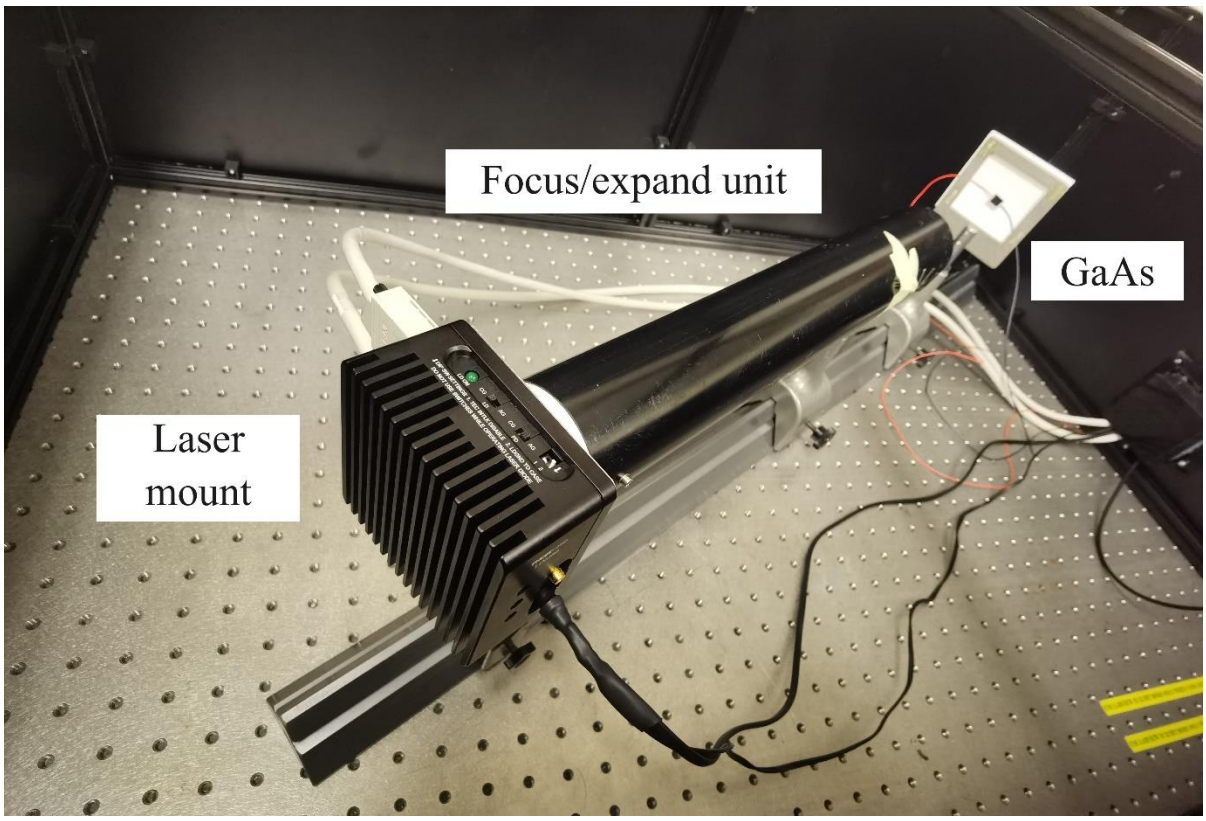

Figure 5-6. The LPT system setup fields

This section will figure out the change rule of the voltage and current when increasing the incident laser power. The system is set up as Figure 5-5. Firstly, the *I-V-R* curve of the PCM is detected by connecting a sliding rheostat to the end. The result shown in Figure 5-7.

Table 5-4. Output I-V-R values of the GaAs irradiated by 150mW laser.

V	*I*	*R*
0.27	14.8	0
0.416	14.7	10
0.592	14.6	20
0.7	15.3	30
0.871	14.8	40
1.039	15.3	50
1.238	15.4	60
1.318	15.5	70
1.467	14.7	80
1.614	14.1	90
1.63	13.58	100
1.81	8.116	200
1.88	5.805	300
1.91	4.408	400
1.98	3.766	500
2.06	3.163	600
2.37	3.077	700
2.45	2.711	800
2.52	2.571	900
2.6	2.483	1000
2.58	1.27	2000
2.57	0.857	3000

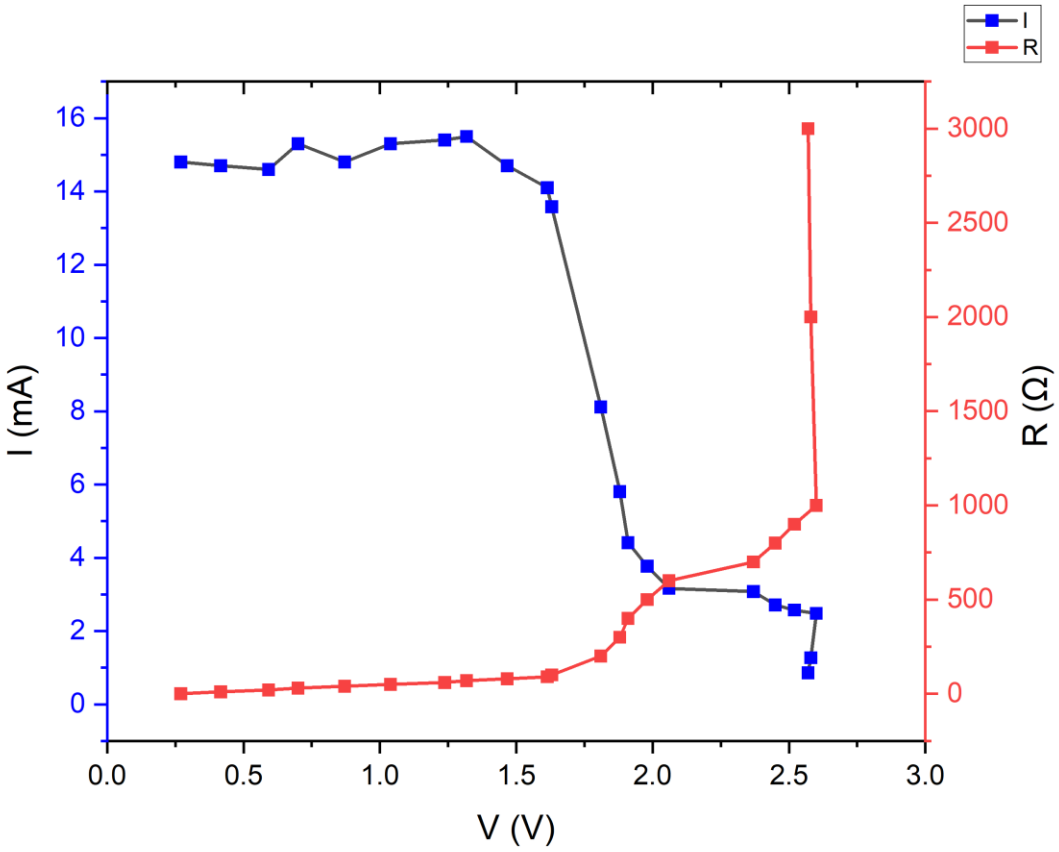

Figure 5-7. Output I-V curve of the GaAs irradiated by 150mW laser.

From the Figure 5-7 and Table 5-4, the maximum power point is around 1.6V and 14 mA, under drive current of 280mA. By calculating the theoretical power transmission efficiency, the laser power could meet the motor running without load. Measuring the voltage and current of a motor can provide insights into how the motor is operating and support the design of closed-loop circuits, The result is exhibited below in Table 5-5:

Table 5-5. The value of electrical characteristics from the output of GaAs under 150 mW laser

I_d(A)	P(W)	I(A)	V(V)
315	172.7	19.408	0.83
316	173.6	19.431	0.95
317	173.7	19.361	1.0072
318	174	19.339	1.0385
319	174.7	19.374	1.07
320	175.3	19.409	1.13
325	178.3	19.618	1.31
330	181.4	19.702	1.4142
335	184.4	19.78	1.4384
340	187.5	19.895	1.4532
345	190.4	20.006	1.47
350	193.6	20.063	1.4808

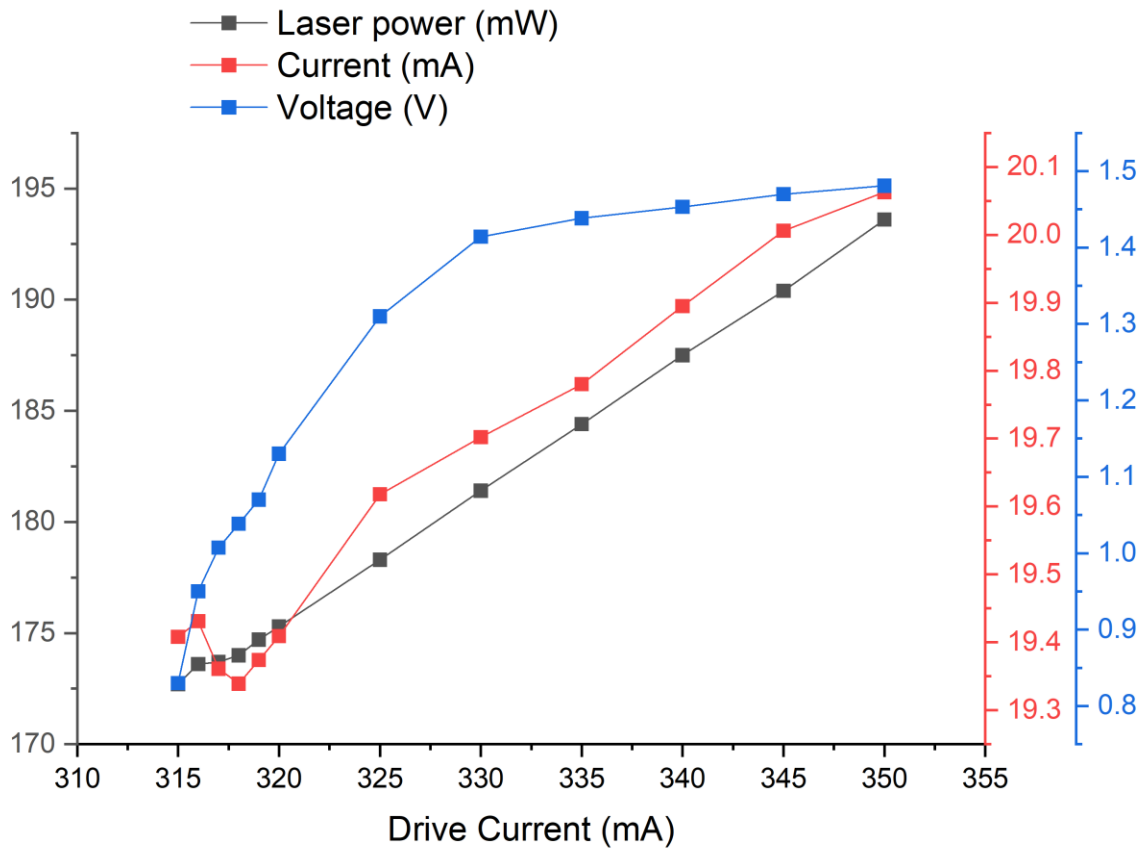

Figure 5-8. The electrical characteristics from the output of GaAs under 150mW laser

The I_d is the laser drive current, and the P is the output power of the laser. From Figure 5-8, the incident laser power is proportion to the drive current. When the incident laser power is increasing, the voltage will rise relatively quickly. The current grows gently, because the increase in speed brings about an increase in no-load torque, which satisfies the conclusion from simulation work that load torque determines steady-state current. Increasing the incident laser power can significantly increase the motor voltage and increase the motor speed.

5.4.4 Steady-state torque and current measurements

In the result of simulation part, the steady-state current is determined by the load torque. To generate load torque to the motor, a 5 cm diameter hub at the end of the motor rotor has been installed, as shown in Figure 5-9. By lifting a weight of a certain weight by winding a fixed thin wire, the load torque of the motor can be determined. By in series of a multimeter, the current can be measured. The motor in this measurement is driven by 5V port of the STM32 board. The result is shown on Table 5-6.

Table 5-6. The weight and corresponding current power by STM32 5V port.

Weight Force(N)	Current(mA)
0	33
1	47
2	59
3	77
4	89
5	102
6	125

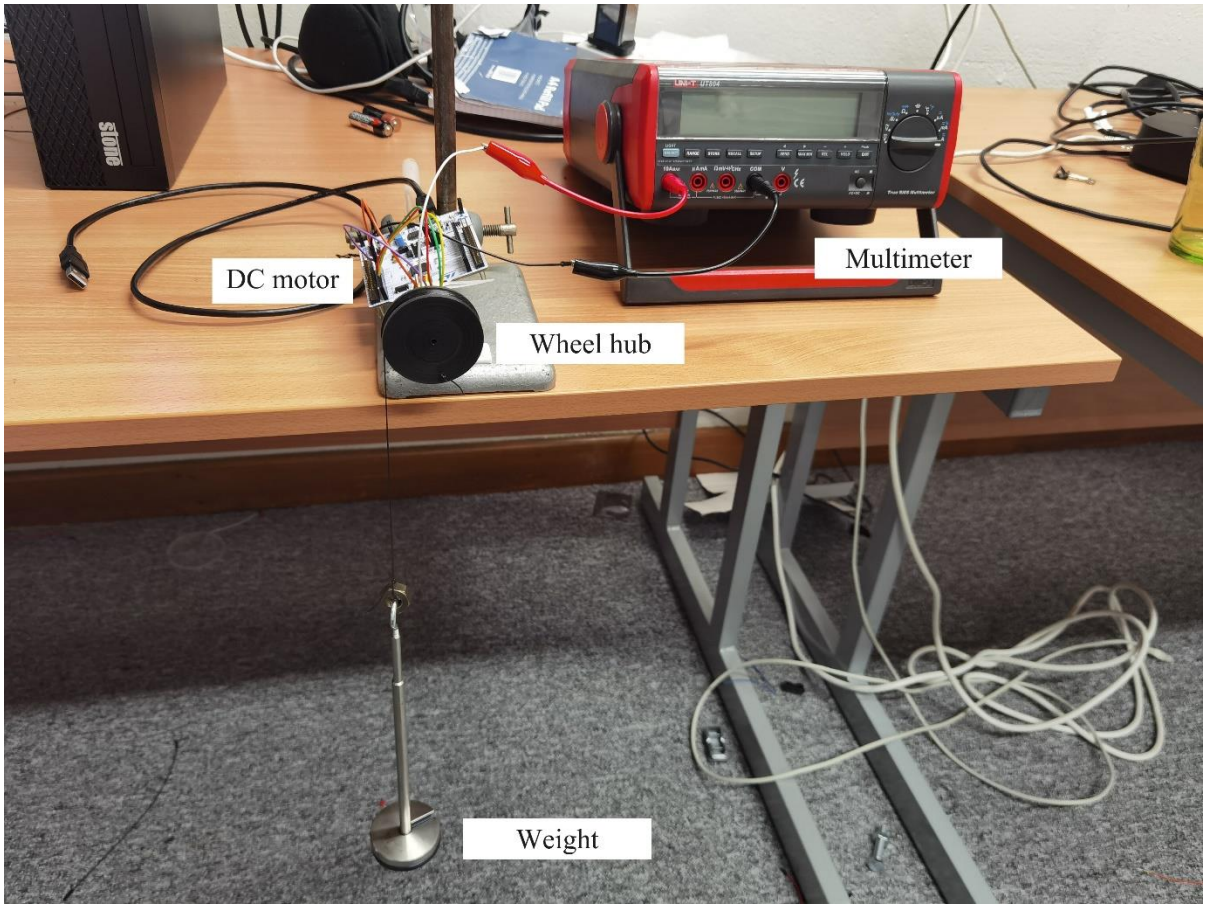

Figure 5-9. Device setup for measurement of torque and current (Powered by 5V port on STM32 board).

Then the power source changed to L450G1 3W laser, driving by the converted electric power, setup as Figure 5-10. The result is shown below in Table 5-7:

Table 5-7. The weight and corresponding current power by L450G1 3W laser.

Weight Force(N)	Current(mA)
0	22
1	33
2	42

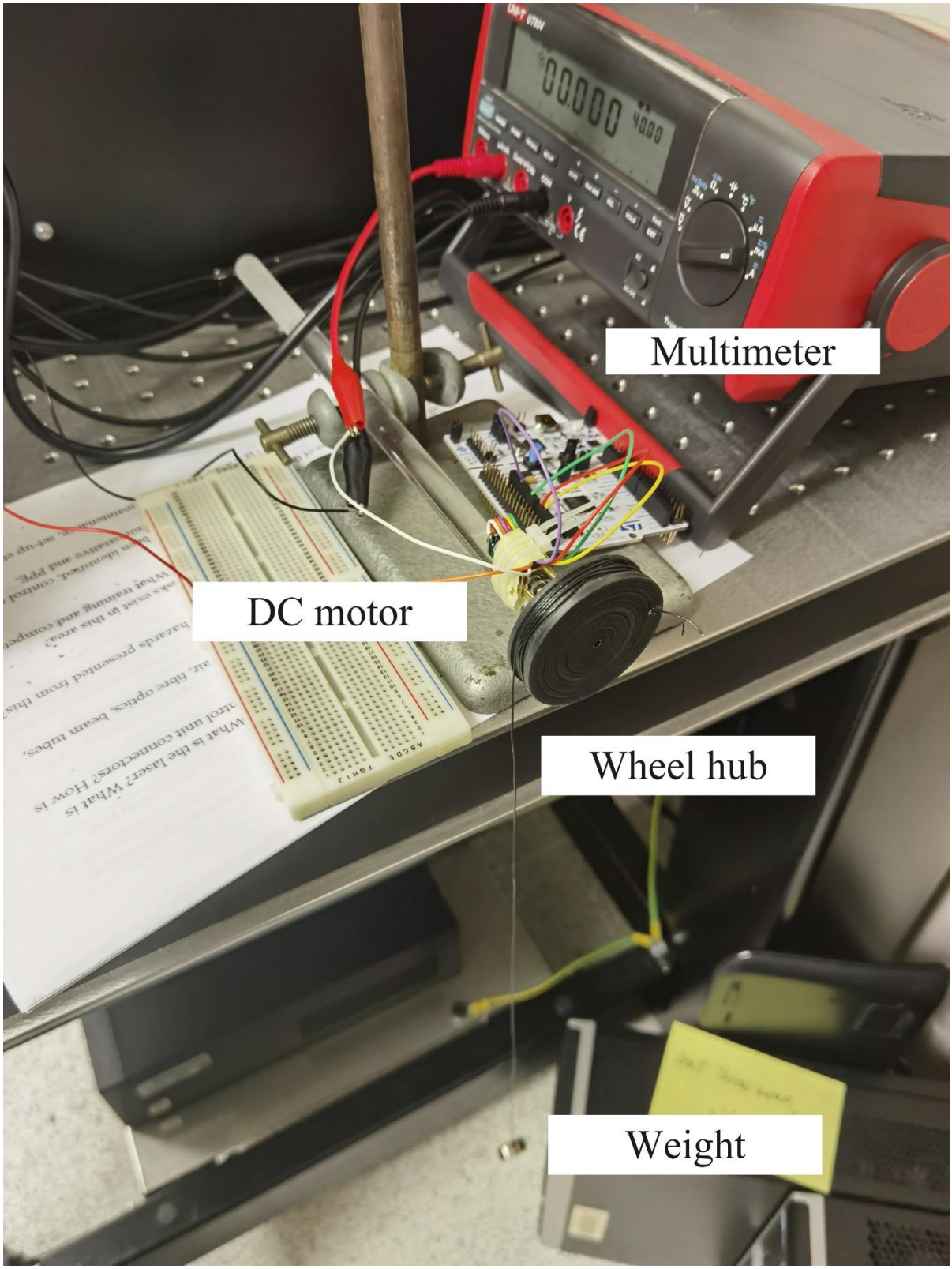

Figure 5-10. Device setup for measurement of torque and current (Powered by L450G1 3W laser).

Due to the output voltage is around 2.58V at no load state, the rotation speed will be lower than driven by 5V STM32 port. Consequently, the motor speed will be lower than driven by

STM32 5V port, and the resistance torque is relatively lower. Although the steady-state current is relatively low, it is consistent with the conclusion that the steady-state current is determined by the load torque.

5.5 Summary

In this section the experiment on laser powered actuator is set up. The experiment equipment's include the safety devices which is the laser enclosure box is designed to protect the operator and the work devices contain laser, PCM, DC motor and power meter. This experiment first verifies when the motor stops, it works as fixed value resistor and the other output power of PCM will go to the resistor which is in series of it. At the same time, increasing the resistor value increases the output size of the PCM and the transmission efficiency of the overall system. Then, while the motor is driven by enough power of laser, the load torque determines the steady-state work current, which satisfies the simulation result.

Chapter 6 Conclusions and Future Works

6.1 Conclusions

This thesis concentrates on how to apply LPT technology to work as a DC motor actuator which could achieve basic drive and control to meet work requirements during steady-state operation. In this comprehensive exploration of Laser Power Transmission (LPT) systems, a thorough investigation has been conducted, encompassing system development, existing applications, and future prospects. While LPT has proven to be a feasible power source, the primary limitation lies in its transmission efficiency, typically around 20%. An in-depth analysis of laser emitter characteristics, transmission media, photovoltaic materials, and overall power conversion efficiency highlights the advantages of Laser Diodes (LDs) in terms of size, ease of implementation, beam alignment, and photovoltaic conversion efficiency. The study identifies avenues for improving LD efficiency, considering factors like accuracy, stability, and wave types.

The choice of transmission media, whether through the atmosphere or optical fiber, is evaluated, emphasizing the atmosphere's simplicity in straight-line transmission. GaAs is recognized for its superior power conversion efficiency. Comparing LPT to other Wireless Power Transmission (WPT) methods, its long transmission distance and ease of implementation position LPT as a suitable actuator for motor drive applications. The proposed LPT system for motor drive is outlined, leveraging high-efficiency equipment and emphasizing the potential through optimization by power electronics.

Expanding the focus to wireless motor speed signal feedback in lase powered actuators, light signal transmission emerges as the method of choice. The study delves into light emitter options, favoring LEDs over LDs for their modulation capabilities and energy efficiency. The analysis distinguishes between analog and digital signal modulation, advocating for a motor speed feedback method aligned with the signal type. The sensorless method is preferred for its cost-effectiveness and simplified system design, with the ripple counting technique and digital light signal modulation proposed for brushed DC motors.

A novel Laser Power Transmission (LPT) motor actuator has been proposed with the aim of achieving long-distance wireless power transmission for motor operation and speed control.

The examined LPT system exhibits a power transfer efficiency of 20.4%, demonstrating its adequacy as a motor actuator. Furthermore, the proposed control method has been validated, showcasing its effectiveness in decreasing the overall system efficiency. Utilizing the DC motor formula and Pulse Code Modulation (PCM) output characteristics, the maximum and minimum motor rotation speeds and torque have been calculated. A method for controlling motor speed by adjusting laser turn-off has been introduced, relying on motor speed feedback to compare with the set value and determine laser on/off. The theoretical derivation of maximum torque after setting the speed establishes a clear understanding of the system's performance limitations, indicating an uncontrollable range beyond this threshold. Steady-state characteristics have been verified through simulations, highlighting the interplay between the external load torque and the steady-state power point. This point is strategically positioned between the maximum torque and maximum speed points. Notably, at time zero, a high voltage peak is observed, attributed to the resistive inductive load characteristics of the DC motor. Within the established control range, the rotation speed of the DC motor remains stable at the set value, and the laser operates in pulse mode. However, when the load torque exceeds the control range, the laser remains continuously on, preventing the speed from reaching the desired value. Changes in reference speed or external load torque prompt motor acceleration or braking, and the resulting current changes determine the direction of the voltage peak.The control range's primary limitations are attributed to laser power and load torque. Future work is directed towards expanding this control range by leveraging feedback signals from the load torque to regulate the laser power. Additionally, introducing a variable load to adjust the maximum power point offers a promising avenue for increasing total system efficiency while concurrently controlling speed, thereby enhancing the applicability of the proposed LPT motor.

The experimental setup validates theoretical simulation findings, emphasizing safety measures in the form of a laser enclosure box. Experiments confirm the dynamic relationship between motor behavior, load torque, and PCM output, supporting the simulation results. This multi-faceted exploration not only contributes to the understanding of LPT systems but also lays the groundwork for future advancements, particularly in expanding control ranges and improving overall system efficiency for diverse applications.

6.2 Future work

6.2.1 Laser power control strategy

Based on the results in the speed control part above, if the control range has to be expanded, the laser power needs to be modified to increase the maximum speed and torque. In order to achieve the closed-loop automatic control, the load torque signal is needed for feedback proposed to the LD. Based on the torque value, the voltage and current can be calculated. The difficulty lies in determining the power curve to achieve the calculated voltage and current, and then enacting the correct adjustment to the appropriate laser value. The existing study shows the relationship between maximum power point current and laser power, albeit under some limitations when building the control loop with the method. The kind of new relationship between laser power and its interaction with current needs to be further studied.

6.2.2 Maximum power point control strategy

The entire system operating at its maximum power point is the ideal case scenario of high efficiency and energy saving. In addition to the dual closed-loop control method, variable loads such as rechargeable batteries can be added. The battery charging efficiency can be adjusted to enable the LPT system to work at the maximum power point and adjust the DC motor speed at the same time. The difficulty lies in the control loop becoming more complex.

6.2.3 Dual closed-loop control strategy of torque and speed

By applying both speed loop and torque loop control to achieve desired motor driven feathers at any speed and external load torque, more information about the relationship between laser power and PCM output curve needs to be studied in order to overcome the limitations of the existing method. This will be a key step to bringing the technology to practical use.

6.2.4 Utilizing light reflection to modulate feedback signal by shutter

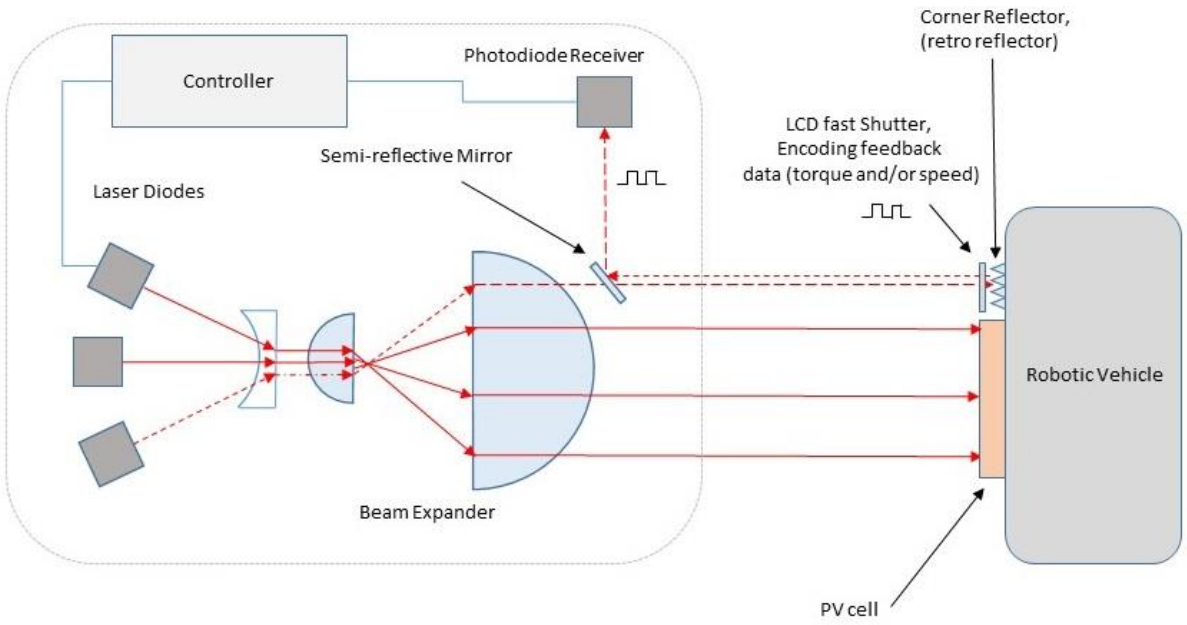

Figure 6-1. Feedback light signal reflection and generation design.

The traditional fibre-based light signal transmission applied in this proposed system requires an additional LED as a feedback signal generator. As shown in Figure 6-1, this method will result in more power loss and complexity. To simplify the feedback system design, an LCD with a faster shutter and a corner reflector is installed. The corner reflector reflects the laser beam in opposite directions. The LCD fast shutter encodes the feedback data from the reflected laser beam by high frequency on/off modulation. The semi-reflective mirror reflects the modulated signal to the receiver. This method needs further validation for accuracy and stability.

Appendix

1. Design for laser enclosure box.

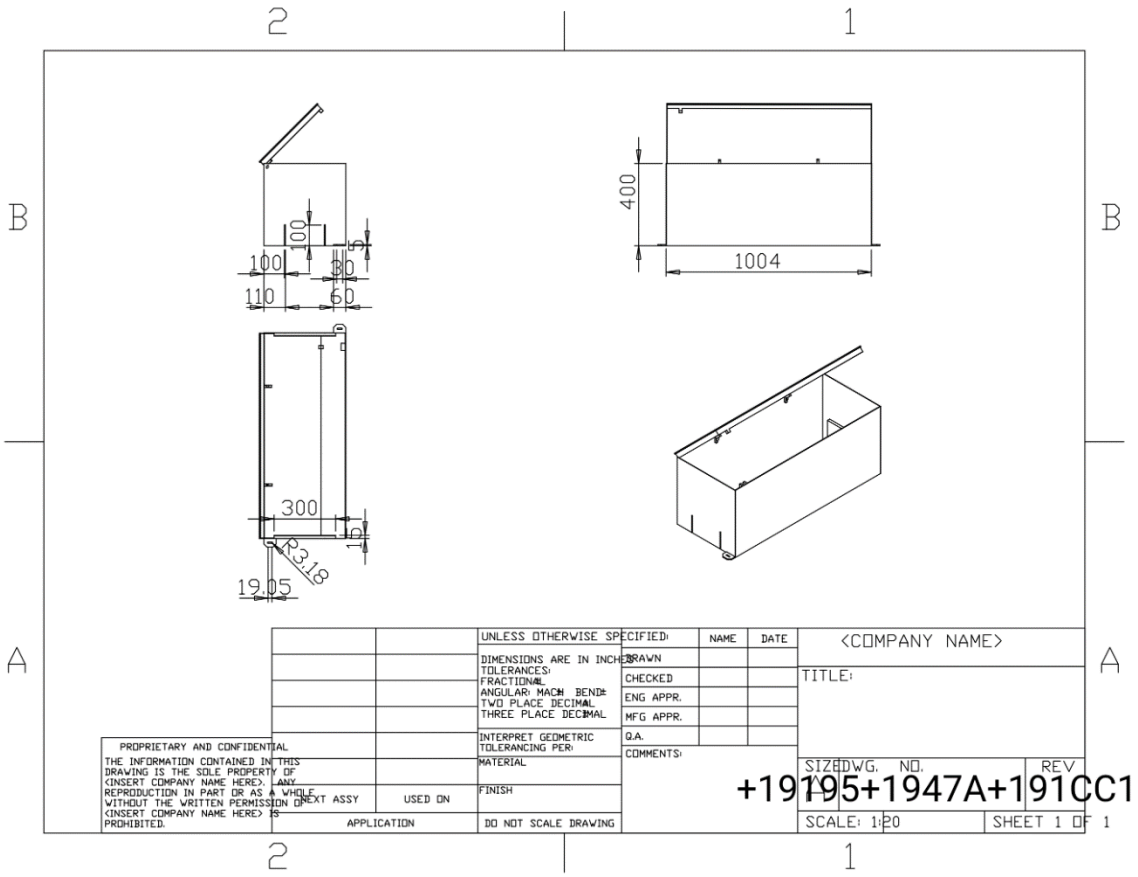

References

[1] T. Nikola, "Apparatus for transmitting electrical energy," *U.S. Patent No. 1,119,732,* January 1 1914.

[2] S. Y. R. Hui, W. Zhong, and C. K. Lee, "A critical review of recent progress in mid-range wireless power transfer," *IEEE Transactions on Power Electronics,* vol. 29, no. 9, pp. 4500-4511, 2013.

[3] W. C. Cheah, S. A. Watson, and B. Lennox, "Limitations of wireless power transfer technologies for mobile robots," *Wireless Power Transfer,* vol. 6, no. 2, pp. 175-189, 2019.

[4] A. Siddiqui, A. Nagani, and R. Ali, "Wireless power transfer techniques: a review," *Recent and Innovation Trends in Computing and Communication,* vol. 3, no. 12, pp. 6711-616, 2015.

[5] K. Jin and W. Zhou, "Wireless laser power transmission: A review of recent progress," *IEEE Transactions on Power Electronics,* vol. 34, no. 4, pp. 3842-3859, 2018.

[6] RCL. https://rclglobal.co.uk/copper-wire-pros-and-cons/ (accessed.

[7] M. Industries. "Copper Wire Pros and Cons." https://meghachem.org/copper-pros-cons.php (accessed 2023).

[8] J. Li, X. Wu, T. Xu, H. Guo, J. Sun, and Q. Gao, "A novel inspection robot for nuclear station steam generator secondary side with self-localization," *Robotics and biomimetics,* vol. 4, pp. 1-9, 2017.

[9] Q. Liu *et al.*, "A novel nuclear station inspection robot," in *2014 4th IEEE International Conference on Information Science and Technology*, 2014: IEEE, pp. 678-681.

[10] DMSI. "The Unfortunate Disadvantages of Using Copper Wires." https://www.dmsimfg.com/2017/09/27/the-unfortunate-disadvantages-of-using-copper-wires/ (accessed 2023).

[11] L. Summerer and O. Purcell, "Concepts for wireless energy transmission via laser," *Europeans Space Agency (ESA)-Advanced Concepts Team,* 2009.

[12] D. Thul *et al.*, "The mobile ultrafast high energy laser facility-A new facility for high-intensity atmospheric laser propagation studies," *Optics and Lasers in Engineering,* vol. 140, p. 106519, 2021.

[13] G.-x. Zhang, S. Chen, S.-g. Xu, B. Luo, and Y.-m. Zhao, "Application and research of laser de-icing in power system," in *2010 IEEE International Power Modulator and High Voltage Conference*, 2010: IEEE, pp. 470-473.

[14] T. S. McComb, R. A. Sims, C. C. Willis, P. Kadwani, L. Shah, and M. Richardson, "Atmospheric transmission testing using a portable, tunable, high power thulium fiber laser system," in *Conference on Lasers and Electro-Optics*, 2010: Optica Publishing Group, p. JThJ5.

[15] V. Alejnikov *et al.*, "Fibre-optic cable for CO and CO2 laser power transmission," *Optics & Laser Technology,* vol. 17, no. 4, pp. 213-214, 1985.

[16] F. Steinsiek, "Wireless power transmission experiment as an early contribution to planetary exploration missions," in *54th International Astronautical Congress of the International Astronautical Federation, the International Academy of Astronautics, and the International Institute of Space Law*, 2003, p. R. 3.06.

[17] D. E. Raible, "High intensity laser power beaming for wireless power transmission," Cleveland State University, 2008.

[18] N. Kawashima and K. Takeda, "Laser energy transmission for a wireless energy supply to robots," *Robotics and Automation in Construction,* vol. 10, pp. 373-380, 2008.

[19] D. E. Raible, "Free space optical communications with high intensity laser power beaming," Cleveland State University, 2011.

[20] D. E. Becker, R. Chiang, C. C. Keys, A. W. Lyjak, J. A. Nees, and M. D. Starch, "Photovoltaic‐concentrator based power beaming for space elevator application," in *AIP Conference Proceedings*, 2010, vol. 1230, no. 1: American Institute of Physics, pp. 271-281.

[21] A. Sahai and D. Graham, "Optical wireless power transmission at long wavelengths," in *2011 International Conference on Space Optical Systems and Applications (ICSOS)*, 2011: IEEE, pp. 164-170.

[22] N. Wang, "Research on the Key Technology of Laser Active Power Supply in Wireless Sensor Networks," *Chongqing University,* 2011.

[23] H. Huang, "Theoretical and Experimental Study on Feedback Resonant Laser Energy Transmission," *Tsinghua University,* 2013.

[24] A. V. Bogachev *et al.*, "Diode-pumped caesium vapour laser with closed-cycle laser-active medium circulation," *Quantum Electronics,* vol. 42, no. 2, p. 95, 2012.

[25] D. Shi, L. Zhang, H. Ma, Z. Wang, Y. Wang, and Z. Cui, "Research on wireless power transmission system between satellites," in *2016 IEEE wireless power transfer conference (WPTC)*, 2016: IEEE, pp. 1-4.

[26] A. Mohammadnia, B. M. Ziapour, H. Ghaebi, and M. H. Khooban, "Feasibility assessment of next-generation drones powering by laser-based wireless power transfer," *Optics & Laser Technology,* vol. 143, p. 107283, 2021.

[27] W. Zhou and K. Jin, "Efficiency optimization inject current characteristic of laser diode for wireless power transmission," in *2015 IEEE Energy Conversion Congress and Exposition (ECCE)*, 2015: IEEE, pp. 3082-3086.

[28] Z. Song, Y. Zhang, X. Huang, D. Shi, S. Wu, and X. Meng. (2018) Energy Transfer Technology of 975 nm Fiber Coupled Semiconductor Laser [J]. *Space Electronic Technology*. 101-105.

[29] M. Röhner, L. Wagner, A. Pietrzak, and R. Hülsewede, "Fiber-coupled high-power diode-lasers with highest radiance," in *2013 High Power Diode Lasers and Systems Conference (HPD)*, 2013: IEEE, pp. 36-37.

[30] H. Zimer *et al.*, "Beam combining technologies for direct diode laser systems at the kW power level," in *2013 High Power Diode Lasers and Systems Conference (HPD)*, 2013: IEEE, pp. 38-39.

[31] A. Unger *et al.*, "The BRIDLE project: High brilliance diode lasers for industrial applications," in *2013 High Power Diode Lasers and Systems Conference (HPD)*, 2013: IEEE, pp. 28-29.

[32] T. Brand, A. Unger, B. Koehler, P. Wolf, A. Beczkowiak, and J. Biesenbach, "Diode laser platform for multi-kW applications," in *2013 High Power Diode Lasers and Systems Conference (HPD)*, 2013: IEEE, pp. 32-33.

[33] M. Helal, S. Bull, S. Kaunga-Nyirenda, J. Lim, and E. Larkins, "Simulation of high-brightness diode lasers with optical feedback from modules and systems," in *2013 High Power Diode Lasers and Systems Conference (HPD)*, 2013: IEEE, pp. 14-15.

[34] U. Witte, S. Hengesbach, M. Traub, M. Strotkamp, B. Jungbluth, and D. Hoffmann, "High brightness diode laser module in the red spectral range for pumping applications," in *2013 High Power Diode Lasers and Systems Conference (HPD)*, 2013: IEEE, pp. 30-31.

[35] S. Hengesbach, U. Witte, M. Traub, and D. Hoffmann, "Design of a DFB/DBR diode laser module including spectral multiplexing based on VBGs," in *2013 High Power Diode Lasers and Systems Conference (HPD)*, 2013: IEEE, pp. 16-17.

[36] S. Bull, S. Kaunga-Nyirenda, and E. Larkins, "Design considerations for high-power external cavity laser diodes," in *2013 High Power Diode Lasers and Systems Conference (HPD)*, 2013: IEEE, pp. 6-7.

[37] D. McCormick, D. Irwin, D. Stapleton, J. Braker, T. Koenning, and S. Patterson, "Ultra-narrow spectral linewidth diode lasers for the pumping of alkalis," in *2015 IEEE High Power Diode Lasers and Systems Conference (HPD)*, 2015: IEEE, pp. 25-26.

[38] U. Witte, M. Hamann, A. Di Meo, D. Rubel, M. Traub, and D. Hoffmann, "High power diode laser with 23W ex 35 μm fibre," in *2015 IEEE High Power Diode Lasers and Systems Conference (HPD)*, 2015: IEEE, pp. 17-18.

[39] R. K. Huang, B. Samson, B. Chann, B. Lochman, and P. Tayebati, "Recent progress on high-brightness kW-class direct diode lasers," in *2015 IEEE High Power Diode Lasers and Systems Conference (HPD)*, 2015: IEEE, pp. 29-30.

[40] H. Zimer *et al.*, "Spectrally stabilized and combined diode lasers," in *2015 IEEE High Power Diode Lasers and Systems Conference (HPD)*, 2015: IEEE, pp. 31-32.

[41] V. Rossin *et al.*, "High power, high brightness diode lasers for kW lasers systems," in *2015 IEEE High Power Diode Lasers and Systems Conference (HPD)*, 2015: IEEE, pp. 35-36.

[42] B. Sumpf, "Wavelength stabilized high-power diode lasers—Devices and applications," in *2016 International Conference Laser Optics (LO)*, 2016: IEEE, pp. R3-3-R3-3.

[43] K. Kleine and P. Balu, "High-power diode laser sources for materials processing," in *2017 IEEE High Power Diode Lasers and Systems Conference (HPD)*, 2017: IEEE, pp. 3-4.

[44] G. Lucas-Leclin, G. Schimmel, P. Albrodt, M. Hanna, and P. Georges, "Coherent combining architectures for high-brightness laser diodes," in *2017 IEEE High Power Diode Lasers and Systems Conference (HPD)*, 2017: IEEE, pp. 49-50.

[45] A. Krasnoshchoka, J. Xu, A. Thorseth, C. Dam-Hansen, and O. B. Jensen, "High luminous flux laser lighting using single-crystal Ce: YAG phosphor," in *2019 IEEE High Power Diode Lasers and Systems Conference (HPD)*, 2019: IEEE, pp. 31-32.

[46] A. M. Rubenchik, M. P. Fedoruk, and S. K. Turitsyn, "Laser beam self-focusing in the atmosphere," *Physical review letters,* vol. 102, no. 23, p. 233902, 2009.

[47] Y. Yao, "Study on Thermal Halo Effect of High Power Laser Propagation in Atmosphere," *Xidian University,* 2009.

[48] B. Xiao, "Design and Implementation of Low Power Intelligent Fiber Energy Transmission System," *Nanjing University of Posts and Telecommunications,* 2017.

[49] X. Zhao, "Study on the Energy Transmissio Characteristics of Fiber Laser with Peak Power," *China Academy of Engineering Physics.,* 2007.

[50] N. Reng and T. Beck, "Transmission properties of all-silica fibres for high-power Nd: YAG lasers," *Optics & Laser Technology,* vol. 25, no. 2, pp. 117-124, 1993.

[51] F. X. Liu, Honggang, "Effect of γ-radiation on optical fiber dispersion," *Infrared and Laser Engineering,* 2016.

[52] M. Zhang, "Experimental Study on Gamma Irradiation Effect of Double Cladding Ultraviolet Fiber," *Atomic Energy Science and Technology,* vol. 53, no. 3, pp. 536-542, 2017.

[53] Q. Zhang, Yun, F. and He, Q, "Research on Space Radiation Damage Mechanism and Performance Improvement of Quartz Fiber," *Fiber and Cable and Its Application Technology,* vol. 6, pp. 7-9, 2020.

[54] J. Wen, "Fabrication and Properties of Radiation Resistant Polarization Keeping Fiber," *Flight Control & Detection,* 2020.

[55] K. Zotov *et al.*, "Radiation-resistant erbium-doped fiber for spacecraft applications," in *2007 9th European Conference on Radiation and Its Effects on Components and Systems*, 2007: IEEE, pp. 1-4.

[56] K. Zotov *et al.*, "Radiation resistant Er-doped fibers: optimization of pump wavelength," *IEEE Photonics Technology Letters,* vol. 20, no. 17, pp. 1476-1478, 2008.

[57] A. Billat, J. Blanc, J. Kuhnhenn, and D. Ricci, "Photobleaching effects in multi-mode radiation resistant optical fibers," in *2017 17th European Conference on Radiation and Its Effects on Components and Systems (RADECS)*, 2017: IEEE, pp. 1-3.

[58] Y. Zhuang, Hua, L. Guo, B, "Research and Design of Laser Energy Converter for Laser Energy Transmission System," *Infrared,* vol. 35, no. 12, pp. 35–40, 2014.

[59] W. Zhou. (2018) Research on Key Technology of Laser Radio Energy Transmission System [D]. *Nanjing University of Aeronautics and Astronautics*.

[60] Y. Zhuang, L. Hua, and B. Guo. (2014) Research and design of laser energy converter for laser energy transmission system [J]. *Infrared*. 35-40.

[61] M. Han, "Study on Photoelectric Conversion Efficiency of GaAs Concentrator Cells Under Laser Irradiation," *Nanjing University of Aeronautics and Astronautics,* 2018.

[62] Anon, "Rapid Development of Photovoltaic Technology," *Dual-use Technology and Products,,* vol. 11, no. 3, 2020.

[63] H. Yugami *et al.*, "Field experiment of laser energy transmission and laser to electric conversion," in *IECEC-97 Proceedings of the Thirty-Second Intersociety Energy Conversion Engineering Conference (Cat. No. 97CH6203)*, 1997, vol. 1: IEEE, pp. 625-630.

[64] N. Kawashima, K. Takeda, and K. Yabe, "Application of the laser energy transmission technology to drive a small airplane," *Chinese Optics Letters,* vol. 5, no. 101, pp. S109-S110, 2007.

[65] C. Balaguer and M. Abderrahim, *Robotics and automation in construction*. BoD–Books on Demand, 2008.

[66] Z. Zhang, Lu, J. Chi, W, "Progress and Prospect of GaAs Solar Cell Technology," *Shanghai Aerospace,* vol. 20, no. 3, pp. 33–38, 2003.

[67] X. Z. Wang, Y, "Research Status and Development Trends of GaAs Trijunction Solar Cells," presented at the National MOCVD Academic Conference, 2012.

[68] A. S. Guo, Q, "Progress of Semiconductor Solar Cell Technology Based on GaAs," *Chinese Journal of Power Sources,* vol. 31, no. 9, pp. 757-758, 2007.

[69] H. Cotal *et al.*, "Highly efficient 32.3% monolithic gainp/gaas/ge triple junction concentrator solar cells," National Renewable Energy Lab.(NREL), Golden, CO (United States), 2000.

[70] K. Nishioka, T. Takamoto, T. Agui, M. Kaneiwa, Y. Uraoka, and T. Fuyuki, "Annual output estimation of concentrator photovoltaic systems using high-efficiency InGaP/InGaAs/Ge triple-junction solar cells based on experimental solar cell's characteristics and field-test meteorological data," *Solar Energy Materials and Solar Cells,* vol. 90, no. 1, pp. 57-67, 2006.

[71] G. S. Kinsey, P. Hebert, K. E. Barbour, D. D. Krut, H. L. Cotal, and R. A. Sherif, "Concentrator multijunction solar cell characteristics under variable intensity and temperature," *Progress in Photovoltaics: Research and Applications,* vol. 16, no. 6, pp. 503-508, 2008.

[72] K. Nishioka, T. Sueto, M. Uchida, and Y. Ota, "Detailed analysis of temperature characteristics of an InGaP/InGaAs/Ge triple-junction solar cell," *Journal of Electronic Materials,* vol. 39, pp. 704-708, 2010.

[73] S. Zimmermann *et al.*, "A high-efficiency hybrid high-concentration photovoltaic system," *International Journal of Heat and Mass Transfer,* vol. 89, pp. 514-521, 2015.

[74] Y. Yang, G. Chen, and L. Guo, "Study on IV Characteristics of Three-junction GaAs Solar Cells," *Semiconductor Technology,* vol. 35, no. 5, pp. 423-426, 2010.

[75] W. Wang, Li, M. Ji, X., "A Novel Fresnel Concentrator for GaAs Cells," *Acta Optica Sinica,* vol. 7, pp. 198-204, 2012.

[76] Z. Wang, Zhang, H. Liu, Y, "Theoretical and Experimental Analysis of Electrical Characteristics of InGaP/GaAs/Ge Three-junction GaAs Photovoltaic Cells," *Proceedings of the CSEE,* vol. 33, no. 27, pp. 168-174, 2013.

[77] N. A. Kalyuzhnyy *et al.*, "Optimization of photoelectric parameters of InGaAs metamorphic laser (λ= 1064 nm) power converters with over 50% efficiency," *Solar Energy Materials and Solar Cells,* vol. 217, p. 110710, 2020.

[78] H. Liu, Y. Zhang, Y. Hu, and Z. Tse, "Laser Power Transmission and Its Application in Laser-Powered Electrical Motor Drive: A Review," *Power Electronics and Drives,* vol. 6, no. 1, pp. 167-184, 2021.

[79] Y. Zhou, Z. Pan, J. Hu, J. Shi, and X. Mo, "Broadband wireless communications on high speed trains," in *2011 20th Annual Wireless and Optical Communications Conference (WOCC)*, 2011: IEEE, pp. 1-6.

[80] Y. Ali, S. Noor, S. Bashi, and M. Hassan, "Microcontroller performance for DC motor speed control system," in *Proceedings. National Power Engineering Conference, 2003. PECon 2003.*, 2003: IEEE, pp. 104-109.

[81] M. F. Al Andzar and R. D. Puriyanto, "PID Control for Temperature and Motor Speed Based on PLC," *Signal and Image Processing Letters,* vol. 1, no. 1, pp. 7-13, 2019.

[82] A. Klee, "Development of a motor speed control system using matlab and simulink, implemented with a digital signal processor," 2005.

[83] P. Olden, K. Robinson, K. Tanner, R. Wilson, and A. H. Basher, "Open-loop motor speed control with LabVIEW," in *Proceedings. IEEE SoutheastCon 2001 (Cat. No. 01CH37208)*, 2001: IEEE, pp. 259-262.

[84] "Optical transmitters and optical receivers." https://wenku.baidu.com/view/95f22d892fc58bd63186bceb19e8b8f67c1cefb6.html?_wkts_=1683493150587 (accessed 2023).

[85] "Chapter 3 Optical transmitters and optical receivers." https://wenku.baidu.com/view/844d9f500e22590102020740be1e650e52eacfb1.html (accessed 2023).

[86] H. Fakham, M. Djemaï, and K. Busawon, "Design and practical implementation of a back-EMF sliding-mode observer for a brushless DC motor," *IET Electric Power Applications,* vol. 2, no. 6, pp. 353-361, 2008.

[87] G. Liu, C. Cui, K. Wang, B. Han, and S. Zheng, "Sensorless control for high-speed brushless DC motor based on the line-to-line back EMF," *IEEE Transactions on Power Electronics,* vol. 31, no. 7, pp. 4669-4683, 2014.

[88] H. Li, X. Ning, and W. Li, "Implementation of a MFAC based position sensorless drive for high speed BLDC motors with nonideal back EMF," *Isa Transactions,* vol. 67, pp. 348-355, 2017.

[89] X. Song, B. Han, and K. Wang, "Sensorless drive of high-speed BLDC motors based on virtual third-harmonic back EMF and high-precision compensation," *IEEE Transactions on Power Electronics,* vol. 34, no. 9, pp. 8787-8796, 2018.

[90] P. Radcliffe and D. Kumar, "Sensorless speed measurement for brushed DC motors," *IET Power Electronics,* vol. 8, no. 11, pp. 2223-2228, 2015.

[91] M. Vidlak, L. Gorel, P. Makys, and M. Stano, "Sensorless Speed Control of Brushed DC Motor Based at New Current Ripple Component Signal Processing," *Energies,* vol. 14, no. 17, p. 5359, 2021.

[92] Q. Zhang, B. Wen, and Y. He, "Rotational speed monitoring of brushed DC motor via current signal," *Measurement,* vol. 184, p. 109890, 2021.

[93] T. Li and J. Zhou, "High-stability position-sensorless control method for brushless DC motors at low speed," *IEEE transactions on power electronics,* vol. 34, no. 5, pp. 4895-4903, 2018.

[94] C. Concari and F. Troni, "Sensorless control of BLDC motors at low speed based on differential BEMF measurement," in *2010 IEEE Energy Conversion Congress and Exposition*, 2010: IEEE, pp. 1772-1777.

[95] G. Prasad, N. S. Ramya, P. Prasad, and G. T. R. Das, "Modelling and Simulation Analysis of the Brushless DC Motor by using MATLAB," *International journal of innovative technology and exploring engineering (IJITEE),* vol. 1, no. 5, pp. 27-31, 2012.

[96] B.-K. Lee and M. Ehsani, "Advanced simulation model for brushless dc motor drives," *Electric power components and systems,* vol. 31, no. 9, pp. 841-868, 2003.

[97] X. Yunxiang, Z. Ping, and N. Haiqing, "A study on high frequency signal injection method of aiming at detecting the rotor position of the salient-pole brushless DC motor," in *2005 International Conference on Electrical Machines and Systems*, 2005, vol. 3: IEEE, pp. 2369-2372.

[98] I. M. Alsofyani and N. R. N. Idris, "A review on sensorless techniques for sustainable reliablity and efficient variable frequency drives of induction motors," *Renewable and sustainable energy reviews,* vol. 24, pp. 111-121, 2013.

[99] R. Kumar, S. Das, P. Syam, and A. K. Chattopadhyay, "Review on model reference adaptive system for sensorless vector control of induction motor drives," *IET Electric Power Applications,* vol. 9, no. 7, pp. 496-511, 2015.

[100] D. M. Stănică, N. Bizon, and M. C. Arva, "A brief review of sensorless AC motors control," in *2021 13th International Conference on Electronics, Computers and Artificial Intelligence (ECAI)*, 2021: IEEE, pp. 1-7.

[101] R. Maamouri, M. Trabelsi, M. Boussak, and F. M'Sahli, "Mixed model‐based and signal‐based approach for open‐switches fault diagnostic in sensorless speed vector controlled induction motor drive using sliding mode observer," *IET Power Electronics,* vol. 12, no. 5, pp. 1149-1159, 2019.

[102] M. Comanescu and L. Xu, "An improved flux observer based on PLL frequency estimator for sensorless vector control of induction motors," *IEEE Transactions on industrial electronics,* vol. 53, no. 1, pp. 50-56, 2006.

[103] A. Kadrine, Z. Tir, O. P. Malik, M. A. Hamida, A. Reatti, and A. Houari, "Adaptive non-linear high gain observer based sensorless speed estimation of an induction motor," *Journal of the Franklin Institute,* vol. 357, no. 13, pp. 8995-9024, 2020.

[104] H. Kubota, I. Sato, Y. Tamura, K. Matsuse, H. Ohta, and Y. Hori, "Stable operation of adaptive observer based sensorless induction motor drives in regenerating mode at low speeds," in *Conference Record of the 2001 IEEE Industry Applications Conference. 36th IAS Annual Meeting (Cat. No. 01CH37248)*, 2001, vol. 1: IEEE, pp. 469-474.

[105] M. Ghanes, J. De Leon, and A. Glumineau, "Observability study and observer-based interconnected form for sensorless induction motor," in *Proceedings of the 45th IEEE Conference on Decision and Control*, 2006: IEEE, pp. 1240-1245.

[106] C.-M. Lee and C.-L. Chen, "Observer-based speed estimation method for sensorless vector control of induction motors," *IEE Proceedings-Control Theory and Applications,* vol. 145, no. 3, pp. 359-363, 1998.

[107] Z. Boulghasoul, Z. Kandoussi, A. Elbacha, and A. Tajer, "Fuzzy improvement on Luenberger observer based induction motor parameters estimation for high performances sensorless drive," *Journal of Electrical Engineering & Technology,* vol. 15, pp. 2179-2197, 2020.

[108] A. Bhaumik and S. Das, "Predictive torque control strategy for speed adaptive flux observer based sensorless induction motor drive in flux-weakening region," *IEEE Transactions on Power Electronics,* vol. 36, no. 12, pp. 14110-14118, 2021.

[109] H. Wang, X. Ge, and Y.-C. Liu, "Second-order sliding-mode MRAS observer-based sensorless vector control of linear induction motor drives for medium-low speed maglev applications," *IEEE Transactions on Industrial Electronics,* vol. 65, no. 12, pp. 9938-9952, 2018.

[110] K. Negadi, A. Mansouri, and B. Khtemi, "Real time implementation of adaptive sliding mode observer based speed sensor less vector control of induction motor," *Serbian Journal of Electrical Engineering,* vol. 7, no. 2, pp. 167-184, 2010.

[111] H. Khouidmi and A. Massoum, "Reduced-order sliding mode observer-based speed sensorless vector control of double stator induction motor," *Acta Polytechnica Hungarica,* vol. 11, no. 6, pp. 229-249, 2014.

[112] H. M. Kojabadi and L. Chang, "Model reference adaptive system pseudoreduced-order flux observer for very low speed and zero speed estimation in sensorless induction

motor drives," in *2002 IEEE 33rd Annual IEEE Power Electronics Specialists Conference. Proceedings (Cat. No. 02CH37289)*, 2002, vol. 1: IEEE, pp. 301-305.

[113] K. Hachiya and T. Ohmae, "Digital speed control system for a motor using two speed detection methods of an incremental encoder," in *2007 European Conference on Power Electronics and Applications*, 2007: IEEE, pp. 1-10.

[114] S. Riyadi, "Control strategy for switched reluctance motor with rotary encoder based rotor position detection," *Advances in Electrical and Electronic Engineering,* vol. 16, no. 3, pp. 261-270, 2018.

[115] M. Bourogaoui, H. B. A. Sethom, and I. S. Belkhodja, "Speed/position sensor fault tolerant control in adjustable speed drives–A review," *ISA transactions,* vol. 64, pp. 269-284, 2016.

[116] P. Mukherjee and M. Sengupta, "Closed loop speed control of a laboratory fabricated brush-less DC motor drive prototype using position sensor," in *2017 National Power Electronics Conference (NPEC)*, 2017: IEEE, pp. 166-171.

[117] H. Arabaci and O. Bilgin, "A novel motor speed calculation method using square wave speed sensor signals via fast Fourier transform," *Turkish Journal of Electrical Engineering and Computer Sciences,* vol. 20, no. 7, pp. 1090-1099, 2012.

[118] M. Baszynski and S. Pirog, "A novel speed measurement method for a high-speed BLDC motor based on the signals from the rotor position sensor," *IEEE Transactions on Industrial Informatics,* vol. 10, no. 1, pp. 84-91, 2013.

[119] A. B. Kulkarni and M. Ehsani, "A novel position sensor elimination technique for the interior permanent-magnet synchronous motor drive," *IEEE Transactions on Industry Applications,* vol. 28, no. 1, pp. 144-150, 1992.

[120] M. Ehsani and B. Fahimi, "Elimination of position sensors in switched reluctance motor drives: state of the art and future trends," *IEEE Transactions on industrial electronics,* vol. 49, no. 1, pp. 40-47, 2002.

[121] P. Alaeinovin and J. Jatskevich, "Filtering of Hall-sensor signals for improved operation of brushless DC motors," *IEEE Transactions on Energy Conversion,* vol. 27, no. 2, pp. 547-549, 2012.

[122] P. Paramo-Balsa, J. M. Roldan-Fernandez, F. Gonzalez-Longatt, and M. Burgos-Payan, "Measurement of the Speed of Induction Motors Based on Vibration with a Smartphone," *Applied Sciences,* vol. 12, no. 7, p. 3371, 2022.

[123] K. Sushmaja and F. Noorbasha, "Implementation of binary shift keying techniques," *Int. J. Eng. Trends Technol.(IJETT),* vol. 4, no. 6, 2013.

[124] A. Goel, "Generation of ASK, FSK and PSK using sample & hold IC LF 398," in *2016 International Conference on Signal Processing and Communication (ICSC)*, 2016: IEEE, pp. 51-54.

[125] G. S. Kishore and H. Rallapalli, "Performance assessment of m-ary ask, fsk, psk, qam and fqam in awgn channel," in *2019 International Conference on Communication and Signal Processing (ICCSP)*, 2019: IEEE, pp. 0273-0277.

[126] W. Li, M. Li, and N. H. Zhu, "All-optical generation of ASK, PSK, and FSK radio-frequency signals," in *2016 Progress in Electromagnetic Research Symposium (PIERS)*, 2016: IEEE, pp. 2362-2362.

[127] A. Sharma, S. Majumdar, A. Naugarhiya, B. Acharya, S. Majumder, and S. Verma, "VERILOG based simulation of ASK, FSK, PSK, QPSK digital modulation techniques," in *2017 International Conference on I-SMAC (IoT in Social, Mobile, Analytics and Cloud)(I-SMAC)*, 2017: IEEE, pp. 403-408.

[128] M. T. Abuelma'atti, "New ASK/FSK/PSK/QAM wave generator using multiple-output operational transconductance amplifiers," *IEEE Transactions on Circuits and Systems I: Fundamental Theory and Applications,* vol. 48, no. 4, pp. 487-490, 2001.

[129] S. Bodkhe, M. Aware, J. Chaudhari, and J. Agrawal, "Speed estimator for induction motor drive based on synchronous speed tracking," *Sadhana,* vol. 40, pp. 1241-1256, 2015.

[130] C. H. Liu, H. C. Chang, and C. D. Wang, "Very low speed sensorless control of induction motor drives using high‐frequency signal injection," *Journal of the Chinese Institute of Engineers,* vol. 28, no. 6, pp. 957-966, 2005.

[131] H. Kiyotake, K. Shinohara, and K. Yamamoto, "Rotor speed detection method for vector control of induction motor without speed sensor utilizing slot harmonics," *Electrical Engineering in Japan,* vol. 169, no. 1, pp. 41-49, 2009.

[132] D.-H. Lee, "Wide-range speed control scheme of BLDC motor based on the hall sensor signal," *Journal of Power Electronics,* vol. 18, no. 3, pp. 714-722, 2018.

[133] S. Singer, B. Rozenshtein, and S. Surazi, "Characterization of PV array output using a small number of measured parameters," *Solar energy,* vol. 32, no. 5, pp. 603-607, 1984.

[134] K. Braimakis and S. Karellas, "Exergy efficiency potential of dual-phase expansion trilateral and partial evaporation ORC with zeotropic mixtures," *Energy,* vol. 262, p. 125475, 2023.

[135] P. V. M. Mena, J J; Kang, S -M; Harton, A V; Wyatt, K W, "A simple rate-equation-based thermal VCSEL model," *Journal of Lightwave Technology,* vol. 17, no. 5, pp. 865-872, May 1999, doi: 10.1109/50.762905.

[136] W. Zhou and K. Jin, "Efficiency evaluation of laser diode in different driving modes for wireless power transmission," *IEEE Transactions on Power Electronics,* vol. 30, no. 11, pp. 6237-6244, 2015.

[137] W. Zhou, K. Jin, M. Wang, and Q. Wu, "Efficiency Evaluation of Laser Based Wireless Power Transmission System," in *2020 IEEE Applied Power Electronics Conference and Exposition (APEC)*, 2020: IEEE, pp. 3147-3150.

END